COST 728/MESOSCALE MODELLING: APPLICATIONS SESSIONS

SIMULATING THE BENZO(A)PYRENE DISTRIBUTION OVER EUROPE FOR 2000 AND 2001
Volker Matthias, Armin Aulinger, Markus Quante - GKSS Research Center, Institute for Coastal Research, Max-Planck-Strasse 1, 21502 Geesthacht, Germany

LONG-TERM SIMULATION OF MESOSCALE FLOW AND AIR POLLUTION DISPERSION OVER TEHRAN, PART I: LOW-LEVEL FLOW FEATURES
Peyman Zawar-Reza[1,2], Mikhail Titov[1], Ghasem Azizi[3], Abbas-Ali Bidokhti[4], Iman Soltanzadeh[4] - [1] Centre for Atmospheric Research, University of Canterbury, Christchurch, New Zealand, [2] Institute of Geography, University of Tehran, Iran, [3] Faculty of Geography, University of Tehran, Iran, [4] Institute of Geophysics, University of Tehran, Iran

METEOROLOGICAL MODELING OF WINTER AND SUMMER PERIODS FOR THE SWISS-CANADIAN RESEARCH PROJECT ON AEROSOL MODELING (SCRAM)
J. Keller[1], Ş. Andreani-Aksoyoğlu[1], A.S.H. Prévôt[1], J.J. Sloan[2], Z. He[2], N. Foppa[3] - [1]Laboratory of Atmospheric Chemistry (LAC), Paul Scherrer Institute, Switzerland, [2]Waterloo Centre for Atmospheric Sciences (WCAS), University of Waterloo, Canada, [3]Federal Office of Meteorology and Climatology MeteoSwiss, Zurich, Switzerland

REGIONAL AIR QUALITY MODEL SIMULATIONS FOR THE SWISS-CANADIAN RESEARCH ON AEROSOL MODELLING (SCRAM) PROJECT
J.J. Sloan[1], S. Taghavi[1], S. Nikzad[1], Z. He[1], Ş. Andreani-Aksoyoğlu[2], J. Keller[2], J. Brook[3] - [1]Waterloo Centre for Atmospheric Sciences (WCAS), University of Waterloo, Canada, [2]Laboratory of Atmospheric Chemistry (LAC), Paul Scherrer Institute, Switzerland, [3]Environment Canada, Air Quality Research Branch, Toronto, Canada

APPLICATION OF MESOSCALE METEOROLOGICAL MODEL ON AIR POLLUTION WARNING SYSTEM
Pornpan Uttamang[1], Surat Bualert[2]and Boonlert Archevarahaprok[3] - [1]Industrial Estate Authority of Thailand [2]Chulalongkorn University, Thailand, [3]Meteorological Department of Thailand.

ANALYTICAL SOLUTIONS OF THE ADVECTION-DIFFUSION EQUATION FOR AREA SOURCES
Young-San Park[1] and Jong-Jin Baik[2] - [1]Climate Environment System Research Center, Seoul National University, Seoul, Korea, [2]School of Earth and Environmental Sciences, Seoul National University, Seoul, Korea

MODELLING PASSIVE TRACER TRANSPORT TO THE HIGH ALPINE SITE JUNGFRAUJOCH
D. Folini[1], S. Ubl[1], P. Kaufmann[2] - 1) Air Pollution and Environmental Technology, Swiss Federal Laboratories for Materials Testing and Research (Empa), Dübendorf, Switzerland, 2) Federal Office of Meteorology and Climatology MeteoSwiss, Zürich, Switzerland, PENINSULA, GREECE

SEA-SALT AEROSOLS (SSA): IMPACT ON ATMOSPHERIC POLLUTION OF THE ATTICA PENINSULA, GREECE
Eleni Athanasopoulou[a], Maria Tombrou[a,] , Spyros Pandis[b] and Armistead G. Russell[c] - [a] National and Kapodistrian University of Athens, Faculty of Physics, Dep. of Applied Physics, Lab. of Meteorology, Athens, Greece, [b] Department of Chemical Engineering, University of Patras, 26500 Patra, Greece, [c] School of Civil and Environmental Engineering, Georgia Institute of Technology, 311 Ferst Drive NW, Atlanta, GA 30332-0512, USA

INFLUENCE OF SAHARAN DUST CONTRIBUTION ON THE PARTICULATE MATTER FORECAST IN SOUTHERN EUROPE
Pedro Jiménez-Guerrero, Carlos Pérez, Oriol Jorba and José M. Baldasano - Barcelona Supercomputing Center – Centro Nacional de Supercomputación (BSC-CNS) Earth Sciences Department, C/ Jordi Girona 29, Edificio Nexus, 08034 Barcelona (Spain)

QUANTIFYING THE INPUT OF WIND BLOWN DUST TO SOUTHERN EUROPEAN CITIES
S Plainiotis[1], K A Pericleous[1], B E A Fisher[2] - [1]University of Greenwich, UK, [2]Environment Agency, UK

AIR QUALITY AND POLLUTION DISPERSION MODELING IN SINGAPORE
M. Skote - Institute of High Performance Computing, 1 Science Park Road, #01-01 The Capricorn, Singapore Science Park II, Singapore 117528

THE DEVELOPMENT AND EVALUATION OF DISPERSION MODELS FOR URBAN AREAS
Wenjun Qian, David Pankratz, Jing Yuan, Tao Zhan, and Akula Venkatram - University of California, Riverside, CA, 92521

ON THE REPRESENTATION OF THE STABLE BOUNDARY LAYER OVER THE LONDON METROPOLITAN AREA IN MESOSCALE MODELS
C. Chemel, Y. Yu, E. Somervell, and R. S. Sokhi - Centre for Atmospheric & Instrumentation Research (CAIR), University of Hertfordshire, Hatfield, UK

SWISS-CANADIAN RESEARCH ON AEROSOL MODELLING (SCRAM)
Ş. Andreani-Aksoyoğlu[1], J. Keller[1], M.R. Alfarra[1], A.S.H. Prévôt[1], J.J. Sloan[2], S. Taghavi[2], S. Nikzad[2], Z. He[2] - [1]Laboratory of Atmospheric Chemistry (LAC), Paul Scherrer Institute, Switzerland, [2]Waterloo Centre for Atmospheric Sciences (WCAS), University of Waterloo, Canada

SIMULATING THE ATMOSPHERIC TRANSPORT AND DEPOSITION OF BENZO(A)PYRENE OVER EUROPE IN 2000 WITH DIFFERENT TIME-VARIANT EMISSION SCENARIOS
Armin Aulinger, Volker Matthias, Markus Quante - GKSS Research Center, Max-Planck-Strasse 1, 21502 Geesthacht, Germany

THE IMPACT OF BIOGENIC VOC EMISSIONS ON PHOTOCHEMICAL OZONE FORMATION DURING A HIGH OZONE POLLUTION EPISODE IN THE IBERIAN PENINSULA IN THE 2003 SUMMER SEASON.
Nuria Castell[1], Rosa Salvador[1], Enrique Mantilla[1], Ariel Stein[2] and Millán Millán[1].- [1] Centro de Estudios Ambientales del Mediterráneo, Valencia, Spain, [2] Earth Resources and Technology on assignment to NOAA/Air Resources Laboratory.

STUDY OF PHOTOCHEMICAL SMOG INCIDENCE IN THE INFLUENCE AREA OF "LA PLANA DE CASTELLON"
Juana M Delgado-Saborit[1, 2], Maria A. Querol-Balaguer[2] & Vicente J Esteve-Cano[2] - (1) University of Birmingham, Division of Environmental Health & Risk Management, Birmingham (UK), (2) Universtat Jaume I, Dept. Quimica Inorganica y Organica, Castellon, (Spain)

PHOTOCHEMICAL MODELING AND OZONE IMPACT OF NEW INDUSTRIAL FACILITIES IN THE SOUTHWESTERN IBERIAN PENINSULA
Enrique Mantilla[1], Nuria Castell[1], Rosa Salvador[1], Ariel Stein[2], and Millán Millán[1]
[1] Centro de Estudios Ambientales del Mediterráneo (CEAM), Valencia, Spai.
[2] Earth Resources and Technology on assignment to NOAA/Air Resources Laboratory.

Proceedings of the 6th International Conference on Urban Air Quality
Limassol, Cyprus, 27-29 March 2007

SIMULATING THE BENZO(A)PYRENE DISTRIBUTION OVER EUROPE FOR 2000 AND 2001

Volker Matthias, Armin Aulinger, Markus Quante

GKSS Research Center, Institute for Coastal Research, Max-Planck-Strasse 1, 21502 Geesthacht, Germany

ABSTRACT

At GKSS, the CMAQ chemical transport model was expanded to treat the carcinogenic polyaromatic hydrocarbon (PAH) benzo(a)pyrene (B(a)P) and other persistent organic pollutants. B(a)P is mainly particle bound and can be transported over long distances. Therefore, it can be deposited in areas far from the main source regions. We simulated the B(a)P distribution over Europe for the years 2000 and 2001. Significant differences exist between different regions in Europe and between winter and summer concentrations. The latter is not only caused by the higher emissions in winter, also the meteorological conditions and, connected to them, the main transport pathways of B(a)P from the source regions into remote areas play an important role. The model is able to represent the temporal evolution and the regional distribution of B(a)P, however simulated concentrations and depositions are significantly higher than measurements at selected EMEP sites. Wet deposition of B(a)P into the North and Baltic Seas was found to be comparable to that in polluted regions like East Germany and therefore higher than modelled air concentrations close to ground would suggest. This indicates that long range transport of persistent pollutants is efficient and that deposition patterns cannot easily be derived from the few existing measurement stations.

1. INTRODUCTION

Polycyclic aromatic hydrocarbons (PAHs) are semivolatile, lipophilic persistent organic pollutants (POPs), which originate primarily from incomplete combustion of organic material. Surveys have revealed that a variety of PAHs possess a high carcinogenic potential to animals and humans (ATSDR, 1995) and are bio-accumulated in the food chain. They can be transported over long distances in the atmosphere resulting in a widespread distribution across the earth, including regions where they have never been used. Due to their toxic and ecotoxic characteristics they pose a threat to humans and the environment, and therefore the international community has called for actions to reduce and eliminate the release of POPs, such as the Protocol to the UN-ECE Convention on Long-range Transboundary Air Pollution (CLRTAP) on POPs. Benzo(a)Pyrene (B(a)P) is the most studied PAH and it is taken as representative for the whole group of PAHs. Because of the significant health risks of PAHs, annual limit values of 1 ng/m^3 for B(a)P will be implemented in the EU by 2013.
To study the atmospheric transport and deposition of PAHs over Europe the Community Multiscale Air Quality (CMAQ) Modeling System developed under the leadership of the US Environmental Protection Agency (Byun and Ching, 1999; Byun and Schere, 2006) has been extended at GKSS to treat also semivolatile POPs, in particular B(a)P. Model runs covering the years 2000 and 2001 giving hourly concentration fields were carried out over Europe and on a smaller grid over the North Sea and its coastal areas. The model results are compared to measurements of B(a)P concentrations in air and to measured depositions in rain water. Sensitivity tests concerning the meteorological input fields show their large influence on the results of the chemical transport model.

2. MODEL SETUP

CMAQ includes gas phase, aerosol and aqueous chemistry. In this study, the CB4 mechanism is used. The aerosol is represented by three size modes (Aitken, accumulation and coarse mode). Each of them is assumed to have a lognormal distribution. In the PAH extension of the model (Aulinger et al., 2007), B(a)P is considered as almost completely connected to particles at ambient temperatures. It can occur in each of the three size modes and also in the gas phase, however typically more than 99 % of the B(a)P mass is connected to organic aerosols in the accumulation mode. Only if the available organic aerosol mass is in the accumulation mode is very small, the partitioning of the aerosol bound B(a)P can be shifted to one of the other modes or even to the gas phase.
The CMAQ model is setup on a 54 x 54 km² grid for Europe and on a nested smaller domain with a 18 x 18 km² grid for the North Sea region. Special emphasis is laid on the representation of the planetary boundary layer to capture vertical transport and dispersion of atmospheric air pollution in coastal environments, where special circulation patterns (e.g. land see breeze effects) can be of importance. Therefore, 30 vertical levels up to 100 hPa with 20 levels below approx. 2500 m are used in a terrain following σ-pressure co-ordinate system.
The meteorological fields are derived from MM5 (Grell et al., 1995) model runs which were driven by ERA40 6 hourly global reanalysis data on a 1x1degree grid. We used four dimensional nudging of the

ERA40 fields and more sophisticated physical parameterisation schemes like Reisner 2 (Reisner et al., 1998) for cloud microphysics, Kain Fritsch 2 (Kain, 2004) for cumulus representation and the MRF (Hong and Pan, 1996) scheme for the boundary layer to produce meteorological data which is as close as possible to wind, temperature and humidity observations. For comparison, meteorological fields for April 2000 were also calculated without nudging. Periods of five days were simulated restarting the model every three days to update the initial conditions and keep them close to the reanalysis.
Emission data for the nitrogen, sulfur and volatile organic compounds as well as for aerosol particles was provided by IER Stuttgart based on EMEP area emissions and EPER point source emissions. The B(a)P emissions are based on annual gridded values from Denier van der Gon et al. (2005). Because the emissions from residential heating (wood and coal burning) are highly dependent on season, we introduced a temporal cycles that depends on ambient temperature for this sector. Weekly and diurnal cycles of the B(a)P emissions were also considered, they were chosen to follow the NO cycle for traffic emissions and the CO cycle for heating processes.

3. RESULTS AND DISCUSSION

The annual mean B(a)P concentration pattern over Europe can be seen in Figure 1. Highest concentrations are found close to the main source regions like the Rhine Ruhr area, south Poland and the Ukraine, but also in the vicinity of large cities like Moscow, Paris and in the Po valley. However, also in regions which are far from the main sources like in south Finland high B(a)P concentrations can be seen in the model results. The differences between the years are quite small in the annual average, but this is caused by the fact that the total amount of emitted B(a)P was the same for both model runs. Larger differences appear in coastal areas like the Adriatic Sea and the northern coast of the Black Sea.
The situation is different for wet deposition, which contributes more than 90 % to the total B(a)P deposition. Significant deposition can be observed over sea, where B(a)P concentrations are usually quite low. In 2000, large parts of the North Sea, the Baltic Sea and the southern Black Sea show high B(a)P wet deposition, the values are comparable to those in eastern Germany and in the Balkans. Over the North Sea and the Baltic Sea, lower B(a)P deposition is simulated for 2001, but the Adriatic Sea and the Black Sea show higher amounts of wet deposited B(a)P than the year before.
Comparisons to measurements of B(a)P in ambient air were carried out for selected EMEP sites. Kosetice in the Czech Republic is located in a rather polluted area in central Europe. The measured annual means were 0.17 ng/m^3 in 2000 and 0.23 ng/m^3 in 2001. The model derived values are significantly higher at 0.86 ng/m^3 in 2000 and 0.78 ng/m^3 in 2001. At Roervik in south west Sweden the measured annual means were about a factor of 3 lower compared to Kosetice and amount to 0.08 ng/m^3 in 2000 and 0.07 ng/m^3 in 2001. The modelled values are again a factor of 3-4 higher at 0.27 ng/m^3 in 2000 and 0.30 ng/m^3 in 2001. Despite this large difference in the absolute values, the time series of the modelled B(a)P concentration (Fig. 3) show high correlations. The annual cycles and also certain peaks in the measurements are captured quite well by the model. Judging the large differences between model and measurements one has to take into account that the measurements are only taken during selected intervals. At Kosetice, the measurements are derived from daily samples taken once a week. At Roervik, weekly samples are taken once a month in 2000, in 2001 they

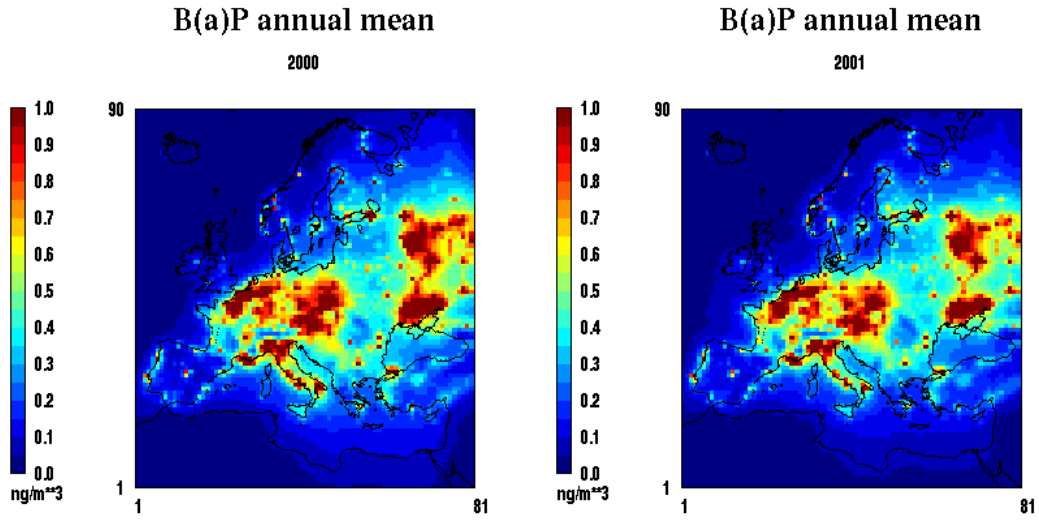

Fig. 1: Annual mean B(a)P concentrations for 2000 and 2001 simulated with CMAQ and a PAH extension.

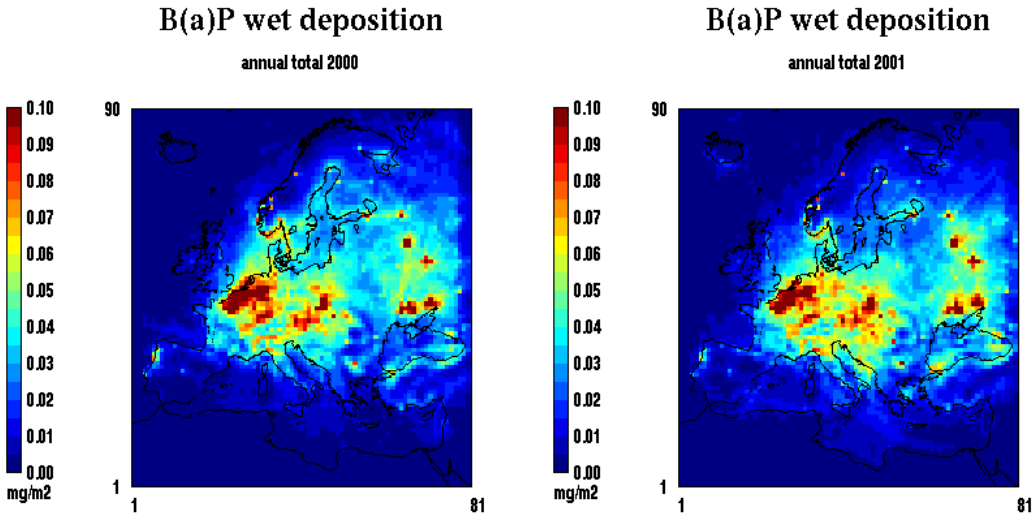

Fig. 2: Annual totals of B(a)P wet deposition in 2000 and 2001 simulated with CMAQ and a PAH extension.

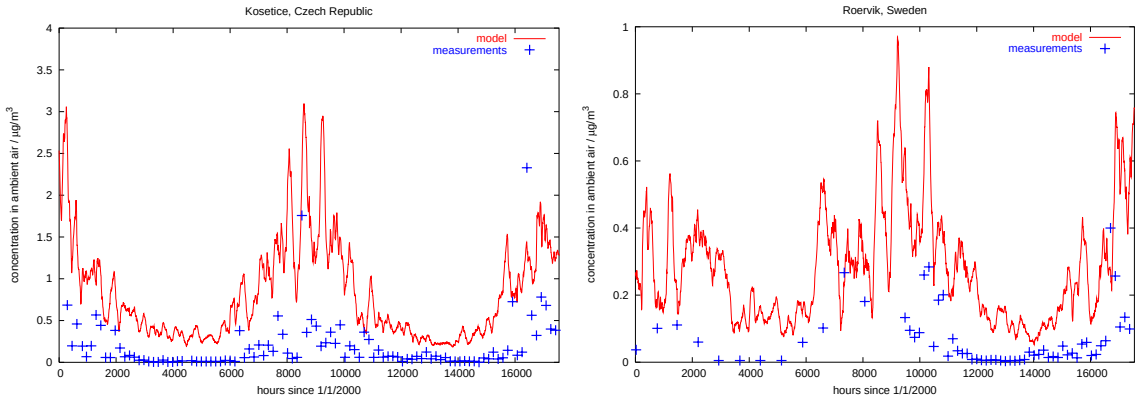

Fig. 3: Time series of modelled and measured B(a)P concentrations in ambient air for 2000 and 2001. Measurements represent two days at Kostice and one week at Roervik. Modelled values are smoothed with a one week gliding average.

were taken on a continuous basis. Having the large variations in ambient air concentrations in mind the latter is certainly the preferred method for B(a)P measurements.

Measured deposition values at EMEP stations in northern Germany, Sweden and Finland show annual averages between 0.001 and 0.006 mg/m^2 while the model values in the grid cells closest to the measurement station range between 0.012 and 0.059 mg/m^2, which means that they are approx. a factor of 10 higher in the model than observed. However, both model and measurements show lower values in 2001 than in 2000, with the exception of Pallas in North Finland where the measured values were higher in 2001.

The use of meteorological fields which were calculated without analysis nudging of wind, temperature and humidity can lead to significantly different results. The differences in B(a)P concentration in the lowest model layer and in the wet deposition pattern for April 2000 are given in Figure 4. The wet deposition shows a different distribution over Europe compared to the nudged case but the total amount is not significantly changed. The B(a)P concentrations are lower in the case without nudging, in particular close to the source regions average concentrations in April can be more than 0.1 ng/m^3 less than in the reference case with full nudging.

4. CONCLUSIONS

Benzo(a)pyrene concentrations in ambient air have been modeled for two years, 2000 and 2001, using an expanded version of the Community Multiscale Air Quality Modelling system (CMAQ). The modeled concentrations are significantly higher than measurements at two EMEP stations in background areas suggest. Nevertheless the temporal evolution over the two years was captured quite well by the model. The reason of the discrepancies in the total amount of B(a)P in air is not yet clear. Uncertainties in the emission data base might play an important role. Chemical degradation of B(a)P which is not considered in the current model version will probably be of minor influence.

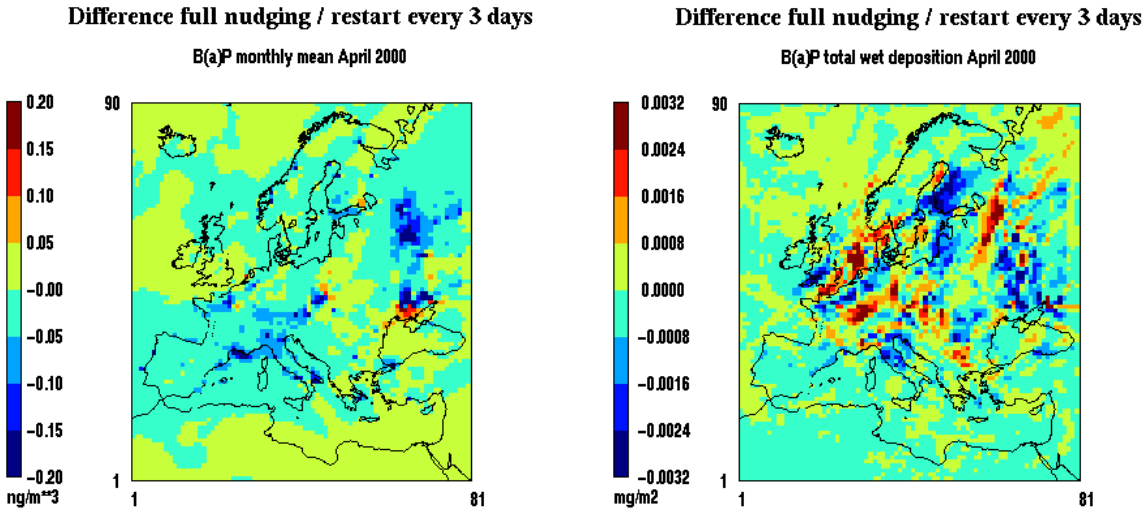

Fig. 4: Changes in modelled concentration and deposition fields by using different meteorological fields for April 2000. The figures show test case (restart every 3 days) minus reference case (full nudging).

Consequently also the B(a)P deposition is significantly higher in the model compared to concentration measurements in rain water. Despite the discrepancies in the total amount, the model gives reliable regional distributions of B(a)P in air and its deposition and it can be used to identify the main transport pathways of persistent organic pollutants into remote regions. Particularly the North and Baltic Seas suffer from higher deposition of B(a)P into water than concentration patterns would suggest.

ACKNOWLEDGEMENTS

US EPA is gratefully acknowledged for the use of CMAQ. We thank NCAR and Penn State University for the use of MM5 and also IER Stuttgart for providing emission data.

REFERENCES

Agency for Toxic Substances and Disease Registry (ATSDR), Toxicological Profile for Polycyclic Aromatic Hydrocarbons (PAHs). Public Health Service, US Department of Health and Human Services, Atlanta, GA, USA, 1995

Aulinger, A., V. Matthias, M. Quante, Introducing a partitioning mechanism for PAHs into the Community Multiscale Air Quality modelling system and its application to simulating the transport of benzo(a)pyrene over Europe, J. Appl. Meteorol., accepted 2007

Byun, D., J.K.S. Ching, Science Algorithms of the EPA Models-3 Community Multiscale Air Quality Modelling System. --EPA report, EPA/600/R-99/030, Office of Research and Development, Washington DC 20406, 1999

Byun, D., K.L. Schere, Review of the Governing Equations, Computational Algorithms, and Other Components of the Models-3 Community Multiscale Air Quality (CMAQ) Modeling System. --Appl. Mech. Rev. **59**, 51-77, 2006

Denier van der Gon, H.A.C., M. van het Bolscher, A.J.H. Visschedijk, P.Y.J. Zandveld, Study of the effectiveness of UNECE Persistent Organic Pollutants Protocol and cost of possible additional measures. Phase I: Estimation of emission reduction resulting from the implementation of the POP Protocol. --TNO-report. B&O-A R 2005/194. Laan van Westenenk 501, P.O. Box 342, 7300 AH Appeldoorn, The Netherlands, 2005

Grell, G., Dudhia, J., and Stauffer, D.R., 1995. A Description of the Fifth-Generation Penn State/NCAR Mesoscale Model (MM5). NCAR Technical Note 398, NCAR, Boulder, Colorado, USA.

Hong, S.Y., Pan, H.L., 1996, Nonlocal boundary layer vertical diffusion in a Medium-Range Forecast Model. Monthly Weather Review 124, 2322.

Kain, J.S., 2004, The Kain-Fritsch convective parameterisation: An update. J. Appl. Meteor. **43**, 170-181

Reisner, J., Rasmussen, R. J., Bruintjes, R. T., 1998, Explicit forecasting of supercooled liquid water in winter storms using the MM5 mesoscale model, QJRMS 124B, 1071.

Proceedings of the 6th International Conference on Urban Air Quality
Limassol, Cyprus, 27-29 March 2007

LONG-TERM SIMULATION OF MESOSCALE FLOW AND AIR POLLUTION DISPERSION OVER TEHRAN, PART I: LOW-LEVEL FLOW FEATURES

Peyman Zawar-Reza[1,2], Mikhail Titov[1], Ghasem Azizi[3], Abbas-Ali Bidokhti[4], Iman Soltanzadeh[4]

[1] Centre for Atmospheric Research, University of Canterbury, Christchurch, New Zealand
[2] Institute of Geography, University of Tehran, Iran
[3] Faculty of Geography, University of Tehran, Iran
[4] Institute of Geophysics, University of Tehran, Iran
*****_Corresponding author_: peyman.zawar-reza@canterbury.ac.nz, Tel: (643) 366-7001 Ext. 7911

ABSTRACT

Tehran, the capital mega-city of Iran has a population of more that 10 million and suffers from poor air quality most of the year. It has seen an unprecedented growth in the last 30 years where emissions from 2 million poorly emission-controlled motor vehicles cause a severe degradation in air quality. A research project is underway to understand and characterise mesoscale flow and dispersion in order to design an air pollution forecasting system for the city. For this purpose, The Air Pollution Model (TAPM) and Weather Research and Forecasting (WRF) model are being tested for their utility. A two month period, one in summer and another in winter, was simulated with both models. Results show that the models are able to simulate the diurnally reversing circulation system over the city. The IOA skill score for TAPM is 0.59 and 0.65 for u- and v-component of wind velocity respectively.

1. INTRODUCTION

Tehran, the capital of the Islamic Republic of Iran is situated in a semi-enclosed inland basin at the foothills of the Alborz Mountain Range (with average height of 2000 mASL; Figure 1). The 11 million inhabitants of the city are exposed to poor air quality for the majority of the year due to high emission levels from motor vehicles and poor ventilation characteristics of the atmosphere. Episodically in winter, the situation gets worse due to a build up of stable nocturnal inversion layer during stagnant anti-cyclonic conditions. Currently, a research programme is underway to study mesoscale flows and air pollution dispersion over Tehran. The first aim of the project is to characterise the mesoscale flow features and air pollution dispersion over Tehran. This paper presents results from two high-resolution non-hydrostatic models The Air Pollution Model (TAPM; Hurley, 2002), and Weather and Research Forecasting (WRF; Skamarock et al., 2005). A detailed emission inventory for Tehran is under preparation; therefore we only discuss the results from the meteorological modules of the models.

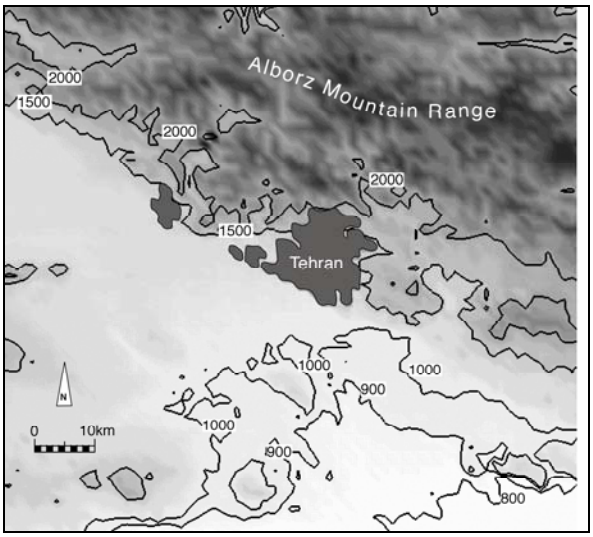

Figure 1: Topography of the Tehran region derived from the TAPM grid. Contour units are in mASL.

It has been recently stated by Tehran's Clean Air Committee that 10,000 people die every year due to air pollution related cardio-pulmonary disease. Using PM_{10} concentrations to illustrate the situation, there are only a few days in the year where the World Health Organisation's standard for PM_{10} (50 micrograms/m^3 for a 24 hour average) is not exceeded (Figure 2). PM10 concentrations are consistently high during summer and autumn, but cleaner periods are observed in winter and spring.

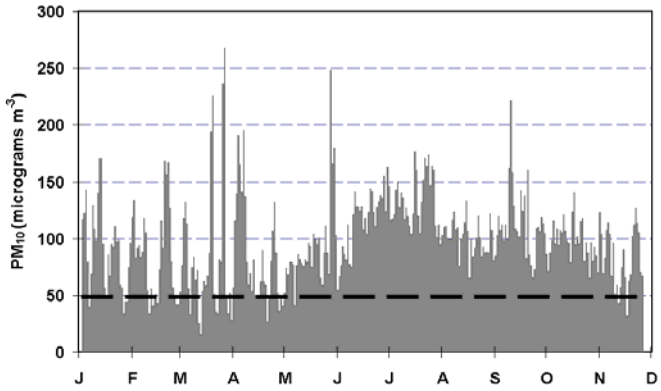

Figure 2: Daily averaged values of PM_{10} for 2003 (excluding December). The black dashed-line is the PM_{10} WHO standard of 50 micrograms/m^3.

The diurnal pattern for PM_{10} is illustrated in Figure 3. For June, two peaks are clearly distinguishable, one for the morning rush hour and another peak at night. This pattern is similar to the diurnal fluctuation of Carbon Monoxide (CO) (not shown here) and is most likely the result of volume of traffic. The hourly averages tend to stay above 100 mircograms/m^3 except for a few hours in the evening. For the month of November, there is only one morning peak evident at 8 A.M., yet compared to June, the PM_{10} concentration at each hour is less. This perhaps shows the contribution by dust in the summer.

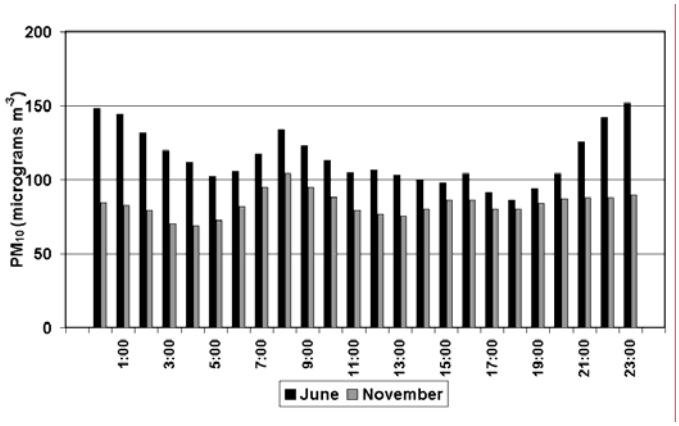

Figure 3: Hourly averages for June and November 2003.

2. METHODOLOGY

To study mesoscale circulations over Tehran, we have employed TAPM and WRF. TAPM was developed by scientists at Commonwealth Scientific and Industrial Research Organisation (CSIRO) in Australia, where as WRF was developed at National Centre for Atmospheric Research (NCAR) in the United States. TAPM is a much simpler (requires modest computational resources) and faster model (about ten times), but does not have the many physics options that are available in WRF. It is beyond the scope of this paper to present a detailed modelling setup with justification, but a general setup is defined next.

TAPM is a three-dimensional incompressible, non-hydrostatic, primitive equations model, which uses a terrain-following coordinate system (Hurley, 2002). The meteorological component of the model is supplied with a dataset derived from the Limited Area Prediction System (LAPS) analysis data from the Australian Bureau of Meteorology. For these series of experiments, the explicit cloud micro-physics option switch was turned on. The simulations presented here use three grids with grid spacing of 27, 9, and 3 km respectively, with each grid having 30 zonal and meridional grid nodes.

WRF, advanced research version 2.1.2 with multi-nesting option was also used. Four domains with spatial resolution 27 km (domain 1) and 1 km (domain 4) and 33 vertical levels for all 4 grids (10 levels in lowest 1500m) were run with no feedback from nest to parent domain (one-way interaction; which is also the same scheme adopted by TAPM). WSM 6-class graupel scheme, Dudhia short-wave radiation scheme, YSU

boundary-layer scheme, Monin-Obukhov surface-layer option and Grell-Devenyi ensemble cumulus scheme were used for physics parameterisation (Skamarock et al., 2005).

3. RESULTS AND DISCUSSION

Research in complex terrain (mountainous) meteorology has shown that superimposed on the perturbed synoptic scale flow, thermally driven mesoscale circulations can be a feature. Therefore a closer examination of observed and simulated local winds for Tehran is necessary. Temporally high-resolution observational data has recently become available in Tehran; most sites are situated in highly urbanised locations where micro-scale flow around the buildings *contaminates* the data. As a means to evaluate model performance, data from Geophysics Institute of University of Tehran was chosen, since the site is in a relatively un-built environment and has good exposure on top of a hill. There are about four other meteorological stations that collect high resolution datasets, but the results are not discussed here. Analysis from the Geophysics site shows that in the northern section of the city – situated on the foothills – a diurnally reversing circulation system exists. A south-easterly up-slope flow is evident predominantly during the day, and then a down-slope northerly becomes the outstanding feature at night (Figure 4a). The 3 km TAPM results also show the same features although due to the coarse resolution of the grid the contours are much smoother (Figure (4b).

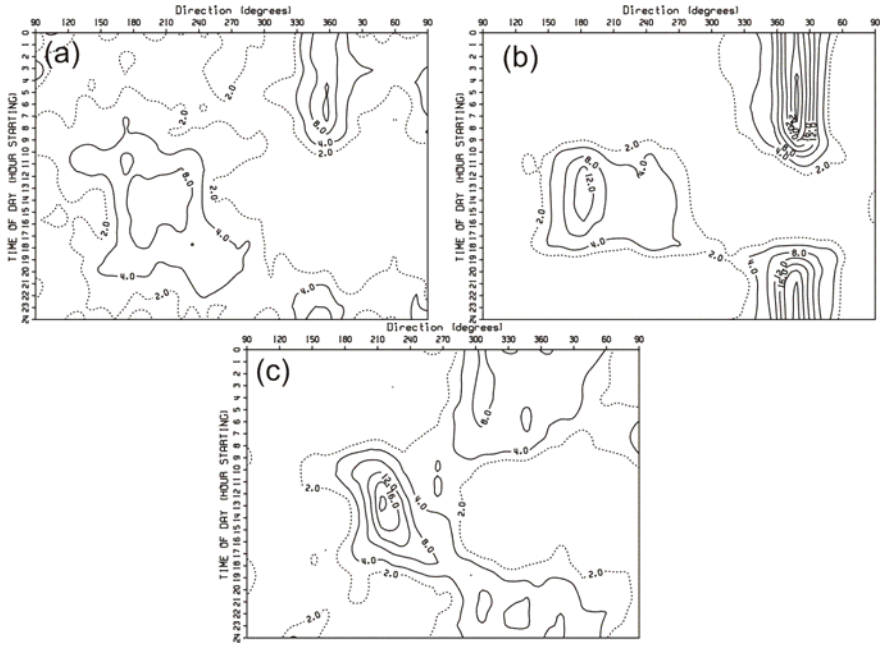

Figure 4: Wind direction frequency distribution for; (a) Geophysics station November 2003, (b) TAPM November 2003, and (c) WRF November 2005.

The 1 km WRF grid also produces the same features. Being a finer resolution than TAPM run the contours are not as smooth, but the modelled data are not comparable since the WRF simulation was performed for November of 2005 (we did not have access to the 2003 re-analysis input data for WRF at the time).

As a means of verifying the performance of TAPM, the Index of Agreement (IOA) was calculated against the Geophysics dataset. The IOA is a measure of the skill of the model in predicting variations about the observed mean; a value above 0.5 is considered to be good (Willmott, 1981). For November IOA is 0.59 and 0.65 for u- and v-component of wind velocity respectively. With the current setup and resolution, TAPM has more skill in capturing the north-south flow (up-slope, down-slope circulation system) than the east-west flow. Figure 5 illustrates the time series of wind velocity components; the almost daily diurnally reversing up- and down-slope flow is easily identifiable here. TAPM shows good skill is simulating the magnitude and duration of the up-slope component on most days, yet it over-estimates the down-slope component significantly. The u-component comparison is not as good as, this maybe due to the rather coarse 3 km grid spacing.

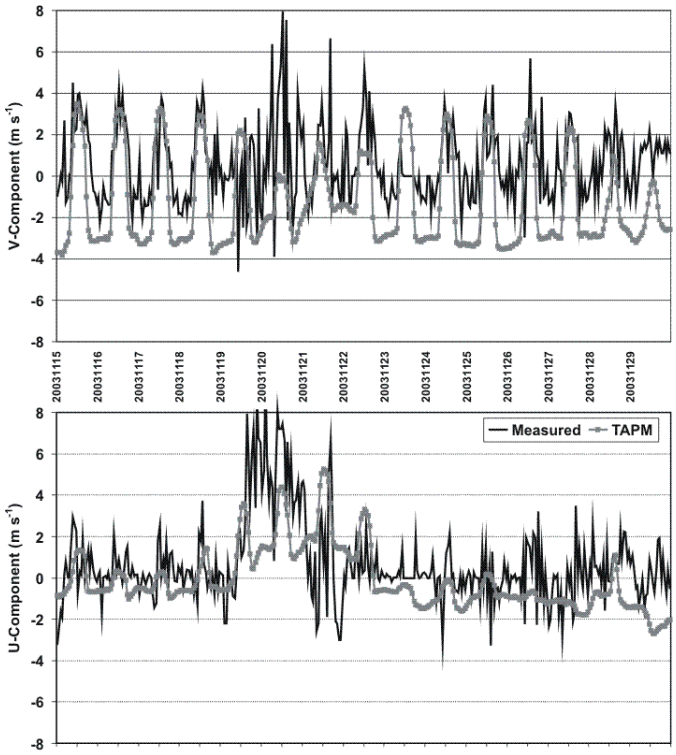

Figure 5: Comparison of u- and v-component of wind velocity for November between TAPM and measurements (only a potion of the time series is shown).

4. CONCLUSIONS

High-resolution month-long simulations with TAPM and WRF capture the main features of the mesoscale flow over Tehran. TAPM has a good skill in simulating the day-time up-slope flow, but consistently overestimates the nocturnal down-slope flow. The next step in this research is preparation of a detailed emissions inventory dataset to be used by the models.

5. ACKNOWLEDGEMENTS

This research is supported by a grant from the Islamic Republic of Iran Meteorological Organisation (www.irimet.net). We would like to thank the Air Quality Control Company (AQCC) of Tehran for providing us with the air pollution dataset. Also, we appreciate the support given to this project by Drs. Kamali, Jamali, Azadi, and Ranjbar from IRIMO.

6. REFERENCES

Skamarock, W. C., Klemp, J.B., Dudhia, J., Gill, D.O., Barker, D.M., Wang, W. and Powers, J.G. 2005. A description of the Advanced Research WRF Version 2. NCAR Tech Notes-468+STR.

Hurley, P. 2002. The Air Pollution Model (TAPM) Version 2. Part 1: technical description. CSIRO Atmospheric Research Technical Paper No. 55 2002. Available at http://www.dar.csiro.au/TAPM.

Willmott, C.J. 1981. On the validation of models, Physical Geography, 2,184-194.

METEOROLOGICAL MODELING OF WINTER AND SUMMER PERIODS FOR THE SWISS-CANADIAN RESEARCH PROJECT ON AEROSOL MODELING (SCRAM)

J. Keller[1], Ş. Andreani-Aksoyoğlu[1], A.S.H. Prévôt[1], J.J. Sloan[2], Z. He[2], N. Foppa[3]

[1]Laboratory of Atmospheric Chemistry (LAC), Paul Scherrer Institute, Switzerland
[2]Waterloo Centre for Atmospheric Sciences (WCAS), University of Waterloo, Canada
[3]Federal Office of Meteorology and Climatology MeteoSwiss, Zurich, Switzerland

ABSTRACT

The focus of the Swiss-Canadian project SCRAM is the simulation of formation and transport of atmospheric aerosols using two chemical transport models (CTM): the Comprehensive Air Quality Model with Extensions (CAMx) and the Community Multiscale Air Quality (CMAQ) modeling system, which includes the Model of Aerosol Dynamics, Reaction, Ionization, and Dissolution (MADRID). Both CTMs are driven by the meteorological model MM5. Two regions will be investigated, Switzerland and Southern Ontario (Canada).

For Switzerland, a winter period during January and February 2006 is investigated. This period is characterized by elevated aerosol concentrations due to anti-cyclonic conditions associated with temperature inversions and low wind patterns. Three nested domains were defined for the MM5 simulations. The coarse domain includes Central and Southern Europe, the fine domains are focused on Switzerland. MM5 was initialized by assimilated data of the aLpine Model (aLMo), the forecast model of MeteoSwiss. Snow information was taken from aLMo data and from snow cover maps based on NOAA AVHRR satellite data. The aLMo data was also used to perform a 4-dimensional data assimilation (FDDA). Preliminary results show that the wind fields show an acceptable agreement with measurements at moderate to high wind speed, whereas the agreement at low wind speed is worse.

The three Canadian domains cover Eastern North America, the Great Lakes and Southern Ontario, respectively. MM5 forecasts were performed for a period between July and September 2001. An example of the wind field is given.

1. INTRODUCTION

In the frame of the Swiss-Canadian project SCRAM the formation and transport of atmospheric aerosols are investigated by using two chemical transport models (CTM): CAMx and CMAQ/MADRID (Andreani-Aksoyoglu *et al.*, 2007). Both CTMs are driven by the meteorological model MM5. The study focuses on two regions, Switzerland and Southern Ontario (Canada). For Switzerland, a highly polluted period in winter 2006 will be simulated. The Canadian time frame covers a three months period in summer 2001. During both periods, extended field experiments in the respective regions have been performed where numerous measurements of gaseous and particulate properties have been taken. This paper deals first with the features of the meteorology during winter episodes in Switzerland. Subsequently, the setup of the model domains and the MM5 parameters are given and first results are shown. Second, we present an example of the results for the Canadian period.

2. WINTER EPISODES WITH ELEVATED PM10 LEVELS IN SWITZERLND (JANUARY / FEBRUARY 2006)

From January 1 to February 10, 2006 extraordinary high PM10 concentrations were measured in all regions of the country. By taking the national air quality station at Zurich as an example, this period can be characterized by two episodes (Fig.1). Further information is available from the "Alpine Weather Statistics", which describes the daily weather features over the Alps by 34 parameters (Wanner *et al.*, 1998). An anti-cyclonic situation with an extended fog layer over the Swiss Plateau prevailed until January 16, causing PM10 concentrations at Zurich of about 100 μg m^{-3}, which is twice the national air quality threshold. This episode was suddenly terminated by precipitation. The second episode from January 24 to February 7 was characterized first by conditions similar to those of the first episode leading to a peak PM10 concentration of 165 μg m^{-3}. Subsequently, however, the concentration gently dropped due to increasing wind speeds.

The meteorology of this period was simulated by MM5 version 3.7.2 (PSU/NCAR, 2005). The three nested domains with 27 km (Europe), 9 km (Switzerland and neighboring countries, Fig.2) and 3 km (Switzerland) resolution were defined. In the current configuration, MM5 runs in the one-way nesting mode initialized by assimilated data of the aLpine Model (aLMo), the forecast model of MeteoSwiss developed in the European consortium COSMO (COSMO, 2002). The grid cell size of aLMo is about 7 km at mid latitudes. Snow information was taken from the water equivalent accumulated snow depth (WEASD) field of aLMo and, for domain 3, from snow cover retrievals based on operational NOAA AVHRR satellite data (Foppa *et al.*, 2004). aLMo data was also used to perform a 4-dimensional data assimilation (FDDA), which is currently applied to domains 1 and 2. Domain 3 is controlled by the lateral boundary derived from domain 2 by using

the MM5 utility NESTDOWN. MM5 met fields were produced in units of 4 days (e.g. Jan 1-4). The last day of a given unit (e.g. Jan 4) is repeated, being the spin-up day of the subsequent unit. As an example, Figure 3 shows the wind field of aLMo (bottom layer), MM5 (bottom layer) and measurements taken at the stations of the Swiss meteorological monitoring network ANETZ (10 m) for Jan 8, 12:00 UTC (13:00 CET). On that day low winds prevailed over the Swiss Plateau and in the Po Basin. The MM5 wind field may substantially differ from the aLMo pattern and from the measurements. These discrepancies decreased on days with higher wind speeds and a prevailing wind direction. Wind vectors measured at exposed elevated locations can hardly been captured by the model. A preliminary comparison of the shortwave downward radiation (supposed to be an indicator of clouds or fog) with MODIS satellite imagery shows that MM5 may produce clouds. Fog, however, is hardly formed by the model. Future investigations will tackle the problem of the parameterization of the various meteorological and microphysical options to get the most realistic set of inputs for the whole time period.

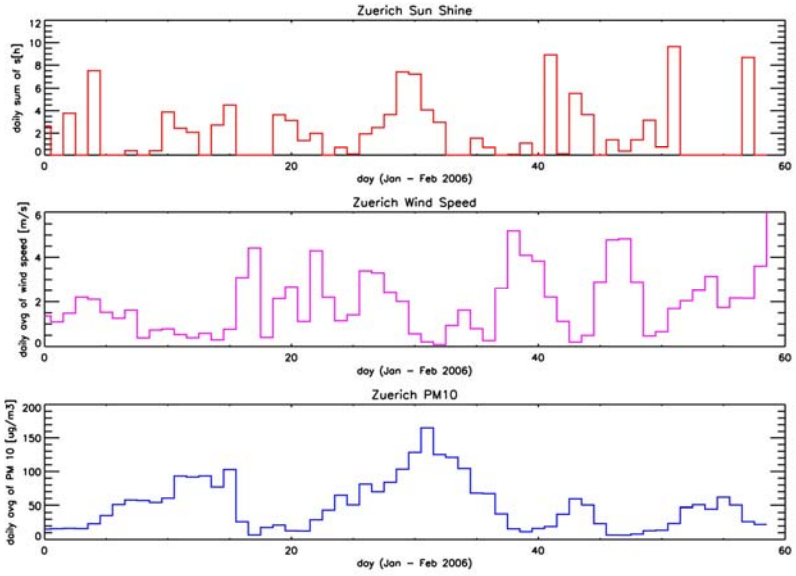

Figure 1: Sun shine duration (top), average wind speed (middle) and PM10 concentration (bottom) at Zurich. January-February 2006.

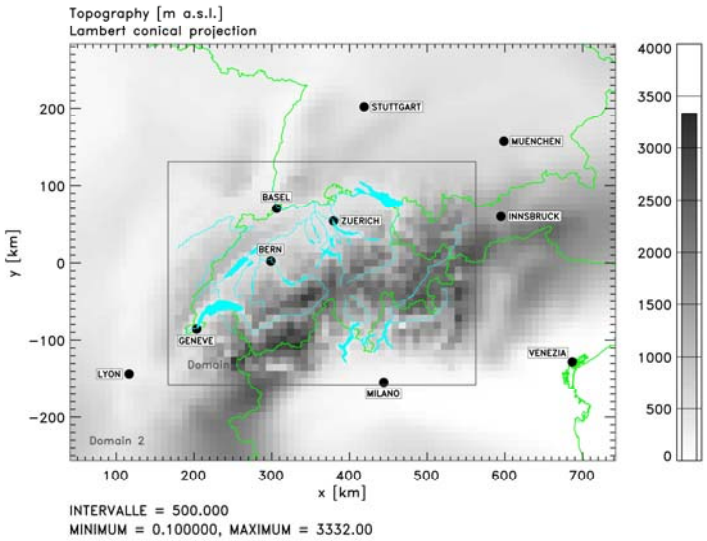

Figure 2: Topography of MM5 domain 2

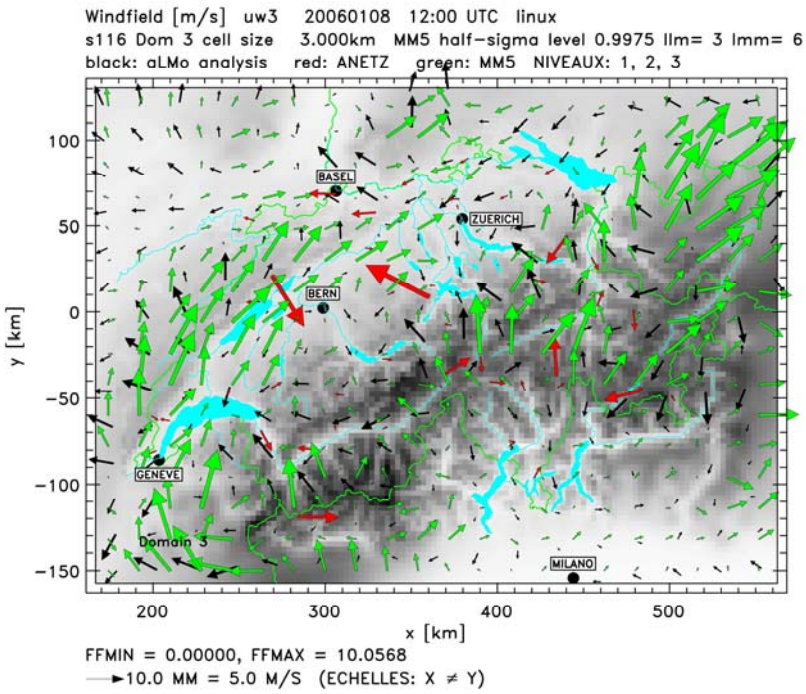

Figure 3: Wind fields of domain 3 on January 8, 2007, 12:00 UTC (13:00 CET). Black: aLMo (bottom layer); green: MM5 (bottom layer); red: ANETZ (10 m)

3. SUMMER EPISODES IN SOUTHERN ONTARIO (JULY-SEPTEMBER 2001)

The Canadian domains have resolutions of 36, 12 and 4 km covering Eastern North America, the Great Lakes and Southern Ontario, respectively (Fig. 4). MM5 was running in the two-way nesting mode and FDDA was applied to all domains. The simulations were performed for a period between July and September 2001. In Fig. 5 an example of wind forecast for domain 2, August 3, 2001, 01:00 UTC (August 2, 20:00 EST) is shown. A high wind speed region extends between Lake Ontario and Lake Huron. Lower velocities are observed over Lake Michigan and in the NW of the domain.

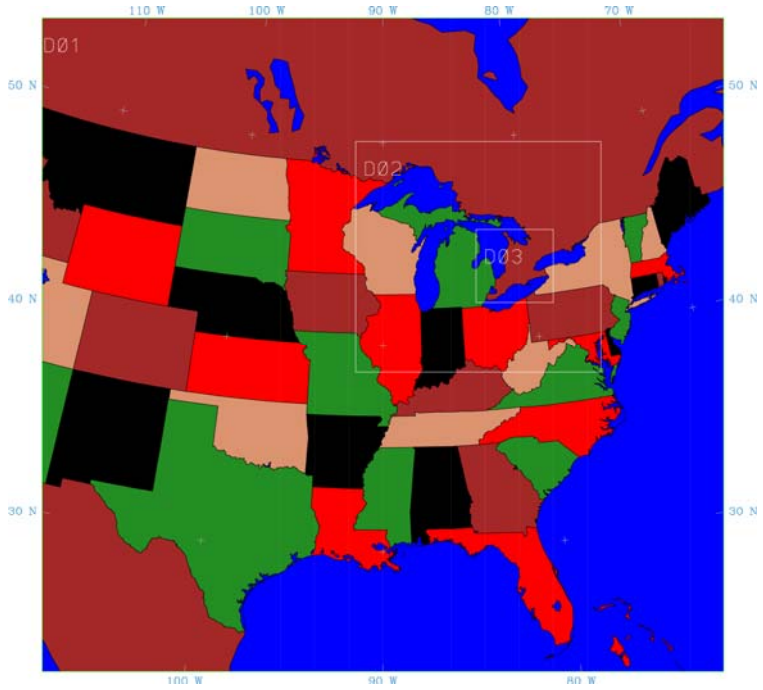

Figure 4: Map of the MM5 domains in Eastern North America and Canada

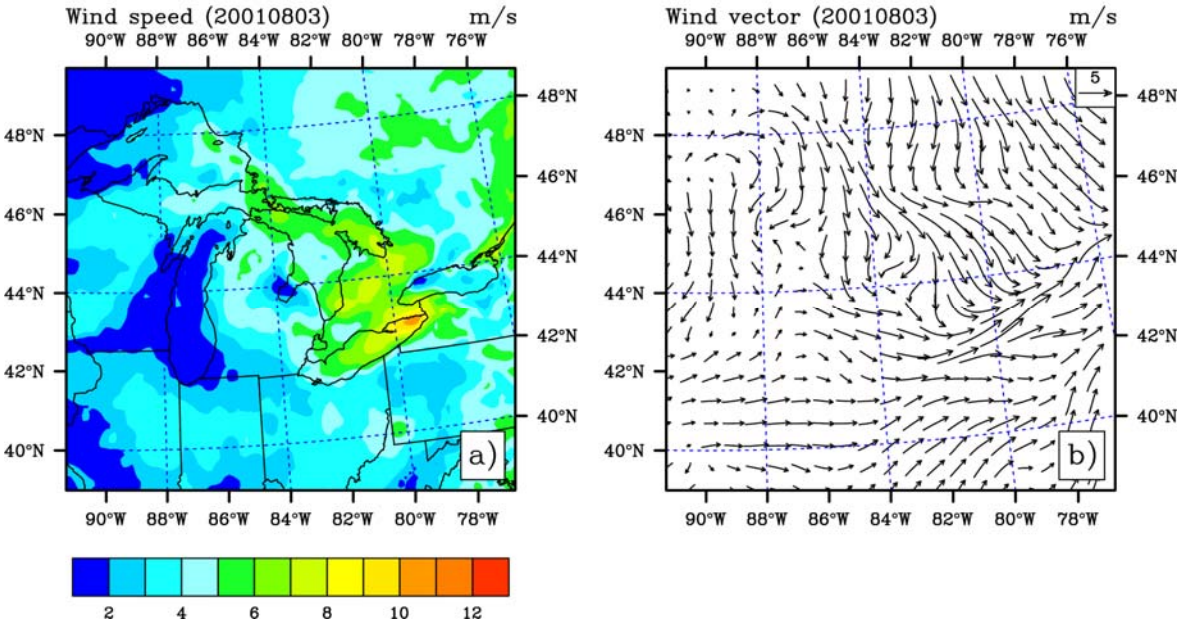

Figure 5: Example of a MM5 wind forecast in domain 2 on August 3, 2001, 01:00 UTC (August 2, 20:00 EST)

4. CONCLUSIONS

Modeling meteorology for winter conditions over the complex terrain of Switzerland is affected by numerous uncertainties. In contrast to summer smog conditions, no distinct mixing layer is developed even on clear days. Changes of the wind patterns due modified parameterizations of the model may substantially affect the concentrations simulated by the CTM. During anti-cyclonic situations, which may prevail several days, wind is low and fog is often formed over the Swiss Plateau, in alpine valleys and in the Po Basin. These features are very difficult to be captured by the model. Further investigations using various parameterizations of the meteorological and microphysical options of MM5 are required to obtain the most realistic met fields ending in simulated concentrations close to the measurements.

ACKNOWLEDGEMENTS

We acknowledge MeteoSwiss for providing aLMo data, Michel Tinguely (PSI) for his assistance in data pre-processing and plotting, and Guenther Zaengl (University of Munich) for his recommendation regarding the parameter setting in MM5. NOAA AVHRR data have been provided by the Institute of Geography, University of Bern, Switzerland.. Air quality measurements of the Swiss monitoring network NABEL were taken by the Swiss Federal Laboratories for Materials Testing and Research (Empa) and made available by the Federal Office for the Environment (FOEN). The collaboration of PSI and WCAS was supported by FOEN and by the Interdisciplinary Tropospheric Research (INTROP) grant of the European Science Foundation (ESF).

5. REFERENCES

Andreani-Aksoyoglu S., Keller J., Alfarra R., Prevot A. S. H., Sloan J., Taghavi S., Nikzad S., He Z. 2007. Swiss-Canadian Research Project on Aerosol Modeling (SCRAM). *6th International Conference on Urban Air Quality (UAQ 2007), March 27-29, 2007*, Limassol (CYP), this conference.

COSMO 2002. *Newsletter No. 2*. Deutscher Wetterdienst, Offenbach (D).

Foppa N., Wunderle S., Hauser A., Oesch D., Kuchen F. 2004. Operational sub-pixel snow mapping over the Alps with NOAA-AVHRR data. *Annals of Glaciology* 38, 245-252.

PSU/NCAR 2005. PSU/NCAR Mesoscale Modeling System. Tutorial Class Notes and User's Guide: MM5 Modeling System Version 3.
http://www.mmm.ucar.edu/mm5/mm5v3/tutorial/presentations/tut-presentations.html.

Wanner H., Salvisberg E., Rickli R., Schüepp M. 1998. 50 years of Alpine Weather Statistics (AWS). *Meteorologische Zeitschrift, N.F.* 7, 99-111.

Proceedings of the 6th International Conference on Urban Air Quality
Limassol, Cyprus, 27-29 March 2007

REGIONAL AIR QUALITY MODEL SIMULATIONS FOR THE SWISS-CANADIAN RESEARCH ON AEROSOL MODELLING (SCRAM) PROJECT

J.J. Sloan[1], S. Taghavi[1], S. Nikzad[1], Z. He[1], Ş. Andreani-Aksoyoğlu[2], J. Keller[2], J. Brook[3]

[1]Waterloo Centre for Atmospheric Sciences (WCAS), University of Waterloo, Canada

[2]Laboratory of Atmospheric Chemistry (LAC), Paul Scherrer Institute, Switzerland

[3]Environment Canada, Air Quality Research Branch, Toronto, Canada

ABSTRACT

We compare the Community Multiscale Air Quality modelling system, including the Model of Aerosol Dynamics, Reaction, Ionization, and Dissolution (*CMAQ-MADRID*) with the Comprehensive Air Quality Model with Extensions (*CAMx*) in two very different applications: the relatively flat Great Lakes region of Southern Ontario and the Alpine terrain of Switzerland. Both models were driven by the same meteorology (generated by *MM5*) in each location. Three nested domains were used in each case. The Swiss study used resolutions of 27, 9 and 3 km to cover Europe, central Europe and Switzerland respectively. The resolutions in the Canadian study were 36, 12 and 4 km, covering eastern North America, the Great Lakes and Southern Ontario, respectively. The major differences between the models are in their gas/particle partitioning algorithms and in their treatment of organic particulate matter (PM) as well as anthropogenic and biogenic secondary organic aerosol (SOA). The major focus of the study is the ability of the models to simulate PM in the major urban areas and transportation routes.

1. INTRODUCTION

Understanding the sources and behaviour of particulate matter (PM) in the urban atmosphere has become increasingly important as its adverse health effects have become better understood (Carero et al., 2001). Regional and federal governments have responded to this perceived danger by increasing their measurements of PM and including these data in regularly published air quality indices (Ontario Ministry of the Environment, 2006). After analysis and policy discussions, such measurements are used to set lower targets on the desirable concentrations of PM (particularly $PM_{2.5}$, because of its adverse health effects). In order to meet these targets, it is necessary to know the sources of the PM and the relative amounts produced by each source. It is difficult to establish such source-receptor relationships with measurements alone, however, so it is customary to use models to assist in the assessment.

It is possible to infer source regions for identifiable episodes of poor air quality using Lagrangian methods, but these in general do not give information about the chemical transformations that occur during transport. Since chemistry plays a very important role in the concentration and identity of pollutants, it is necessary to employ a chemical transport model (CTM) if a quantitative description of the pollutant concentrations is required. This is particularly important – and difficult – for the case of PM because in this case the chemistry is both complex and poorly understood.

Under the terms of the SCRAM collaboration, we have begun to explore the sources, chemistry and transport of PM in two locations – Switzerland and the part of Southern Ontario that is surrounded by lakes Huron, Erie and Ontario. These domains have roughly the same area and their situations – continental locations with significant industrial activity nearby – are similar. The terrain, however, (and hence the meteorology) is dramatically different. Other differences, such as those in the emissions and land use, also affect the air quality, but compared to the geographical differences, these play a relatively smaller role. Extensive measurements of PM and other pollutants have been carried out in these regions respectively by the Laboratory for Atmospheric Chemistry (LAC) of the Paul Scherrer Institute in Switzerland and by the Air Quality Research Branch (AQRB) of Environment Canada in Ontario. The purpose of the SCRAM collaboration is to interpret and analyse these measurements using Eulerian CTM methods in order to determine the regional pollutant concentrations and elucidate the effects of the meteorology, terrain, emissions, etc. on their concentrations and regional distributions. The measurements in Switzerland were made during January and February 2006 in urban and motorway sites and those in Canada were made during comprehensive field campaigns in Ontario and Quebec during the summers of 2001 and 2006. Only data from the former are available at this time.

2. METHODS

The focus of the work is on the formation and chemistry of PM in the target domains, so CTMs having good capabilities for the simulation of PM were chosen for the work. The WCAS group used the *CMAQ-MADRID* 2004 Model (Pun, B. *et al.*, 2005; Zhang et al., 2004), which consists of the version of *MADRID* implemented within the October 2004 release (version 4.4) of the *SMOKE/CMAQ* modelling framework (Byun, D. W. and Ching, J. K. S, 1999). This CTM system uses a sectional treatment for simulating the formation and fate of PM in the atmosphere. It has gas-to-particle conversion for both inorganic and organic species, but neglects coagulation. It uses the *CB4* chemistry mechanism; the *ISORROPIA* model (Nenes, Pilinis, and Pandis, 1999) for thermodynamic equilibria of inorganic species; the reduced *MADRID 1a* SOA module and the *RADM* mechanism for cloud chemistry. The LAC group used *CAMx* (version 4.40) (Environ., 2006), which has the *ISORROPIA* and *SOAP* modules for aerosol modelling. Both groups used the *MM5* meteorological modelling system (PSU/NCAR, 2005) Version 3.7.2 (LAC) and Version 3.7.3 (WCAS).

The PM measurements in Ontario, with which the simulations will be compared, were made during two campaigns. The Study of the Health Effects of the Mix of Urban Air Pollutants (SHEMP) was carried out from February 2000 to August 2002 at the Gage Occupational and Environmental Health Unit of the University of Toronto, which is an urban site located in downtown Toronto. The Supersite Transboundary Intensive Field Study (STIFS) was carried out from June 2001 to January 2002 at the Gage site as well as three other locations: Egbert, a rural site 50 km south of Georgian Bay; Simcoe, a rural site 20 km north of Lake Erie and St Anicet, an urban site in Montreal Quebec. The data from both campaigns, which have been archived by (NARSTO, 2001), consist of measurements of total PM carbon, organic and inorganic ions.

3. RESULTS AND DISCUSSION

Two major influences affect the distribution of pollutants in Southern Ontario: long range (transboundary) transport and local emissions. Long range transport and the associated summertime climatology in Southern Ontario associated with high ozone episodes was identified some time ago (Heidorn and Yap, 1986; Mukammal E.I, 1982; Schichtel and Husar, 2001; Yap, Ning, and Dong, 1988) and similar conclusions have been drawn more recently for the long range transport of $PM_{2.5}$ (Brook et al., 2007). The typical synoptic meteorology associated with summertime transboundary O_3 and PM transport involves the passage of high pressure regions either through or south of Southern Ontario in a northwest to Southeast direction. The anticyclonic circulation around such systems draws air from the central and eastern US into Southern Ontario. Figure 1 shows our *MM5* calculation of the pressure and wind vectors associated with two high pressure systems, averaged for the five day period from 25 to 30 June 2001. The synoptic pattern consists of two high pressure regions and the associated trough between them. The leading one has passed into the Atlantic, to the lower right of the figure, while the trailing one, indicated by "H" in the figure, is over the southern part of James Bay. The southwest to northeast circulation in the trough between these high pressure regions draws contaminated air from the States south and west of the Great Lakes, resulting in elevated levels of ozone and PM in Southern Ontario. Simultaneously, towards the end of the episode, air flows from Ontario and Quebec into the New England States, causing similar effects on the air quality in those locations. Such episodes are very frequent during the summer months in this part of North America, causing significant transboundary pollutant flows. They are a major factor in the summertime background PM and ozone spatial distributions in this domain.

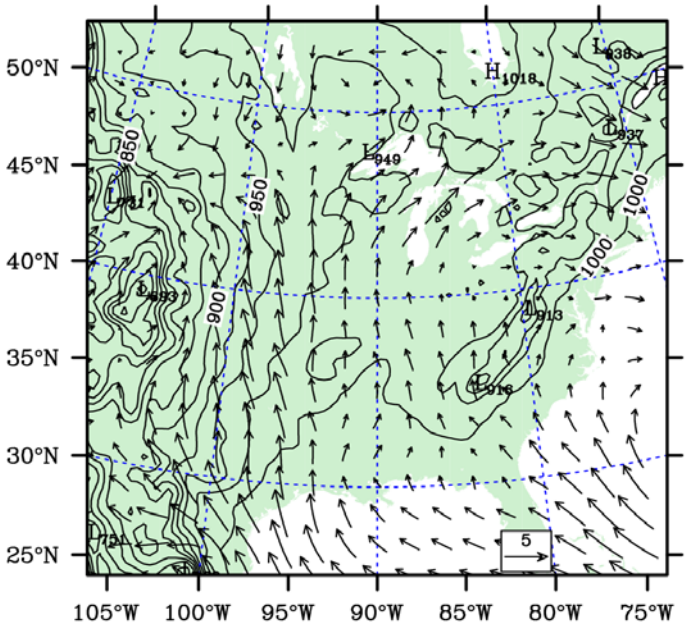

Figure 1: Meteorology for June 25-30, 2001, illustrating typical synoptic summer circulation

In the smaller (Southern Ontario) domain that is the focus of this study, the local emissions are dominated by vehicular traffic in the urban areas and various point sources including smelters (Hamilton), refineries and chemical plants (Sarnia) and coal fired power plants (Lambton and Nanticoke).

The mobile sources of $PM_{2.5}$ dominate the emissions strongly. Figure 2 shows the typical afternoon pattern of total $PM_{2.5}$ emissions for June 2001. The great majority of this is from mobile sources. The Greater Toronto Area (GTA, which has a population of about 5.4 million, coincides with the highly elevated $PM_{2.5}$ emissions on the north west shore of Lake Ontario. The majority of the remainder of the population of Southern Ontario (about 8 million) is in the strip around the western end of the lake, which also shows elevated $PM_{2.5}$ emissions.

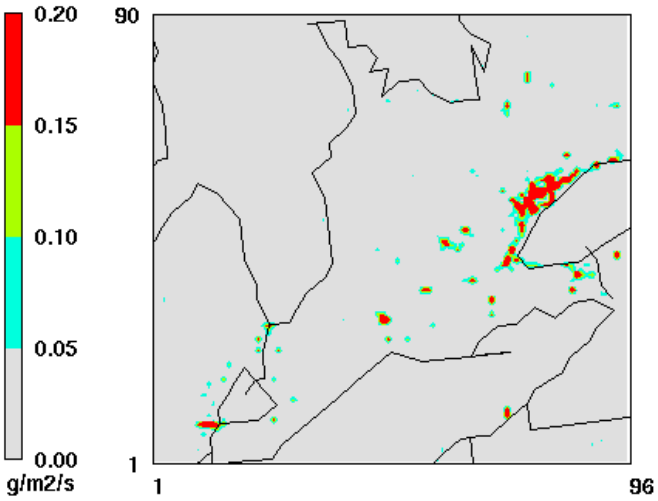

Figure 2. Typical afternoon pattern of total $PM_{2.5}$ emissions in Southern Ontario for June 2001.

We show the monthly average $PM_{2.5}$ concentrations in Figure 3. The total $PM_{2.5}$ concentrations are shown in Figure 3a and the contribution to these concentrations from the two power plants (3920 MW and 1975 MW; marked by "+" in Figure 3a), are shown in Figure 3b. Only the PM from the largest plant is visible at the scale of the figure. Its contribution to the total concentration is about two orders of magnitude less than the vehicle-dominated concentrations in the urban areas. Most of the $PM_{2.5}$ from the power plants are secondary sulfate aerosols and their spatial distribution illustrates again the predominantly southwest to northeast circulation typical of the summer in this region.

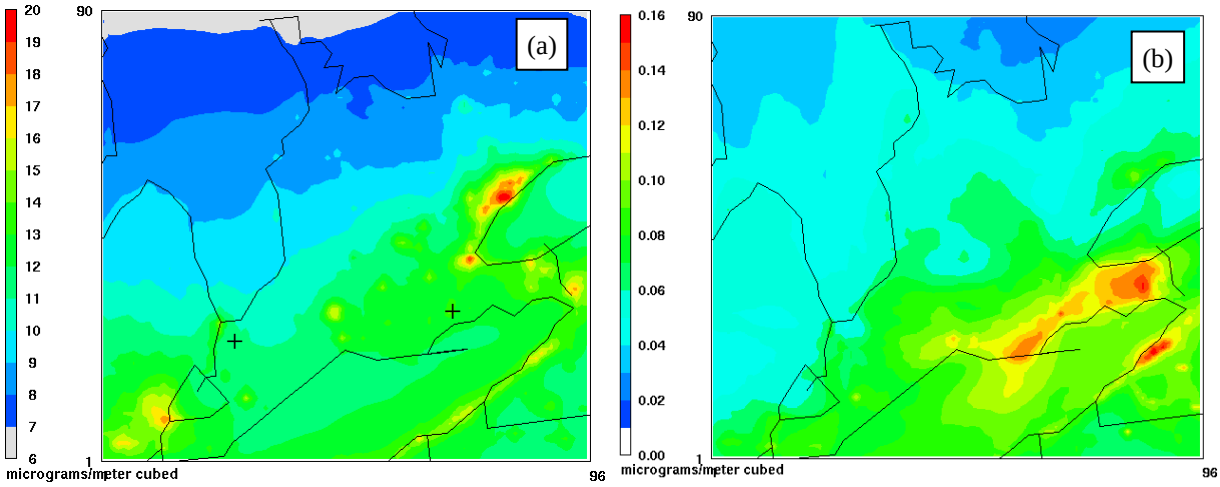

Figure 3. Spatially resolved hourly average $PM_{2.5}$ concentrations in Southern Ontario. (a) Total $PM_{2.5}$ concentrations. (b) Contribution from coal fired power plants.

4. CONCLUSIONS

We report results obtained under the SCRAM collaboration, which involves chemical transport modelling of air quality in Switzerland (winter) and Southern Ontario (summer) using the *MM5* meteorology model to drive both the *CAMx* and *SMOKE/CMAQ* models. This paper discusses preliminary simulations in Southern Ontario using the *SMOKE/CMAQ* system. It shows that the typical synoptic meteorology causes transboundary transport of pollutants from south west of the Great Lakes into Ontario and from Ontario and Quebec into New England. As a result of the former air flow, there are frequent high PM and ozone episodes in Southern Ontario during the summer months. The PM emissions in Southern Ontario are dominated by mobile sources in the urban areas. The maximum local concentration of $PM_{2.5}$ contributed by two coal fired power plants, is approximately two

orders of magnitude smaller than that from mobile sources. Most of the PM from the coal plants is secondary sulfate, which is formed by the oxidation of SO_2 and SO_3 to $SO_4^=$ and the subsequent hygroscopic growth of the nucleation mode particles as they move through regions of higher relative humidity. Further simulations with the *SMOKE/CMAQ* system, which are currently under way, will compare the details of the PM microphysics and heterogeneous chemistry using the *MADRID* model. Thereafter, the same calculations will be carried out for the Swiss domain.

5. ACKNOWLEDGEMENTS

The collaboration between PSI and WCAS was supported by the committee for Interdisciplinary Tropospheric Research: (INTROP) of the European Science Foundation (ESF). The WCAS is grateful for financial support from Ontario Power Generation Ltd and the Natural Sciences and Engineering Research Council of Canada.

6. REFERENCES

NARSTO, http://eosweb.larc.nasa.gov/PRODOCS/narsto/table_narsto.html, (2001)

PSU/NCAR Mesoscale Modelling System. Tutorial Class Notes and User's Guide: MM5 Modelling System Version 3, PSU/NCAR, http://www.mmm.ucar.edu/mm5/mm5v3.html, (2005)

Air Quality in Ontario, Ontario Ministry of the Environment, http://www.ene.gov.on.ca/envision/techdocs/index.htm#airquality, (2006)

Brook, J.R. et al., 2007. Regional Transport and Urban Contributions to Fine Particle Concentrations in Southeastern Canada. Journal of the Air & Waste Management Association 52, 855-866.

Byun, D. W. and Ching, J. K. S, Science Algorithms of the EPA Models-3 Community Multiscale Air Quality (CMAQ) Modelling System, Report EPA-600/R-99/030, Washington DC. U. S. Environmental Protection Agency, 1999.

Carero, A.D.P. et al., 2001. Genotoxic effects of carbon black particles, diesel exhaust particles, and urban air particulates and their extracts on a human alveolar epithelial cell line (A549) and a human monocytic cell line (THP-1). Environmental and Molecular Mutagenesis 37, 155-163.

Environ., User's Guide, Comprehensive Air Quality Model with Extensions (CAMx), Version 4.40, Report California Environ International Corporation, 2006.

Heidorn, K.C. and Yap, D., 1986. A Synoptic Climatology for Surface Ozone Concentrations in Southern Ontario, 1976-1981. Atmospheric Environment 20, 695-703.

Mukammal E.I, 1982. Meteorological conditions associated with ozone in Southwestern Ontario, Canada. Atmospheric Environment, 16, 2095-2106.

Nenes, A., Pilinis, C., and Pandis, S.N., 1999. Continued development and testing of a new thermodynamic aerosol module for urban and regional air quality models. Atmospheric Environment 33, 1553-1560.

Pun, B., Karamchandani, Prakash, Vijayaraghavan, K., Chen, S. Y., and Seigneur, C., Models-3/Community Multiscale Air Quality Model (CMAQ) User's Guide to Alternative Modules: Model of Aerosol Dynamics, Reaction, Ionization, and Dissolution (MADRID), Mercury (Hg), and Advanced Plume Treatment (APT), Report CP194-05-1, Atmospheric & Environmental Research, Inc., 2005.

Schichtel, B.A. and Husar, R.B., 2001. Eastern North American transport climatology during high- and low-ozone days. Atmospheric Environment 35, 1029-1038.

Yap, D., Ning, D.T., and Dong, W., 1988. An Assessment of Source Contributions to the Ozone Concentration in Southern Ontario 1979-1985. Atmospheric Environment 22, 1161-1168.

Zhang, Y. et al., 2004. Development and application of the model of aerosol dynamics, reaction, ionization, and dissolution (MADRID). Journal of Geophysical Research-Atmospheres 109,

Proceedings of the 6th International Conference on Urban Air Quality
Limassol, Cyprus, 27-29 March 2007

APPLICATION OF MESOSCALE METEOROLOGICAL MODEL ON AIR POLLUTION WARNING SYSTEM

Pornpan Uttamang[1], Surat Bualert[2] and Boonlert Archevarahaprok[3]

[1]Industrial Estate Authority of Thailand
[2]Chulalongkorn University, Thailand.
[3]Meteorological Department of Thailand.
[*]E-mail: Surat.B@chula.ac.th

ABSTRACT

The application of mesoscale meteorological model on air pollution warning system was performed on three nested domains with horizontal grid dimensions of 36, 12 and 4 km., respectively. The data were from the third domain only, which covers Bangkok metropolitan and Bangkok vicinity. This study was divided to three parts. Part A, the effects of land use on meteorological prediction. Part B, the comparison of atmospheric stability prediction between MM5 and met-preprocessor in dispersion model and Part C, application meteorological data on warning system. The comparisons between MM5 land use simulations and Bangkok land use patterns in 2001 show 60.7% of MM5 land use simulations was close to land use patterns of Bangkok and MM5 show urban area was less than land use patterns about 28.6%. The result of effects of land use on meteorological prediction (Part A) found that MM5 can predict temperature, wind speed, wind direction sensible heat and friction velocity at night close to observation data that used modified land use pattern. However, friction velocity at noon and atmospheric stability prediction from this case were different from observation. The comparison of atmospheric stability between model predictions and observation data found 30.2-55.1% of model prediction close to observation in stable condition. Part B, GAMMA-Met (a met-preprocessor in GAMMA) is used for this study. The comparison between MM5's forecasting and GAMMA-Met found MM5 show the best agreement to observation data. Thus MM5 was suitable to apply on air pollution warning system. However, there was error from the atmospheric stability prediction from MM5. Therefore, using the PBL height prediction for warning system with atmospheric stability prediction from MM5 will give a better result than using atmospheric stability prediction only. The atmospheric conditions that need to make a warning are stable condition, neutral condition and low PBL height.

Key words: MM5, Warning system, Atmospheric stability, PBL height, Land use

1. INTRODUCTION

Meteorological condition is the major factor for air pollution. The meteorological parameters such as wind speed, wind direction are the factor for diluting air pollutant in the atmosphere. If the atmosphere is suitable for dispersion process, the pollutant concentration will be low. The parameter that can be used as an indicator for atmosphere is atmospheric stability. Boundary layer theory used Monin-Obukhov length to categorize atmospheric stability which was more reliable than Pasquill-Gifford stability class. That relates to MM5 model which is Weather forecast model and can calculate Monin-Obukhov length. Therefore, the objective of the study are 1) application of MM5 on Bangkok, Thailand 2) development of air pollution warning system for Bangkok.

2. METHODOLOGY

1) Study area

(1) Chalumprakia meteorological station operates by Royal Thai meteorological department located in Bangkok. Land covers of Bang-Na station are green area, constructed area, water surface, and road around 17.33, 68.15, 9.7 and 4.82 percent of 1 km^2 nearby station, respectively.

(2) Dong-Mung meteorological station operates by Royal Thai meteorological department located in Bangkok. Dong-Mung was a international airport.

2) The Modeling System

Fifth-Generation Mesoscale Model (MM5) was used for forecasting meteorological conditions and atmospheric stability which was used to predict pollutant concentration and air pollution warning system. MM5 (Version 3) with two-way nesting calculation technique was divided study area (1,792 km^2) into three domains (Figure 1). The smallest and inner domain was 4 x 4 km^2. The domains were cover the area of Bangkok (central of the domain) and some parts of Nonthaburi , Phatumtanee, Chachangsol, Samutprakan, Samutsakorn provinces and gulf of Thailand. Land cover of the study area that was used for modeling system were USGS land cover data and land cover developed by Department of Land Development (Thailand) in year 2005.

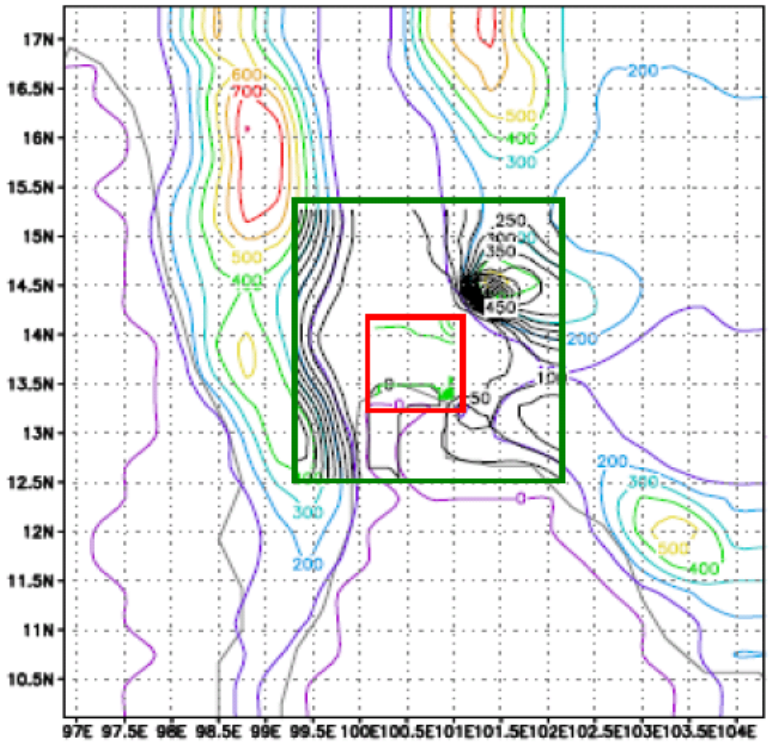

Figure 1. Domain and the study area

3) Measurement

The MM5's results were compared to meteorological measurement. Don-Mung and Chalumprakia meteorological stations (operated by Thai Meteorological Office) were used to measure meteorological condition. Furthermore, 3-D Sonic anemometer at 10m height was installed and collected wind component at the study area. The measurements were conducted on wet and dry seasons in 2004 (Table 1). Ambient air temperature, wind speed, wind direction and wind component were measured by using WMO standard equipments.

Table 1 Measurements periods

Stations	Season	
	Wet	Dry
Chalumprakia station	2-5 October 2004	22-25 December 2004
Don-Mung station	17-20 October 2004	27-30 December 2004

3. RESULT and DISCUSSION

Land cover data of MM5, Terrain (USGS data) and the data developed by Department of Land Development (Thailand) were used to forecast meteorological condition. The land cover data showed a difference on urban (increase around 28%) and agriculture area (decrease around 18%) (Table 2). MM5 showed a good agreement on surface meteorological parameters especially on the land cover data set which was developed in Thailand. Furthermore, sensible heat flux, Friction velocity and atmospheric stability (forecasted by MM5) were compared to the measurement. The forecasting of sensible heat flux showed a good relationship to the measurement (Figure 2) but MM5 showed over-forecasting on friction velocity (Figure 3). Comparison of atmospheric stability, MM5 showed fair agreement (30.3-55.1 %) to the measurement.

Table 2 Comparison of Land cover between Terrain data and Department of Land development (Thailand) on the study area.

Land Cover	Terrain data	Dept. of Land development	Difference (%)
Urban	15.2	43.8	+28.6
Dryland Crop. Past.	25.0	6.3	-18.8
Irrg. Crop. Past.	52.7	37.5	-15.2
Grassland	0.9	8.9	+8.0
Shrubland	2.7	0.9	-1.8
Mixed forest	0.9	0.0	-0.9
Bar. Sparse Veg.	2.7	2.7	0.0

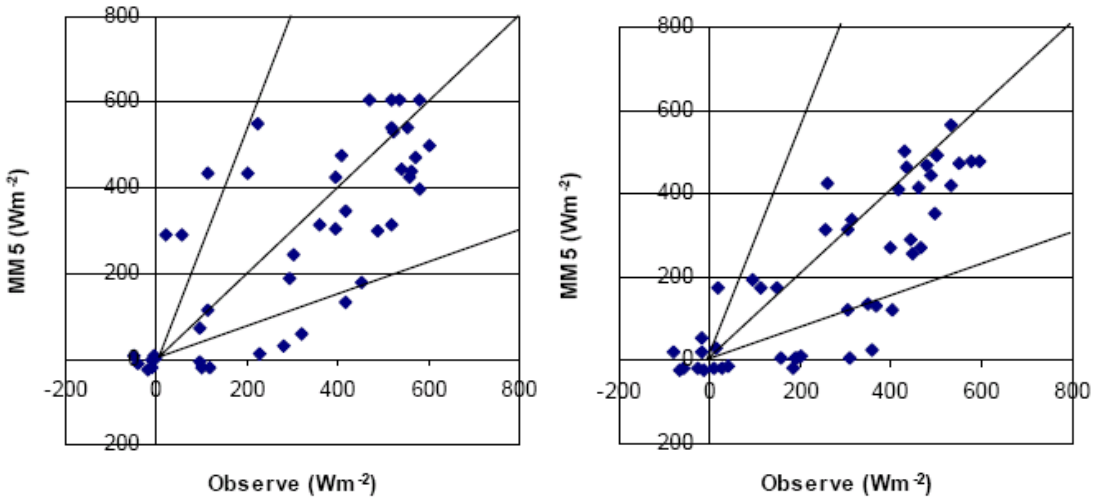

(a) wet season (b) dry season

Figure 2 Comparison of MM5's sensible heat flux forecasting and measurement

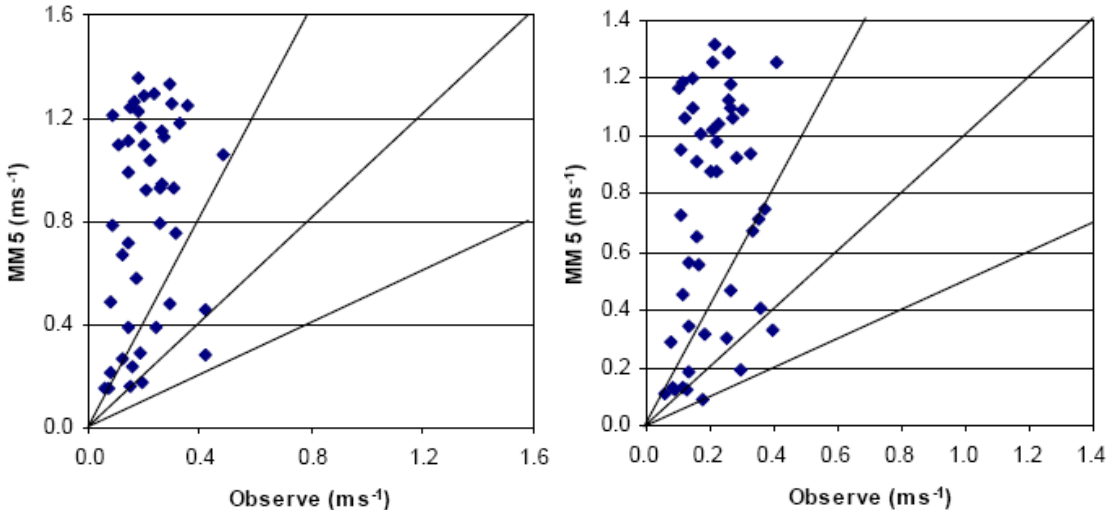

(a) wet season (b) dry season

Figure 3 Comparison of MM5's friction velocity forecasting and measurement

To develop air pollution warning system, atmospheric stability (Monin-Obukhov length) and Planet Boundary Layer (PBL) height were used as major factors to consider level of the warning. In principle, stable condition and low planet boundary layer are the critical condition of air pollution. As show in Figure 4, CO concentration nearby study area showed high concentration on stable condition and low plane boundary layer height.

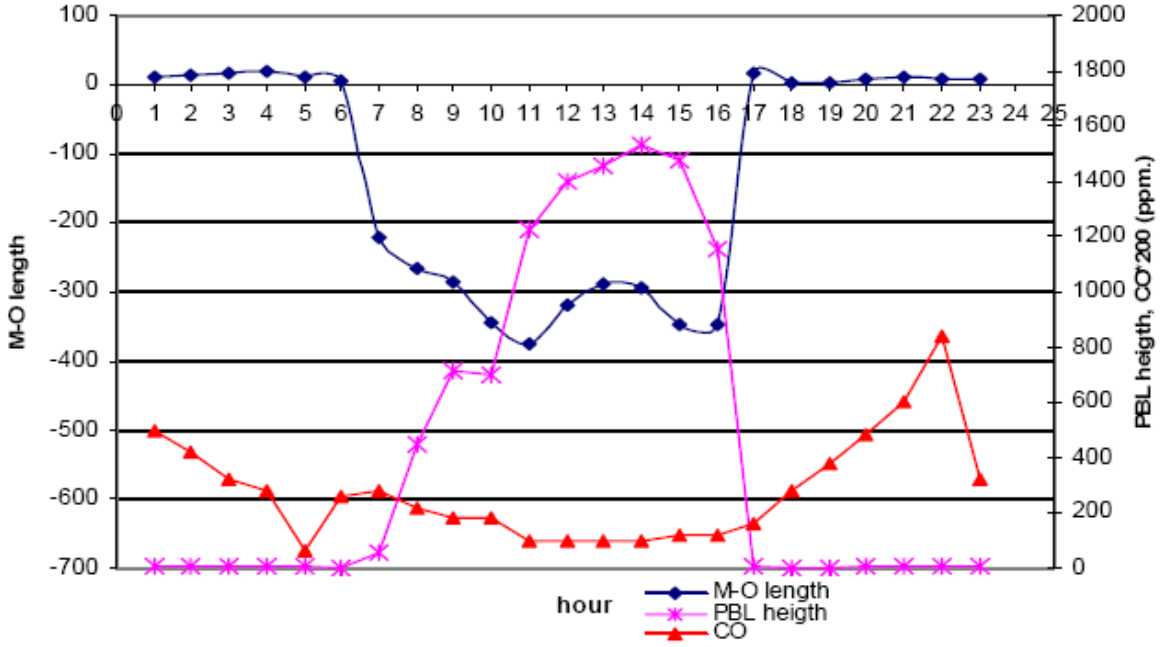

Figure 4 Application of MM5's forecasting on air pollution.

4. CONCLUSIONS

1) MM5 can be applied for weather forecasting in Bangkok, Thailand.
2) Land cover is a factor for the model forecasting.
3) Boundary layer parameters, Monin-Obukhov length and planet boundary layer are used for warning criteria.

5. ACKNOWLEDGEMENTS

The meteorological data was received from Meteorological Department of Thailand. Their assistance is gratefully acknowledged.

ANALYTICAL SOLUTIONS OF THE ADVECTION-DIFFUSION EQUATION FOR AREA SOURCES

Young-San Park[1] and Jong-Jin Baik[2,]*

[1]Climate Environment System Research Center, Seoul National University, Seoul, Korea
[2]School of Earth and Environmental Sciences, Seoul National University, Seoul, Korea

ABSTRACT

Advection-diffusion equation is solved analytically using the superposition method for a continuous ground-level finite area source. The wind speed, vertical eddy diffusivity, and standard deviation of a plume in the crosswind direction are assumed to vary by power laws. The concentrations of the diffused substance at surface increase along downwind direction inside source area and decrease rapidly behind the downwind edge. The concentrations are sensitive to exponents in power functions of wind speed and vertical eddy diffusivity inside source area, while to standard deviation of a plume in the crosswind direction downwind of source area. The solutions for finite area source are compared to those for infinite area and point sources, respectively. Their ratios along the plume centreline are greatly dependent on the crosswind diffusivity.

1. INTRODUCTION

The estimation of pollutants dispersion from area sources is useful in regulatory planning or risk assessment in urban areas or hazardous waste sites. The analytical solutions of the advection-diffusion equation are of fundamental importance since all the influencing parameters are expressed in mathematically closed form. Finite area sources can be treated as a continuum of point sources. Integration of solutions of a point source is very straightforward as long as the relevant integral formula is available.

Since the analytical solution for finite area source is not available, the analytical solutions for infinite area and point sources have been applied instead so far for the receptors near the source and far downwind from the source, respectively, on the basis of assumption that finite area can be treated as an area infinite in crosswind direction or point. The concentration for a finite area source is compared to those for infinite area and point sources, of which types of solutions are simpler.

2. METHODOLOGY

Advection-diffusion equation for which K-theory is applied is as follows

$$u\frac{\partial c}{\partial x}=\frac{\partial}{\partial y}\left(K_y\frac{\partial c}{\partial y}\right)+\frac{\partial}{\partial z}\left(K_z\frac{\partial c}{\partial z}\right) \tag{1}$$

The diffusion in the parallel direction to wind is neglected. The wind speed (u) and vertical eddy diffusivity (K_z) are assumed to vary with height by power laws, respectively; $u(z)=az^p$ and $K_z(z)= bz^n$ where the parameters a, b, m, and n depend on the atmospheric conditions and surface roughness. The lateral eddy diffusivity (K_y) is represented by the following expression (Huang, 1979);

$$K_y(x,z)=\frac{1}{2}u(z)\frac{d\sigma_y^2(x)}{dx} \tag{2}$$

where σ_y^2 is the mean square displacement along the crosswind direction of the flow.

The solution of Equation (1) for a ground-level point source (Yeh and Huang, 1975; Lin and Hildemann, 1996; Brown and Arya, 1997) is integrated for the ranges of finite source area which extends from $x=x_1$ to $x=x_2$ and from $y=y_1$ to $y=y_2$ in x and y directions, respectively as follows (Chrysikopoulos, et al., 1992),

$$\begin{aligned} c(x,y,z) &= \int_{x_1}^{x_2}\int_{y_1}^{y_2} c(x-x_s,y-y_s,z)\,dy_s\,dx_s \\ &= \int_{x_1}^{x_2}\int_{y_1}^{y_2} \frac{Q}{\sqrt{2\pi\left[\sigma_y^2(x)-\sigma_y^2(x_s)\right]}}\frac{\alpha}{a\Gamma(1-\nu)}\left(\frac{a}{b\alpha^2}\right)^{1-\nu}\frac{1}{(x-x_s)^{1-\nu}} \\ &\qquad \exp\left(-\frac{(y-y_s)^2}{2\left[\sigma_y^2(x)-\sigma_y^2(x_s)\right]}\right)\exp\left(-\frac{az^\alpha}{b\alpha^2(x-x_s)}\right)dy_s\,dx_s \end{aligned} \tag{3}$$

* Jong-Jin Baik; jjbaik@snu.ac.kr, +82-2-880-6990

where x_s and y_s are coordinates of a point source in x and y directions, Q is a source strength which is uniform inside source area, α =2+p-n, and ν =(1-n)/α . σ_y is assumed to vary as σ_y =Rx^r where R is a constant which depends on the atmospheric conditions. The exponent r is set to 0.5 in order to solve the integration analytically.

Using

$$\int x^{-a} erf\left(\frac{b}{\sqrt{x}}\right)dx = \frac{x^{-a}}{a-1}\left[-b\sqrt{\frac{x}{\pi}}\,\Gamma\left(a-\frac{1}{2},\frac{b^2}{x}\right)\left(\frac{b^2}{x}\right)^{\frac{1}{2}-a} - x\,erf\left(\frac{b}{\sqrt{x}}\right)\right], \tag{4}$$

the solution of integrations at ground level is

$$c(x,y,0) = \frac{Q\alpha}{2a\nu\Gamma(1-\nu)}\left(\frac{a}{b\alpha^2}\right)^{1-\nu}\left\{\left[f(x_1,y_1)-f(x_1,y_2)\right]-H(x_2,x)\left[f(x_2,y_1)-f(x_2,y_2)\right]\right\} \tag{5}$$

where

$$f(x_0,y_0) = \frac{1}{\sqrt{\pi}}\left(\frac{y-y_0}{R\sqrt{2}}\right)^{2\nu}\Gamma\left(\frac{1}{2}-\nu,\frac{(y-y_0)^2}{2R^2(x-x_0)}\right)+(x-x_0)^{\nu}\,erf\left(\frac{y-y_0}{R\sqrt{2(x-x_0)}}\right)$$

H(a,b) is the Heaviside step function, and for a>b, H(a,b)=0, otherwise H(a,b)=1. Γ is the gamma function and *erf* is the error function. When this superposition method is applied to the area source which is infinite in the lateral direction, the analytical solution is completely identical to that derived by using similarity theory by Lebedeff and Hameed (1975).

3. RESULT AND DISCUSSION

The solutions are mainly functions of the atmospheric parameters; ν and R (or σ_y) which are dependent on atmospheric condition. Three cases are calculated for a test and the values of parameters set for each case are shown in Table 1. The source area is set to a square with the length, L in one side. The concentrations of the diffused substance increase along downwind direction from the leading edge to the downwind edge inside source area squared and decrease rapidly behind the downwind edge. But their rates of change along distances depend on the magnitude of the parameters. For different ν values the concentrations normalized by source strength differ greatly inside source area but the differences are very small out of the source area (Fig. 1a). On the other hand, for different R values the concentrations differ relatively a little greater outside than inside source area (Fig. 1b).

Table1. Values of parameters for tests

a	p	b	n	ν
2	0.41	0.1	0.53	0.25
4	0.30	0.2	0.30	0.35
6	0.19	0.3	0.03	0.45

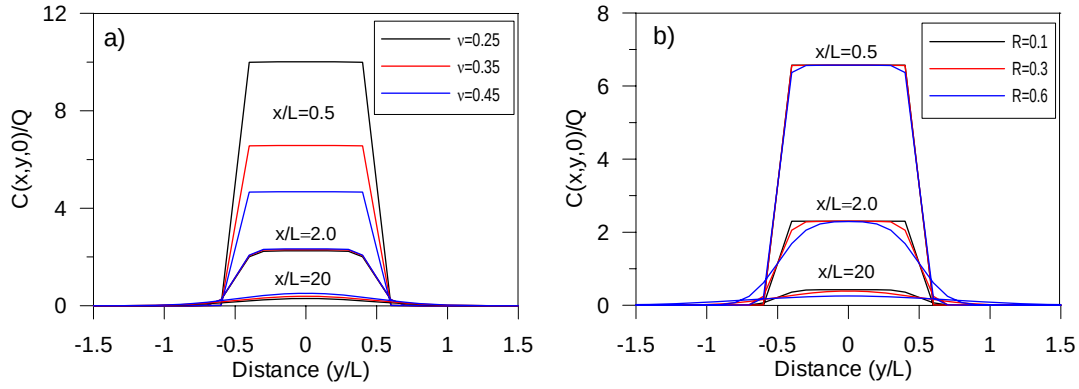

Figure 1. Normalized concentrations, C/Q at ground level along crosswind direction at 3 locations, x/L=0.5 (top 3 lines), 2 (middle 3 lines), and 20 (bottom 3 lines) for 3 values of a) ν (0.25, 0.35, and 0.45) with R fixed as R=0.3 and b) R (0.1, 0.3, and 0.6) with ν fixed as ν =0.35, respectively.

The concentrations along plume centreline for finite area source are compared to those from the analytical solutions for infinite area source for 6 ν values and 5 R values (Fig. 2). The ratios are one at the source area and decrease gradually further downwind. The changes of ratios along downwind distance are very sensitive to R values. The greater the R values, the greater the decrement of the ratio. But the variations of ratios have a unique line for different ν values.

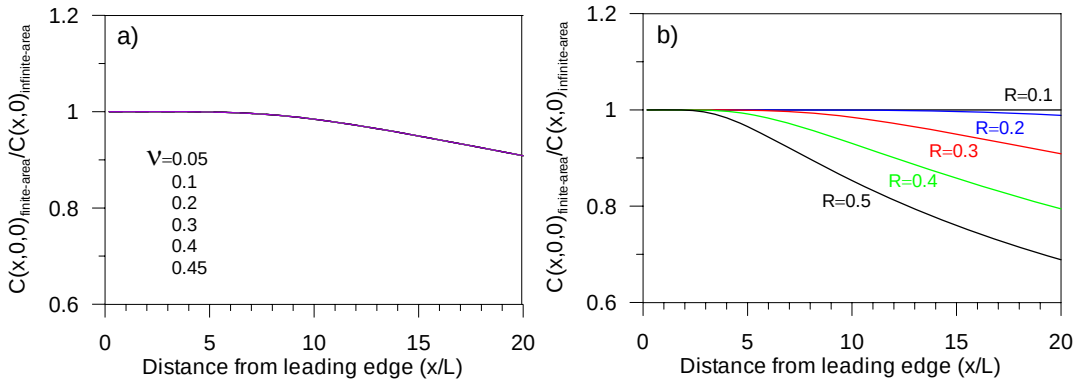

Figure 2. Ratios of concentrations at ground level along the plume centerline for the finite area source to those for the infinite area source with the width, L for the cases of a) 6 values of ν (0.05, 01, 0.2, 0.3, 0.4, and 0.45) with R fixed as R=0.3 and b) 5 values of R (0.1, 0.2, 0.3, 0.4, and 0.5) with ν fixed as ν =0.35, respectively.

The concentrations along plume centreline for finite area source are compared to those for a point source located on center of compared finite source area (Fig. 3). The ratios increase gradually behind downwind edge with distance approaching to one and are very sensitive to R values. The ratios are proportional to R values. But the ratios are irrelevant to ν values.

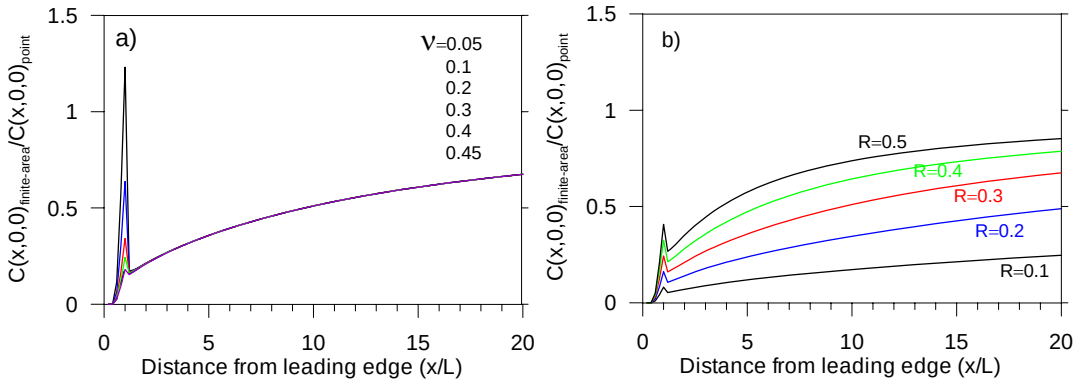

Figure 3. Same as Figure 2 except for the ratios for the point source located in the center of finite area source.

The analytical solutions for 3 types of source show a unique relation for atmospheric parameters (ν or, n and p) which are responsible for vertical diffusion. On the other hand, the relations between 3 types of solution are highly sensitive for the parameters (σ_y) which are responsible for lateral diffusion. Therefore, when the concentration of diffused substance from the finite area source is substituted by the solutions for infinite area or point source, of which types of solutions are much simpler, the atmospheric conditions and locations of the receptor should be considered.

4. ACKNOWLEDGEMENTS

This work was funded by the Korea Meteorological Administration Research and Development Program under Grant CATER 2006-2202.

5. REFERENCES

Brown, M. J., Arya, S. P., Snyder. W. H. 1997. Plume descriptors derived from a non-Gaussian concentration model. Atmos. Environ. 31, 183-189.

Chrysikopoulos, C. V., Hildemann, L. M., Roberts, P. V. 1992. A 3-dimensional steady-state atmospheric dispersion deposition model for emissions from a ground-level area source. Atmos. Environ. 26, 747-757.

Huang, C. H. 1979. Theory of dispersion in turbulent shear-flow. Atmos. Environ. 13, 453-463.

Lebedeff, S. A., Hameed, S. 1975. Steady-state solution of the semi-empirical diffusion equation for area sources. J. Appli. Meteo. 14, 546-549.

Lin, J. S., Hildemann, L. M. 1996. Analytical solutions of the atmospheric diffusion equation with multiple sources and height-dependent wind speed and eddy diffusivities. Atmos. Environ. 30, 239-254.

Yeh, G. T., Huang, C. H. 1975. Three-dimensional air pollutant modeling in the lower atmosphere. Bound.-Layer Meteor. 9, 381-390.

Proceedings of the 6th International Conference on Urban Air Quality
Limassol, Cyprus, 27-29 March 2007

MODELLING PASSIVE TRACER TRANSPORT TO THE HIGH ALPINE SITE JUNGFRAUJOCH

D. Folini[1], S. Ubl[1], P. Kaufmann[2]

1) Air Pollution and Environmental Technology, Swiss Federal Laboratories for Materials Testing and Research (Empa), Dübendorf, Switzerland

2) Federal Office of Meteorology and Climatology MeteoSwiss, Zürich, Switzerland

ABSTRACT

The Swiss high Alpine measurement station Jungfraujoch (3580 m asl) is ideally located to monitor a significant part of central European air pollutant emissions. Although close to major European emission sources, it is often reached by clean background air. To better interpret measured concentrations we determine their potential source regions by means of a backward Lagrangian particle dispersion model (LPDM). Originally from the German Weather Service (DWD), we use the LPDM with wind fields from the numerical weather prediction model COSMO of MeteoSwiss (grid spacing 7km x 7km). We present first results of a sensitivity study of our LPDM, applied to the site of Jungfraujoch. The receptor height above model ground is found to be a particularly sensitive parameter. Comparing measured and modelled CO over an eight day period in late October 2004 indicates better results for lower receptor heights, close to the model ground.

1. INTRODUCTION

The Swiss high Alpine measurement station Jungfraujoch (46° 33'N, 7° 59`E, 3580 m above sea level) is ideally located to monitor a significant part of central European air pollutant emissions. On the one hand, the station is remote enough (high elevation and only sparse settlements within at least 25 km radius) to be often reached by clean background air (Baltensperger et al. 1997; Lugauer et al. 2000). On the other hand, Jungfraujoch is close to major European emission sources, like the highly industrialized Po-valley in northern Italy, parts of the Rhone-valley in south-east France, or the Rhur-valley in the west of Germany. Occasionally, the station is reached by polluted boundary layer air from these regions, thus is able to monitor corresponding emissions. The station is a global site in the global atmosphere watch (GAW) program.

The complex surrounding topography of Jungfraujoch makes the interpretation of these measurement data particularly demanding. Meteorological transport processes on large and small scales need to be taken into account. On the local scale, a thermally induced diurnal cycle is often observed on fair weather days in late spring and summer. The cycle peaks around 6 pm local time and is observed, for example, in aerosol data (Baltensperger et al. 1997). On the synoptic scale, föhn episodes play an import role. Zellweger et al. (2003) observe highest NO_y mixing ratios during south föhn events. According to the same authors, föhn events at Jungfraujoch are about twice as frequent in spring/summer than in autumn/winter, while synoptic lifting (e.g. due to fronts) shows no such seasonal dependence. Finally, pronounced long-range, intercontinental transport events are occasionally registered at Jungfraujoch as well. Over the course of summer 2000, Guerova et al. (2006) identify 9 major episodes of transatlantic transport of O_3 to the Jungfraujoch.

Our ultimate goal is the use of long time-series of Jungfraujoch measurement data to investigate changing European emission patterns of long-lived trace gases. This requires that we are able to interpret several years of measurement data (in contrast to short-duration case studies) at hourly or daily resolution (in contrast to monthly mean values). First steps in this direction were already taken by Reimann et al. (2004) who used trajectory statistics (Seibert et al. 1994) to identify potential emission regions of various hydrochlorofluorocarbons (HCFCs) for the years 2002 to 2004. These trajectory statistics we now want to replace by a Lagrangian particle dispersion model (LPDM) which we run in receptor oriented mode. The long time-series we aim at exclude fine tuning of the LPDM and encourage the use of operationally available wind field data. In the present paper we investigate how well, given the constraints just mentioned, we can reproduce measured CO concentrations at Jungfraujoch during an eight day period in late October 2004.

High quality, operationally available wind-fields for Jungfraujoch are the analyzed wind fields from the numerical weather prediction model COSMO of MeteoSwiss. They are available for each hour, on a 7 km x 7 km grid, with 45 vertical levels reaching up to 20 hPa. As LPDM we use, for consistency reasons, the LM-LPDM which is in operational use at the MeteoSwiss and German weather service (DWD) in case of a nuclear accident emergency. For relatively flat terrain, the performance of this model has been ascertained by the DWD (Glaab et al. 1998). In the present paper, we focus on the application of the model to the high Alpine site of Jungfraujoch and, in particular, on its sensitivity to the receptor height above model ground.

2. METHOD: BACKWARD LPDM

The basic features of the LM-LPDM are given in Glaab et al. (1998), along with an evaluation against the European Tracer Experiment (ETEX) measurements. Here we restrict ourselves to a few important aspects and differences between the LM-LPDM we use and the model as it is described in Glaab et al. (1998). As we are interested in the interpretation of measurement data from one particular site, we run the LM-LPDM in backward or receptor-oriented mode (Seibert and Frank 2004; Stohl et al. 2005). A number N of particles are released over a certain time interval Δt_r at the geographical position of Jungfraujoch. The particles are then followed backward in time, tracing the path the air parcels have taken before their arrival at the station. The position X_n of each particle trajectory in 3d space is given by

$$X_n(t+\Delta t) = X_n(t) + V_n(t)\,\Delta t$$
$$V_n(t) = \overline{V}_n(t) + V'_n(t)$$

where Δt is the time increment (negative for backward simulations). The velocity vector V_n is composed of the mean wind field $\overline{V}_n$ (from COSMO) and the turbulent velocity V'_n. To compute the latter we solve the Langevin diffusion equation with a slightly different Markovian chain formulation than Glaab et al. (1998). For the vertical diffusion w' we use the well-mixed formulation given by Wilson et al. (1993) for stationary inhomogeneous Gaussian turbulence. For the horizontal diffusion u' and v' we use the cheaper but not strictly well-mixed formulation by Legg and Raupach (1982). This is justified as Uliasz (1994) showed that lateral dispersion in mesoscale is caused mostly by vertical mixing combined with wind shear while the horizontal turbulent velocities have little effect. The update formulae for the turbulent velocity fluctuations thus read

$$u'_n(t) = R_{u,n}\,u'_n + (1-R_{u,n}^2)^{1/2}\,\sigma_{u,n}\,\lambda$$
$$v'_n(t) = R_{v,n}\,v'_n + (1-R_{v,n}^2)^{1/2}\,\sigma_{v,n}\,\lambda$$
$$w'_n(t) = R_{w,n}\,w'_n + (1-R_{w,n}^2)^{1/2}\,\sigma_{w,n}\,\lambda + \frac{\Delta t}{|\Delta t|}\,T_{Lw,n} + 0.5\,(1-R_{w,n})\left(1+\frac{w'^2}{\sigma_{w,n}^2}\right)\frac{\partial \sigma_{w,n}^2}{\partial z}$$

All quantities on the right hand side are taken at time t-Δt. The correlation functions $R_{*,n}$ are computed as $R_{*,n} = \exp(-|\Delta t| / T_{L*,n})$, with * = u,v,w and $T_{L*,n}$ the corresponding Lagrangian time scales. σ is the standard deviation of the turbulent velocities, λ a random number out of a normalized Gaussian distribution. The parameterizations of σ and $T_{L*,n}$ are consistent with those in COSMO. Details can be found in Glaab et al. (1998), from where it can also be taken that $\sigma_{u,n} = \sigma_{v,n}$ and $T_{Lu,n} = T_{Lv,n}$.

The output of the LM-LPDM consists of a 3d residence time field. It gives the time which the particles (the air mass measured at the receptor) spent in a particular grid box of our 3d computational domain. From this 3d data a 2d residence time map is obtained by summing over the lowest lying 500 m above model ground. Summing further also over this 2d map yields the total, integrated residence time within the 500 m sampling layer. It gives the total time the air spent during the back-tracking time within the 500 m. An upper limit to this total residence time is the total tracking time of the particles. Reaching this upper limit would imply that the measured air, before reaching the measurement site, resided exclusively within the lowest lying 500 m above ground during the entire back tracking time.

The input data for the LM-LPDM may be grossly divided into two parts, the wind field data and a set of input parameters governing the details of the particle release and tracking. As wind fields we take analysed wind fields from COSMO, the operational weather prediction model of MeteoSwiss. COSMO is a non-hydrostatic, fully compressible, limited-area model. A generalized terrain-following vertical coordinate system with hybrid sigma-pressure levels is used. The model domain extends roughly from Ireland to eastern Poland and from Denmark to Sicily. Lateral boundary values are taken from the ECMWF model. The development of COSMO takes place within the frame of the Consortium for Small-Scale Modelling, COSMO, http://www.cosmo-model.org, where more information may be obtained. In our LPDM we use wind fields with a time spacing of 3 hours. Other input parameters concern mostly the particle release and sampling. Within the frame of this work we use 25000 particles for each 3 hour release interval. We trace the particles backward in time for 60 hours. As sampling height for the 2d residence time map we take the above mentioned 500 m. We use receptor heights of 80 m and 400 m above model ground (see Section 3). The vertical and horizontal time steps are 1s and 300 s respectively.

3. RESULTS

The results we present here are part of a larger sensitivity study we are currently working on. From this larger study we take that the receptor height above model ground is a most sensitive input parameters for our backward LM-LPDM simulations at Jungfraujoch. While Jungfraujoch is located at 3580 m asl in reality, its height is only about 2720 m asl within the frame of our model topography. The four closest lying grid points of our 7 km x 7 km mesh reflect the complex topography in that their height varies by several hundred meters: 2416 m, 2616 m, 3085 m, and 2416 m.

For the period from October 26, 2004, 12:00 UTC, to November 3, 2004, 12:00 UTC we have computed 64 residence time maps for two different receptor heights, 80 m and 400 m above model ground. During this period, Jungfraujoch received air mainly from southern directions, especially the Po-valley in northern Italy. Each of the computed residence time maps covers a 3h sampling interval at Jungfraujoch. The maps we multiplied with the gridded EMEP CO inventory for the year 2003 to obtain modelled CO concentrations for Jungfraujoch (http://www.emep.int). Plotting the modelled CO concentrations for the two different receptor heights against each other reveals, Figure 1, that the CO concentration are generally lower for the higher receptor height.

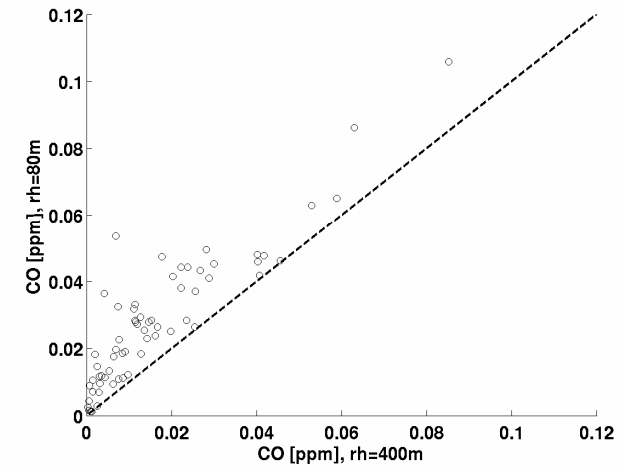

Figure 1. Modelled CO (EMEP multiplied with residence time maps, no CO background) for receptor heights of 400 m (x direction) and 80 m (y direction). For the time period considered, a larger receptor height results in a clearly smaller CO concentration.

To compare modelled and measured CO concentrations, we subtracted from the latter an estimated (based on the measured data) CO background concentration of 0.083 ppm. The corresponding CO time series are shown in Figure 2: modelled CO for 80 m (dashed black) and 400 m receptor height (dotted grey), as well as measured CO, interpolated onto the 3h intervals of our residence time maps (solid black). Measured and modelled concentrations appear to match better for 80 m receptor height than for 400 m. As can be seen, modelled concentrations can both exceed (at the beginning and end of the considered period) or underestimate measured values. The model values using 80 m receptor height appear to reproduce measured values

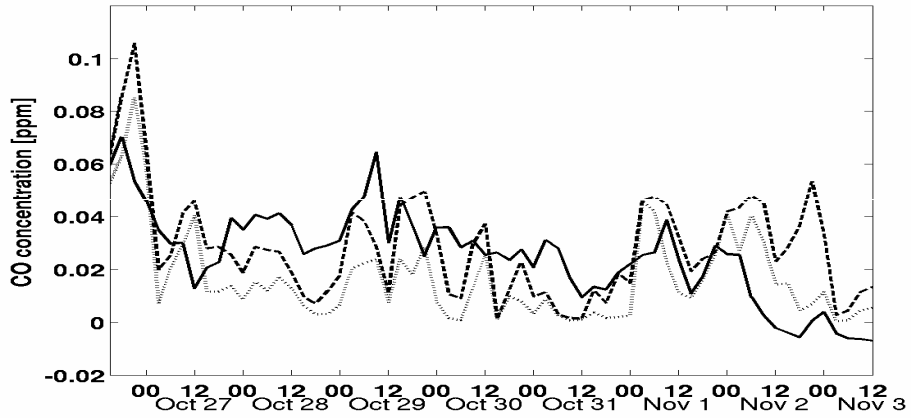

Figure 2. CO concentration (background subtracted) at Jungfraujoch in October 2004, measured (solid black) and modelled with receptor heights 80 m (dashed black) and 400 m (dotted grey) above model ground. For details see text.

generally somewhat better than the 400 m receptor height values. Time averages of the concentrations in Figure 2 indeed agree better for the 80 m data (12% larger average than the measured data) than for the 400 m data (33% smaller average than measured data). Of the 80 m data, 36% deviate by more than 50% from measured concentrations. For the 400 m data this Figure is 60%. Correlations, on the other hand, are comparable: r = 0.42 and 0.46 for the 80 m and 400 m data respectively.

4. SUMMARY AND CONCLUSIONS

We presented LPDM simulations for the high Alpine site Jungfraujoch, using numerical wind fields from the numerical weather prediction model COSMO of MeteoSwiss (grid spacing 7 km x 7 km). We focused on the impact of the receptor height above model ground as the height of Jungfraujoch strongly differs considerably between reality (3580 m asl) and model (2720 m asl). Two sets of model data (80 m and 400 m receptor height) were compared with measured CO concentrations. Time averages of modelled and measured concentrations agree better for the lower receptor height. Correlations between modelled and measured data are, on the other hand, essentially the same for both receptor heights. While further comparison between model and reality (longer time series, other seasons) are certainly imperative these first results indicate that our LPDM is generally capable of reproducing transport processes to Jungfraujoch reasonably well.

5. ACKNOWLEDGEMENTS

We acknowledge computational resources for this project, on a NEC SX5, granted by the Swiss Center for Scientific Computing SCSC / CSCS, Manno, Switzerland.

6. REFERENCES

Baltensperger, U., Gäggeler, H. W., Jost, D. T., Lugauer, M., Schwikowski, M., Weingartner, E., and Seibert, P. 1997. Aerosol climatology at the high-alpine site Jungfraujoch, Switzerland. JGR 102, 19707-19716.

Glaab, H., Fey, B., and Jacobsen, I. 1998. Evaluation of the emergency dispersion model at the Deutscher Wetterdienst using ETEX data. Atmos. Env. 32, 4359-4366.

Guerova, G., Bey, I., Atti, J. L., Martin, R. V., Cui, J., and Sprenger, M. 2006. Impact of transatlantic transport episodes on summertime ozone in Europe. ACP 6, 2057-2072.

Legg, B. J. and Raupach, M. R. 1982. Markov-chain simulation of particle dispersion in inhomogeneous flows: The mean drift velocity induced by a gradient in Eulerian velocity variance. Boundary Layer Meteorology 24, 3-13.

Lugauer, M., Baltensperger, U., Furger, M., Gäggeler, H. W., Jost, D. T., Nyeki, S., and Schwikowski, M. 2000. Influences of vertical transport and scavenging on aerosol particle surface area and radon decay product concentrations at the Jungfraujoch (3454 m above sea level). JGR 105, 19869-19880.

Reimann, S., Schaub, D., Stemmler, K., Folini, D., Hill, M., Hofer, P., Buchmann, B., Simmonds, P. G., Greally, B. R., and O'Doherty, S. 2004. Halogenated greenhouse gases at the Swiss High Alpine Site of Jungfraujoch (3580 m asl): Continuous measurements and their use for regional European source allocation. JGR 109, 5307-5318.

Seibert, P., Kromp-Kolb, H., Baltensperger, U., Jost, D. T., Schwikowski, M., Kasper, A., and Puxbaum, H. 1994. Trajectory analysis of aerosol measurements at high alpine sites. Transport and Transformation of Pollutants in the Troposphere, Borrell, P. et al. (ed).

Seibert, P. and Frank, A. 2004. Source-receptor matrix calculation with a Lagrangian particle dispersion model in backward mode. ACP 4, 51-63.

Stohl, A., Forster, C., Frank, A., Seibert, P. , and Wotawa, G. 2005. Technical note: The Lagrangian particle dispersion model FLEXPART version 6.2. ACP 5, 2461-2474.

Uliasz, M. 1994. Lagrangian particle modeling in mesoscale applications. Environmental Modeling II, Computational Mechanics Publications, Zannetti, P. (ed).

Wilson, J. D., Legg, B. J., and Thomson, D. J. 1983. Calculation of particle trajectories in the presence of a gradient in turbulent-velocity variance. Boundary Layer Meteorology 27, 163-169.

Zellweger, C., Forrer, J., Hofer, P., Nyeki, S., Schwarzenbach, B., Weingartner, E., Ammann, M., and Baltensperger, U. 2003. Partitioning of reactive nitrogen (NO_y) and dependence on meteorological conditions in the lower free troposphere. ACP 3, 779-796.

SEA-SALT AEROSOLS (SSA): IMPACT ON ATMOSPHERIC POLLUTION OF THE ATTICA PENINSULA, GREECE

Eleni Athanasopoulou[a], Maria Tombrou[a], Spyros Pandis[b] and Armistead G. Russell[c]

[a] National and Kapodistrian University of Athens, Faculty of Physics, Dep. of Applied Physics, Lab. of Meteorology, Athens, Greece
[b] Department of Chemical Engineering, University of Patras, 26500 Patra, Greece
[c] School of Civil and Environmental Engineering, Georgia Institute of Technology, 311 Ferst Drive NW, Atlanta, GA 30332-0512, USA

ABSTRACT

In the present study, we examine the ability of SSA to enhance predicted aerosol concentrations at marine-affected locations in Athens (Attica peninsula, Greece). An SSA emissions algorithm is developed and linked to the CAMx model (Environ, 2004). Gas/particle mass transfer is dynamically calculated for the coarse mass, which leads to a quadrupling of aerosol NO_3^- at the city center from representing reactions involving NO_3^- and NaCl. Simulations reveal that the sea-salt component of aerosol concentrations is important all over Attica during the selected event and reaches 30% at the city center. NO_3^- seems to show the greatest influence from the sea salt production mechanisms compared to SO_4^{2-} and NH_4^+. In addition, 95% of the NO_3^- is due to the chemistry involving its precursor's reaction with Na^+, which is enhanced in areas where Na^+ is in excess after neutralizing SO_4^{2-}.

1. INTRODUCTION

Sea salt aerosol (SSA) participates in atmospheric chemistry by interacting with atmospheric pollutants, particularly in urban environments. Specifically, addition of NaCl to an urban aerosol leads to its reaction with HNO_3, resulting in more NO_3^- ($NaNO_3$), as well as to the production of Na_2SO_4. These reactions mainly produce coarse aerosol and lead to a Cl^- "deficit" in aerosol mass (Seinfeld and Pandis, 1998). SSA primarily affects coastal environments but its role becomes important inland during sea breeze conditions, which contribute to the stagnation of local pollution and carry NO_3^- and SO_4^{2-} laden air mass.

For the reasons articulated above, an SSA emissions algorithm is developed and implemented in the Eulerian, aerosol model CAMx (Environ, 2004). The main area of interest is Athens (Attica peninsula, Greece), which is surrounded by three harbors, an airport and many industrial sources and is one of the most polluted European cities. The main goal of this study is to examine the ability of SSA to enhance the predicted aerosol concentrations in marine-affected locations in the Athens basin. The selected event for application involves a sea-breeze period surrounding the Attica peninsula, allowing for the examination of the air-sea chemical interactions, together with the direct participation of SSA in aerosol mass.

2. METHODOLOGY

In order to assess the role of SSA production on aerosol concentrations, two simulations are performed over a domain centred on the Attica peninsula using a 2 km horizontal resolution (Figure 1). The SSA emissions are applied in the one simulation, thus differences in aerosol concentrations predicted by the two simulations reflect their role in aerosol formation over the Athens basin.

Meteorological fields used in CAMx are produced by the fifth generation Penn State/NCAR Mesoscale Model, MM5 (Anthes and Warner, 1978). The modeling system is applied for a summer synoptic condition characterized by a relatively weak synoptic wind flow that favors the development of sea-breeze circulation (S-SW flow) over the Athens basin event (24 June, 1998). The local S-SW flow starts developing at 0900LST over land and at 1200LST over the Saronic Gulf, is fully developed during the afternoon hours (Figure 1) and starts weakening around 2100LST.

The anthropogenic and biogenic emission fields used in simulations cover most gaseous and aerosol species emitted from area and point sources. A comprehensive SSA emission parameterization is applied over the sea surface (~50% of the total surface). The algorithm combines two open-ocean source functions (Gong, 2003; Clarke et al., 2006) and the surf-produced aerosols are calculated by De Leeuw et al. (2000). These equations calculate the number flux density of droplet generation as a unique function of wind speed at 10m above sea level and at a specific ambient relative humidity. The algorithm incorporates correction factors proposed by Zhang et al. (2005a, 2005b) and Lewis and Schwartz (2005) that relate the size of SSA to the local relative humidity and

salinity. The translation of number to mass fluxes depends on particle density and solute weight fraction, as defined by Zhang et al. (2005a). The chemical composition of seawater can satisfactorily be applied in the simulations (Seinfeld and Pandis, 1998; Lewis and Schwartz, 2004). Figure 1 shows the spatial distribution of aerosol emissions and point sources in the nested domain.

Regarding boundary conditions, the 'nesting' technique reduces the uncertainty in model predictions caused by the uncertain boundary conditions. In our case, the domain of Attica peninsula is nested in a domain over Greece Additionally, simulations include a 3-day 'start-up' period to minimize the role of the applied initial concentrations.

CAMx incorporates the ISORROPIA module (Nenes et al., 1998) to calculate gas/particle partitioning for inorganic aerosol constituents The mass transfer between gas and aerosol phases is calculated by using the hybrid approach (Capaldo et al., 2000), which assumes instantaneous equilibrium between gases and fine aerosols (equilibrium approach) and solves the mass transfer rate equations for the coarse mass (dynamic approach). The reason for such a consideration is that small particles achieve equilibrium with the gas phase within a few minutes, while mass transfer rates are more limiting and vary for larger particles, involving NO_3^- and NaCl. 2.5μm was chosen as the threshold diameter between the two approaches, in order to achieve both speed and accuracy during simulations (Capaldo et al., 2000; Koo et al., 2003).

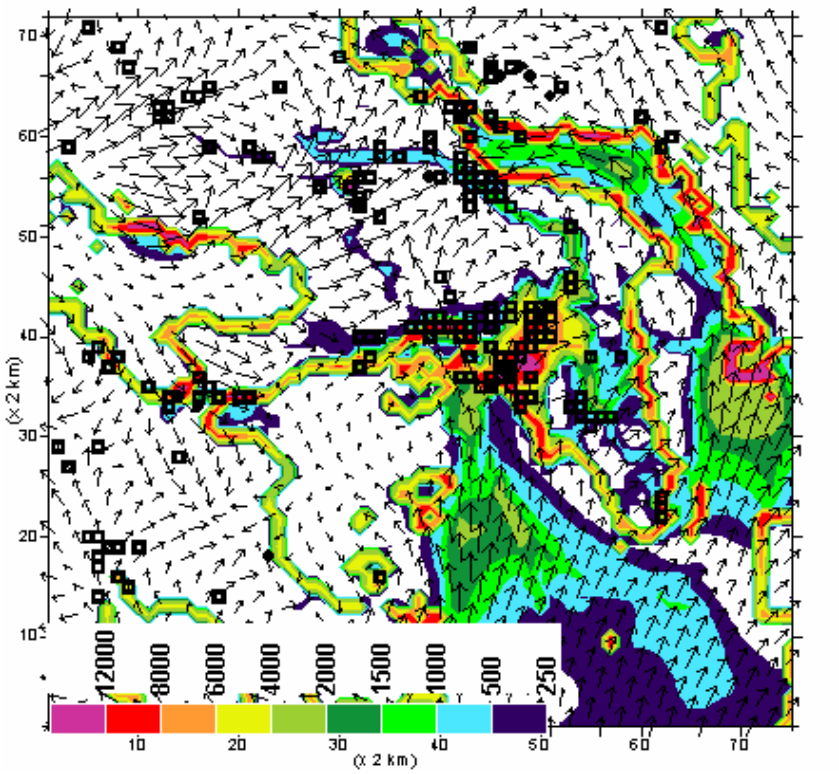

Figure 1. Nested application domain. Also shown: the wind field, point sources and the aerosol emission rates (g hr $^{-1}$cell $^{-1}$) at 1800LST (24 June, 1998).

3. RESULTS AND DISCUSSION

Simulations reveal that the sea-salt component of aerosol concentrations is important all over Attica during the selected event. The greatest influence of SSA production at the Athens basin is observed during 1800LST (figure 2a) for the reason described in the previous section. SSA is the 30% of the total aerosol concentration in the city center, and is up to 20% even at very distant areas from the coast. Over the sea surface, SSA remains above 30% and it can even rise to 90% of the total aerosol concentration, depending on the wind field and the SSA emissions (Figure 1).

Analysing the daily average concentrations of SSA at the city center, it is found that the sea salt ions (Na^+, Cl^-, Mg^+ etc.) reach about 68%. SO_4^{2-} reaches 13%, but this value is shaped by both primary SO_4^{2-} emitted from the sea (60%) and secondary Na_2SO_4 production. The latter is more important in areas with high SO_2 emissions, namely where the point sources are located (Figure 1). The NO_3^- mass that is generated by the SSA influence reaches 17% of the inorganic aerosol mass at the city center, while NH_4^+ production is slightly affected by the sea (2%).

Since NO_3^- seems to show the greatest influence from the sea production mechanisms compared to the other secondary inorganic ions, it is further investigated. The concentration predictions shown in figure 2b are satisfactory compared to measurements (Scheff and Valiozis, 1990; Eleftheriadis et al., 1998a, b; Torfs and Grieken, 1997). It should be noted here that the scenario without the SSA emissions results in trivial amounts of NO_3^- mass production over the whole domain (5% of the current predictions). In addition, the dynamic approach of the coarse mass transfer between phases results in a quadrupling of aerosol NO_3^- at the city center. Thus, simulations without the above, result in great model underestimations.

The spatial distribution of NO_3^- concentrations is namely shaped by the NO_x emissions, the Na^+ abundance and the wind direction. More analytically, the three peak values are observed in areas where Na^+ fully neutralizes the SO_4^{2-} and further reacts with NO_3^-. The dominant peak at the south of the domain is a strong NO_3^- penetration from the south, where high Na^+ production rates combined with NO_x emissions from the ships resulted in a concentration peak (up to 4μg m^{-3}) during the previous hours that is transferred northerly by the well-established S-SW flow. The other two peaks coincide with rich Na^+ areas during the same hour, combined with the high local industrial activity (figure 1). The effect of SSA on NO_3^- over the Athens basin is also apparent and follows the spatial distribution of emissions (figure 1) and of the SSA percentage (figure 2a).

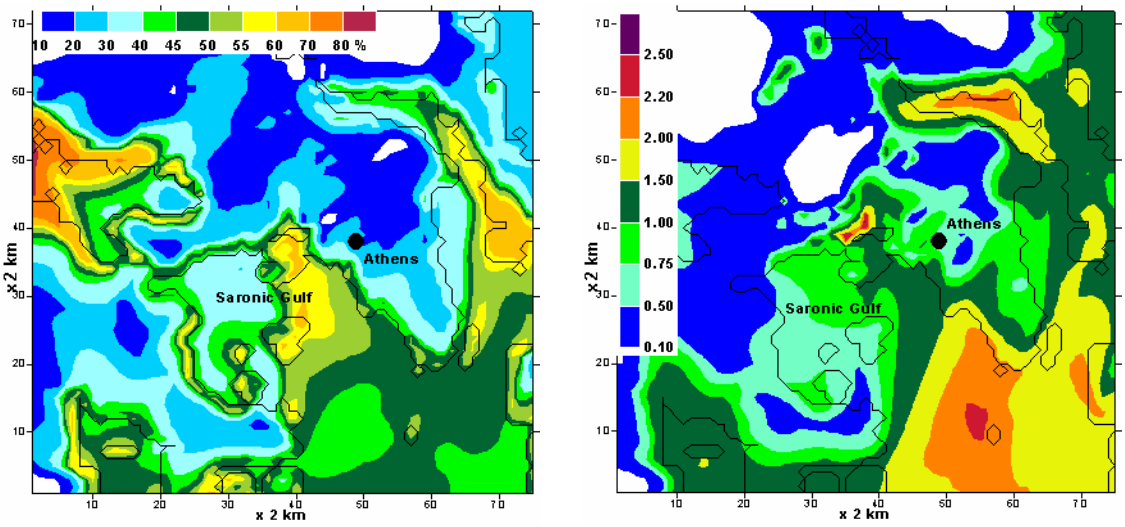

a b

Figure 2. Spatial distribution of the predicted a) SSA percentage in total aerosol concentrations, b) aerosol NO_3^- concentrations (μg m^{-3}), at 1800LST (24 June, 1998).

4. CONCLUSIONS

Numerical simulations over the Athens basin (Attica peninsula, Greece) show that the SSA component of aerosol is approximately 30% in the city center and remains above 20% even at very distant areas from the coast. Over the sea surface, it fluctuates between 30% and 90%, depending on the wind field and the SSA emissions.

NO_3^- seems to show the greatest influence from the sea production mechanisms compared to SO_4^{2-} and NH_4^+, reaching 17% of the inorganic aerosol mass at the Athens city center. In addition, the 95% of the NO_3^- produced mass over the whole domain is due to its precursor reaction with Na^+, which is effectively simulated by the dynamic gas/particle mass transfer. The resulting concentration predictions are quite satisfactory compared to measurements over the same area.

Peak NO_3^- values are predicted in areas where Na^+ fully neutralizes the SO_4^{2-} and further reacts with NO_3^-. These areas are strongly affected by increased SSA production and high local anthropogenic activity, both produced either locally or transported by the wind flow.

5. ACKNOWLEDGEMENTS

This study is conducted in the frame of a research project financed by the General Secretariat of Research and Technology (Ministry of the Environment, Greece).

6. REFERENCES

Anthes, R.A., Warner, T.T. 1978. The development of hydrodynamic models suitable for air pollution and other meteorological studies. Monthly. Weather. Rev. 106, 1045-1078.

Capaldo, K.V., Pilinis, C., Pandis, S.N. 2000. A computationally efficient hybrid approach for dynamic gas/aerosol transfer in air quality models. Atmos. Environ. 34, 3617-3627.

Clarke, A. D., Owens, S. R., Zhou, J. 2006. An ultrafine sea-salt flux from breaking waves: Implications for cloud condensation nuclei in the remote marine atmosphere. J. Geophys. Res. 111, D06202, doi:10.1029/2005JD006565.

De Leeuw, G., Neele, F.P., Hill, M., Smith, M.H. and Vignati, E. 2000. Production of sea spray aerosol in the surf zone. Journal of Geophysical Research 105 (D24), 29397-29410.

Eleftheriadis, K., Balis, D., Ziomas, I., Colbeck, I., Manalis, N. 1998a. Atmospheric aerosol and gaseous species in Athens, Greece.Atmos. Environ. 32, 2183-2191.

Eleftheriadis, K, Chung, M.C., Colbeck, I. 1998b. Atmospheric aerosol formation over Athens. J Aerosol Science 29, S25-6.

ENVIRON, 2003. Development of an Advanced Photochemical Model for Particulate matter: PMCAMx, cited at www.environcorp.com.

Gong, S.L. 2003. A parameterization of sea-salt aerosol source function for sub- and super-micron particles. Global Biogeochemical Cycles 17 (4), (8-)1 – (8-)6.

Koo, B.Y., Ansari, A.S., Pandis, S.N., 2003. Integrated approaches to modeling the organic and inorganic atmospheric aerosol components. Atmos. Environ 37, 4757–4768.

Lewis, E.R., Schwartz, S.E., 2004. Sea Salt Aerosol Production: Mechanisms, Methods, Measurements, and Models: A Critical Review. American Geophysical Union, Washington, DC.

Lewis, E.R., Schwartz, S.E., 2005. Comment on ‘‘Size distribution of sea-salt emissions as a function of relative humidity’’.

Nenes, A. Pandis S.N., Pilinis, C. 1998. ISORROPIA: A New Thermodynamic Model for Inorganic Multicomponent Atmospheric Aerosols, Aquatic Geochem. 4:123-152.

Seinfeld, J.H., Pandis, S.N. 1998. Atmospheric chemistry and physics. Wiley – Interscience publication.

Zhang, K.M., Knipping, E.M., Wexler, A.S., Bhave, P.V., Tonnesen, G.S., 2005a. Size distribution of sea-salt emissions as a function of relative humidity. Atmos. Environ. 39 (18), 3337–3373.

Zhang K.M., Knipping, E.M., Wexler, A.S., Bhave, P.V., Tonnesen, G.S. 2005b. Reply to comment on ‘‘Size distribution of sea-salt emissions as a function of relative humidity’’.

INFLUENCE OF SAHARAN DUST CONTRIBUTION ON THE PARTICULATE MATTER FORECAST IN SOUTHERN EUROPE

Pedro Jiménez-Guerrero, Carlos Pérez, Oriol Jorba and José M. Baldasano
Barcelona Supercomputing Center – Centro Nacional de Supercomputación
(BSC-CNS) Earth Sciences Department, C/ Jordi Girona 29, Edificio Nexus, 08034 Barcelona (Spain)

ABSTRACT

The complex atmospheric conditions in southern Europe during summer involve the superposition of phenomena occurring at different scales exerting a high influence in the levels of particulate matter and its composition. Namely, the contribution of mineral aerosols is very high due to the frequent occurrence of Saharan dust events. Nowadays, none of the operational daily forecasts in Europe include the influence of Saharan dust. In order to account for this, the BSC-CNS currently operates air quality forecasts in the Iberian Peninsula with MM5-EMEP-CMAQ-DREAM modelling system (http://www.bsc.es/projects/earthscience/aqforecast-en/). The necessity of coupling both modelling systems is addressed by the study of a summer episode combining regional pollution and Saharan dust in the Iberian Peninsula covering from June 19th to July 12th, 2006.

1. INTRODUCTION

The most serious air quality problems in southern Europe are related to high levels of PM10, NO_2 and O_3. Indeed, atmospheric chemistry transport model simulations and observations have shown that summertime aerosol levels in the entire Mediterranean troposphere are among the highest in the world. In this region precipitations are poor and irregular. Furthermore, it has been shown that Saharan dust decisively contributes to the exceedances of the PM10 limit values of Directive 1999/30/CE (e.g. Rodríguez et al., 2001; Querol et al., 2004).

One of the topics in which the European Commission has shown a greater concern, through initiatives as GMES is the necessity of developing actions that allow increasing the knowledge on transport and dynamics of pollutants to assure the accomplishment of legislation and to inform the population about the levels of pollutants. The regulation is especially demanding when the threshold levels are exceeded. In this case, it demands a detailed diagnosis of those areas where the exceedances are found and a forecast of the evolution of ground-level concentrations. However, nowadays, to the authors' knowledge, none of the available operational daily forecasts in Europe include the influence of Saharan dust in a non-climatologic basis. When considering only European anthropogenic emissions, chemistry-transport model simulations underestimate the PM10 concentrations by 30–50%, using the current knowledge about aerosol physics and chemistry (Vautard et al., 2005). In order to account for this, the Barcelona Supercomputing Center currently operates air quality forecasts in the Iberian Peninsula with MM5-EMEP-CMAQ-DREAM modelling system (http://www.bsc.es/projects/earthscience/aqforecast-en) over Southern Europe on a daily basis. The necessity of coupling CMAQ and DREAM modelling systems is addressed by the study of a summer long event (June 19th-July 12th, 2006) of Saharan dust transport towards southern Europe. As a first approach, the natural dust contribution from DREAM (http://www.bsc.es/projects/earthscience/DREAM) is added on-line to the output of CMAQ.

2. METHODS

The domain of operational simulations covers an area of 1392 x 1104 km^2 centred in the Iberian Peninsula. The MM5 numerical weather prediction model has been used to operationally provide the meteorology parameters to CMAQ chemistry transport model. The MM5 options used for the simulations were: MRF scheme for the PBL parameterization; Kain-Fritsch cumulus scheme; Dudhia simple ice moisture scheme, the cloud-radiation scheme, and the five-layer soil model. Emissions used for the domain of Europe and the Iberian Peninsula are derived from EMEP emissions database, on an hourly basis. The cells from the European EMEP mesh have a resolution of 50-km in polar coordinates; emissions in the Iberian Peninsula are disaggregated into a grid of 24-km resolution in Lambert coordinates. The biogenic emissions (included in EMEP sector 11) are not derived from EMEP, but estimated following the methods implemented in EMICAT2000 (Parra et al., 2006). The Community Multiscale Air Quality Modeling System (CMAQ) represents the state-of-the-science in atmospheric chemistry, simulating the main atmospheric chemistry, transport and deposition processes involved in the domain defined. The particulate matter species included are sulphates, nitrates, ammonia, aqueous aerosols, primary and secondary aerosols of anthropogenic and

biogenic origin, elemental carbon and other primary particulate matter. In addition, the code is parallelized for its implementation in cluster and supercomputation structures. There is also a great experience of works previously made in the Iberian Peninsula (Jiménez et al. 2006a; 2006b). The model used to provide the concentrations of natural dust to CMAQ chemistry transport model is the Dust REgional Atmospheric Model (DREAM©) (Nickovic et al., 2001). It was developed to simulate, diagnose or predict the atmospheric cycle of the mineral aerosol. It is integrated in the NCEP/Eta atmospheric model. DREAM is a fully operative tool extended and accepted by the scientific community, and nowadays provides operational forecasts over the Mediterranean and Canary Islands and Eastern Asia.

3. RESULTS AND DISCUSSION

In order to implement new model versions for operational applications there is a need for extensive checking and validation with observations. As a first approach, the natural dust contribution from DREAM is coupled on-line to the anthropogenic output of CMAQ by a simple addition of outputs (Figure 1). DREAM qualitative and quantitative validation studies using data from lidar stations, sun-photometers and satellite have outlined the good skills of the model concerning both the horizontal and vertical extent of the dust plume in the region (e.g. Perez et al., 2006). The performance of the system for predicting PM10 levels has been statistically evaluated by an on-line comparison of the first-layer simulations results of CMAQ and CMAQ+DREAM and the values measured on-line in two different stations located in the Mediterranean part of the domain: a urban station with high influence of traffic (Barcelona-Eixample) and a background station (Cubelles).

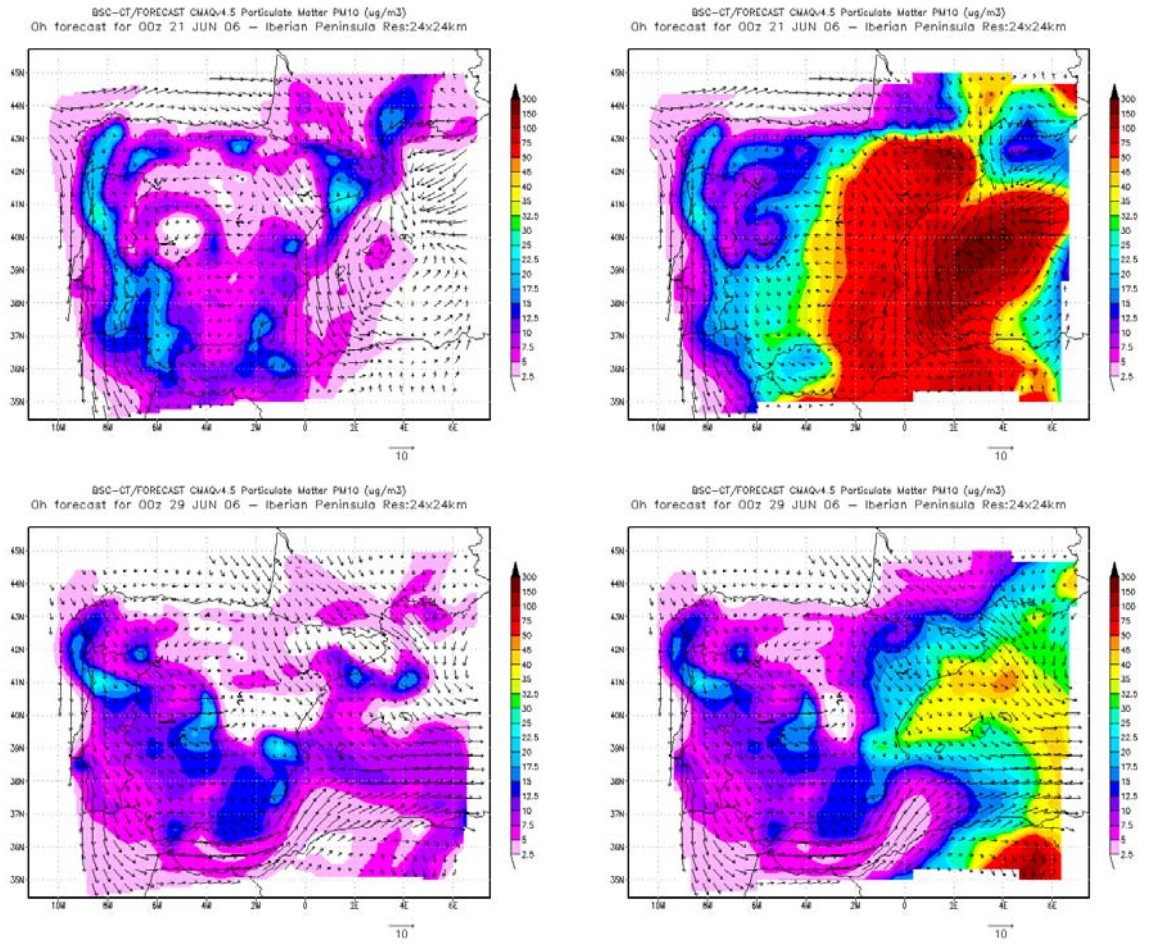

Figure 1. Forecast of PM10 concentration for June 21st (up), and June 29th (down), 2006 in the case of considering the CMAQ (left) or CMAQ+DREAM (right) modelling system.

The European Directive 1999/30/EC does not define criteria for modelling performance in the case of hourly and daily average concentration (this accuracy objective is 50% for annual average). Boylan and Russell (2006) have proposed model performance goals and criteria that vary as a function of particulate matter

concentration. The goal has been met when both the mean fractional error (MFE) and the mean fractional bias (MFB) are less than or equal to +50% and ±30%, respectively. The criteria has been met when both the mean fractional error and the mean fractional bias are less than or equal to +75% and ±60%, respectively. As derived from Table 1, the performance goals are not achieve by CMAQ or DREAM when applied uncoupled. For CMAQ and DREAM, the MFB exceeds the ±30% as an average behaviour during the episode (-38.7% and -55.6%, respectively); also, for DREAM, the MFE does not meet the performance goal (55.6%). However, if we consider the CMAQ+DREAM system, both the performance goals and criteria accomplish with the advised values (-7.7% for MFB and 10.1% as MFE). For CMAQ+DREAM, the highest MFB and MFE is -23.9% and 23.9%, in that order, for June 30th. Therefore, the performance goals are achieved for daily averages on every day just in the case of applying CMAQ+DREAM system (Table 1).

Table 1. Summary of the statistical evaluation of PM10 in the forecasting system for the stations included in the study during June 19th to July 12th, 2006*.

	Barcelona-Eixample	Cubelles	**AVERAGE**
Bias(C) (μg m^{-3})	-37	-20	**-29**
Bias(D) (μg m^{-3})	-47	-23	**-35**
Bias(C+D) (μg m^{-3})	-14	-1	**-7**
MNBE(C) (%)	-50.8	-43.6	**-47.2**
MNBE(D) (%)	-68.2	-58.1	**-63.2**
MNBE(C+D) (%)	-18.9	-1.8	**-10.3**
MNGE(C) (%)	50.8	43.6	**47.2**
MNGE(D) (%)	68.2	58.1	**63.2**
MNGE(C+D) (%)	19.5	8.4	**14.0**
MFB(C) (%)	-41.8	-35.7	**-38.7**
MFB(D) (%)	-60.7	-50.4	**-55.6**
MFB(C+D) (%)	-14.0	-1.5	**-7.7**
MFE(C) (%)	41.8	35.7	**38.7**
MFE(D) (%)	60.7	50.4	**55.6**
MFE(C+D) (%)	14.4	5.8	**10.1**

*C: CMAQ; D: DREAM; C+D: CMAQ+DREAM; MNBE: mean normalised bias error; MNGE: mean normalised gross error; MFB: mean fractional bias; MFE: mean fractional error

Furthermore, categorical statistics (Kang et al., 2005; Eder et al., 2006) have also been used to evaluate the different ensembles of the forecast (considering CMAQ alone, DREAM alone or coupled CMAQ+DREAM), including parameters such as the model accuracy (A), bias (B), probability of detection (POD), false alarm rate (FAR) and critical success index (CSI). With respect to the categorical forecasting for PM10 (Table 2), statistical parameters indicate that the accuracy (percent of forecasts that correctly predict an exceedance or non-exceedance) substantially improves when using CMAQ+DREAM for the particulate matter forecasts. In the case of considering the threshold established in the European regulations (50 μg m^{-3}, 24-hr average), for the urban station of Barcelona-Eixample the skill score accuracy improves from 16.7% with CMAQ, 20.8% with DREAM to 70.8% when using both models coupled. For the background station of Cubelles, the accuracy increases from 79.2% with CMAQ and 91.7% with DREAM to 95.8% in the case of using CMAQ+DREAM for providing daily-average forecasts. The value of the bias (B<1 for all models) indicates that exceedances are generally underpredicted by each model, especially in the city of Barcelona, which corresponds with the value of the MNBE obtained for discrete evaluations. This underestimation is minor for the CMAQ+DREAM configurations (bias under 0.2 for both thresholds and stations), clearly improving the bias for CMAQ and DREAM alone versions, that may achieve 0.9. Also the critical success index (CSI) and the probability of detection (POD) are used. Both parameters perform similarly during the whole extent of the episode, importantly increasing their score when using CMAQ+DREAM. For the 50 μg m^{-3} threshold as a daily average, the CSI and the POD involve identical scores, improving in the urban station from 9.1% and 13.6% for CMAQ and DREAM, in that order, to 68.2% with CMAQ+DREAM. In the background station, the scores for CMAQ, DREAM and CMAQ+DREAM increase from 16.7% and 66.7% to achieve 83.3%. Last, the fifth categorical parameter, the false alarm rate (FAR) indicates the number of times that the model predicted an exceedance that did not occur. This metric is zero for all the modelling system options and stations (which also agrees with the tendency to underprediction for CMAQ and DREAM alone).

Table 2. Categorical (skill scores) statistical evaluation (50 μg m^{-3} threshold) of PM10 in the forecasting system for the stations of Barcelona (urban) and Cubelles (background) during June 19th to July 12th, 2006*.

	Barcelona-Eixample			Cubelles		
	C	D	C+D	C	D	C+D
A (Accuracy)	16.7	20.8	70.8	79.2	91.7	95.8
CSI (Critical Success Index)	9.1	13.6	68.2	16.7	66.7	83.3
POD (Probability of Detection)	9.1	13.6	68.2	16.7	66.7	83.3
B (Bias)	0.9	0.9	0.3	0.8	0.3	0.2
FAR (False Alarm Rate)	0.0	0.0	0.0	0.0	0.0	0.0

*C: CMAQ; D: DREAM; C+D: CMAQ+DREAM

4. CONCLUSIONS

In this study we have coupled CMAQ anthropogenic outputs with DREAM natural dust forecasts in an operational way by simple adding both model outputs in the BSC-CNS Air Quality Forecast Modelling System. The novel approach was tested for a major episode of air pollution combining regional pollution and Saharan dust outbreaks over the Mediterranean on June-July 2006 in order to assess the improvements of CMAQ+DREAM coupling on chemical weather forecasting for particulate matter. The modelling system demonstrates high agreement with air quality data from stations in southern Europe. The performance goals for PM10 simulations are achieved for daily averages on every day during the episode just in the case of applying CMAQ+DREAM system. Also, the discrete and categorical scores of the forecasting modelling system (skill scores) improve substantially in the domain of study when including the Saharan dust contributions to the forecasting system.

5. ACKOWLEDGEMENTS

This work was funded by the projects CICYT CGL2006-08903 and CICYT CGL2006-11879 of the Spanish Ministry of Education and Science and CALIOPE project of the Spanish Ministry of the Environment.

6. REFERENCES

Boylan, J.W., Russell, A.G., 2006. PM and light extiction model performance metrics, goals, and criteria for three-dimensional air quality models. Atmospheric Environment 40, 4946-4959.

Eder, B., Kang, D., Mathur, R., Yu, S., Schere, K., 2006. An operational evaluation of the Eta-CMAQ air quality forecast model. Atmospheric Environment 40, 4894-4905.

Jiménez, P., Jorba, O., Parra, R., Baldasano, J.M., 2006a. Evaluation of MM5-EMICAT2000-CMAQ performance and sensitivity in complex terrain: High-resolution application to the northeastern Iberian Peninsula. Atmospheric Environment 40, 5056-5072.

Jiménez, P., Lelieveld, J., Baldasano, J.M., 2006b. Multiscale modeling of air pollutants dynamics in the northwestern Mediterranean basin during a typical summertime episode. Journal of Geophysical Research 111, D18306, doi:10.1029/2005JD006516

Kang, D., Eder, B.K., Stein, A.F., Grell, G.A., Peckham, S.E., McHenry, J., 2005. The New England air quality forecasting pilot program: development of an evaluation protocol and performance benchmark. Journal of the Air & Waste Management Association 55, 1782–1796.

Parra R., P. Jiménez, J.M. Baldasano. Development of the high spatial resolution EMICAT2000 emission model for air pollutants from the north-eastern Iberian Peninsula (Catalonia, Spain) . Environmental Pollution, 140, 200-219.

Pérez, C., S. Nickovic, J. M. Baldasano, M. Sicard, F. Rocadenbosch, V. E. Cachorro, 2006. A long Saharan dust event over the Western Mediterranean: lidar, sun photometer observations and regional dust modeling. Journal of Geophysical Research 111, D15214, doi:10.1029/2005JD006579.

Querol, X., Alastuey, A., et al., 2004. Levels of particulate matter in rural, urban and industrial sites in Spain. The Science of Total Environment 334–335, 359–376.

Nickovic, S., A. Papadopoulos, O. Kakaliagou, G. Kallos, 2001. Model for prediciton of desert dust cycle in the atmosphere. Journal of Geophysical Research 106, 18113-18129

Rodríguez, S., Querol, X., Alastuey, A., Kallos, G. Kakaliagou, O., 2001. Saharan dust contribution to PM10 and TSP levels in Southern and Eastern Spain. Atmospheric Environment 35, 14, 2433 - 2447.

Vautard, R., Bessagnet, B., Chin, M., Menut, L., 2005. On the contribution of natural Aeolian sources to particulate matter concentrations in Europe: Testing hypotheses with a modelling approach. Atmospheric Environment 39, 3291-3303.

QUANTIFYING THE INPUT OF WIND BLOWN DUST TO SOUTHERN EUROPEAN CITIES

S Plainiotis[1], K A Pericleous[1], B E A Fisher[2]
[1]University of Greenwich, UK [2]Environment Agency, UK

ABSTRACT

The Sahara desert is the most significant source of particulate pollution not only to the Mediterranean region, but also to the Atlantic and beyond [e.g. Moulin *et al.*, 1998]. In this paper, PM10 exceedences recorded in the UK and the Mediterranean are studied and their source investigated, using Lagrangian Particle Dispersion (LPD) methods.

1. INTRODUCTION

Although particulate matter in the atmosphere is thought to present one of the most significant current risks to human health, scientific understanding of the behaviour and health effects of PM is still far from comprehensive. For example, there is insufficient understanding of the sizes and the chemical characteristics of the ambient PM mixture that determine its toxicity [WHO 2004]. Furthermore, the PM chemical composition is not well identified in many areas in Europe, as there is need for more monitoring stations, able to distinguish individual particle components or their origins [NGO 2006]. Research studies which help to reduce this knowledge gap and which support the policymaking are sorely needed and air pollution experts have underlined the need for more research and monitoring regarding particle composition. Much attention has been given to anthropogenic sources and in comparison, little attention has been given to natural sources of airborne particles such as wind-blown dusts, volcanic eruptions and sea-salts which are capable of measurement but cannot be controlled.

A proposed new directive summarises and consolidates four existing directives (1996/62/EC, 1999/30/EC, 2000/69/EC and 2001/81/EC) as well as the Council Decision 97/101/EC on the exchange of information and data on ambient air pollution. These directives set limit and target values for ambient air quality for some of the most important pollutants in our outdoor air. The draft Directive recognises that transboundary air pollution can involve particles, however alert and information thresholds do not appear to apply to particulate matter. Particulate matter is subject to assessment using both: 1) an "upper assessment threshold" meaning a level below which a combination of measurements and modelling techniques may be used to assess ambient air quality; and 2) a "lower assessment threshold" meaning a level below which modelling or objective-estimation techniques alone may be used to assess ambient air quality. It is proposed that where natural contributions to pollutants in ambient air can be determined with sufficient certainty; these can be subtracted when assessing compliance with air quality limit values.

One way of treating such events is by chemical speciation of PM. Samples of particles on filters may be analysed for the main compounds, in order of diminishing importance: Particles are made of a mix of different components, some of them originating from natural sources such as for example re-suspended soils, sea salt, pollens and spores, some of them originating from anthropogenic sources, such as combustion processes or re-suspended road dust.

Apart from this not being practical on a routine basis, the additional sampling may not be able to distinguish episodes of mineral dust blow, which are locally derived, from those, which have travelled a long distance. Often, both natural and anthropogenic components are clustered together in a single air-borne particle. This is where the techniques of this paper should be applied. In this paper we investigate long-range transport of desert dust affecting Europe and its prediction through modelling. Particulate exceedences observed recently which have been attributed to Saharan dust storms are the focus of this study. Earlier studies by the same team, have similarly investigated the role of volcanoes and large open fires [Plainiotis *et al*., 2005a, 2005b, 2005c; Pericleous *et al.,* 2006].

This paper contains a brief description of the methodology adopted in this project. This is followed by a description of the input data used and examples of typical pollution episodes.

2. DATA AND METHODS

Particle dispersion models generally use meteorological fields and emission inventories as input, and calculate time-dependent concentration fields as output, using suitable models for the relevant physical processes such as advective or convective transport, mixing by diffusion, and mass transfer through dry or wet deposition, or chemical reaction. Figure 1 shows a schematic of the system put together for this research, featuring two Lagrangian Particle Dispersion (LPD) models (FLEXPART and HYSPLIT).

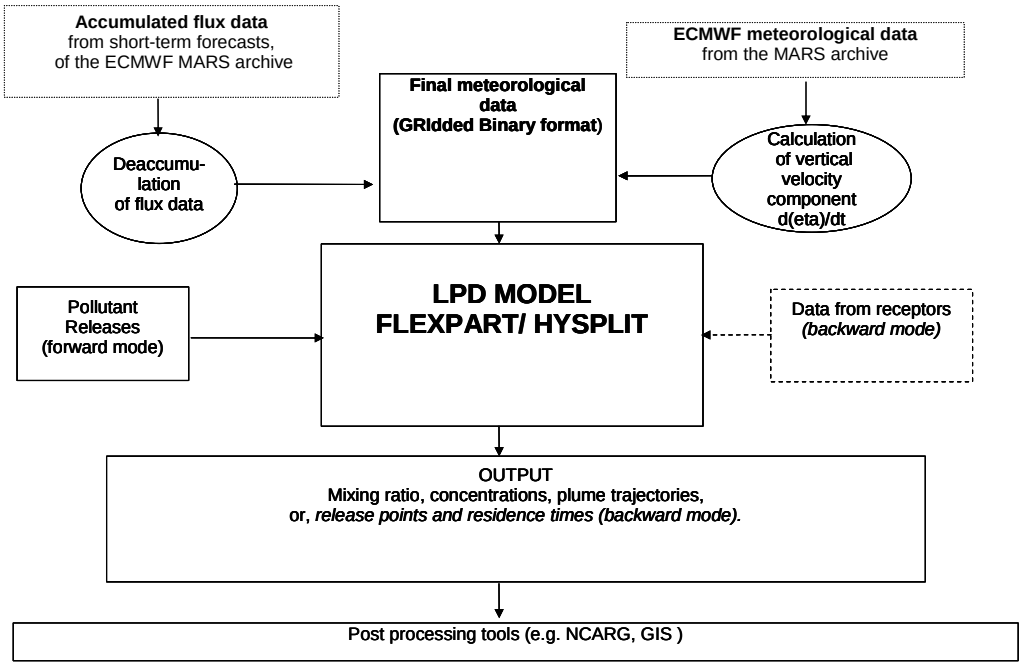

Figure 1: Schematic of the dust dispersion model environment, showing, the LPD engine (FLEXPART, of HYSPLIT) at its centre

The "Hybrid Single Particle Lagrangian Integrated Trajectory" (HYSPLIT) model was developed jointly by the National Oceanic and Atmospheric Administration (NOAA) and Australia's Bureau of Meteorology. The binary installation files are available for download from (http://www.arl.noaa.gov/ready/hysplit4.html). Due to lack of space, no further details of the model will be given here, with the exception of the sand entrainment treatment necessary for this work.

In order to model the dust emission caused in a Sahara desert storm, the dust emission model of Draxler et al. (2001) is employed (HYSPLIT version 4.7). The emission module is based on the concept that threshold friction velocity is dependent on surface roughness which in turn is correlated with soil properties. The emission area is divided into a matrix of points and those points are set as possible point sources in HYSPLIT, provided they are located inside the area identified as desert in a land-use internal database. A dust emission rate is computed from each cell of the resulting emission matrix (up to a maximum value of 1 $mg/m^2/s^1$), when the local wind velocity exceeds the threshold velocity for the soil characteristics of the emission cell [Westphal *et al., 1987*]. Finally, the emitted material is dispersed and transported using the standard methodology of HYSPLIT [Draxler and Hess, 1997]. There is no special treatment in FLEXPART for this, and consequently it was not used in these particular case studies.

3. SIMULATION EXAMPLES

North Africa is the largest global source of atmospherically transported desert dust in the world. Exports of desert dust plumes to the North Atlantic Ocean and the Mediterranean Sea occur several times per year and the most striking effects of dust transport outside the Sahara manifest in the Atlantic Ocean near the Western African coast, particularly in summer. Dust outbreaks in the Mediterranean generally have minor intensity [Prospero 1981; Meloni et al, 2007]. The dust vertical distribution is different for the two paths [Alpert et al., 2004]: the dust generally travels below 5 km altitude over the tropical Atlantic [Karyampudi et al., 1999], while it often reaches 8 km altitude over the Mediterranean [Alpert et al., 2004; Plainiotis et al., 2005a, 2005b; Pericleous et al.,2006].

On a regular yearly base, about 80–120 Tg of dust per year are transported to the Mediterranean [Meloni et al., 2007]. The occurrence of dust events in the Mediterranean has manifested a seasonal behaviour. The temperature difference of cold marine Atlantic air and warm continental air are responsible for the creation of the intense Sharav cyclones, south of Atlas mountains that cross North Africa during spring and summer [e.g. Moulin *et al.*, 1998; Rodriguez *et al.*, 2001]. In spring the Sharav cyclones carry desert dust toward the Eastern Mediterranean, while in summer the most intense activity occurs in the Central Mediterranean; by the end of summer a low-pressure system over the Balearic Islands drives the dust plumes towards the Western Mediterranean [Meloni *et al.,* 2007]. Two characteristic examples of simulations of desert dust outbreaks are shown here.

3.1 Case Study 1: During early March 2000, several particulate (PM10) monitors recorded exceedences of the 50μg/m3 target throughout the UK. The maximum hourly concentration was recorded at Plymouth (290μg/m3) with Port Talbot also monitored several exceedences on March 3rd. The weather was characterised by strong westerly winds and widespread rainfall associated with a low pressure system to the north of Scotland, conditions usually associated with relatively unpolluted air [Ryall, D.B. *et al.*, 2002]. Some of the likely sources were the Icelandic volcano Hekla, which began erupting on the 26 February 2000 and dust transported from the North African Saharan desert. Weather datasets (hor. resolution: 0.5° lat/lon) were retrieved from the ECMWF Mars Archive for the period between 25/02/00 and 04/03/00. A sample result is shown in Figure 2, where the forward tracking simulation of HYSPLIT is compared against satellite observations (TOMS aerosol index) showing good qualitative agreement.

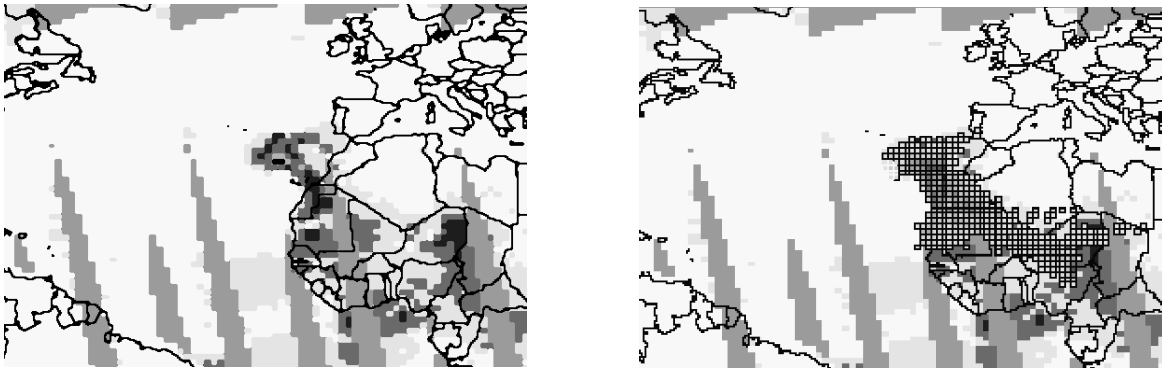

Figure 2. Haze distribution on 12:00 26/02/00 observed by the NASA TOMS aerosol index and comparison with predicted dust particle positions (right, blue area) HYSPLIT

3.2 Case Study 2: On the last days of February 2006 a thick cloud of dust from the Sahara Desert enveloped Greece and other areas of the South-East Mediterranean, leading to the cancellation of many flights. The islands of Crete and Cyprus were especially hard hit. Hospitals in Crete reported a significant increase in patients with respiratory problems. PM10 concentration measurements at the sampling station "Finokalia" in Crete, showed evidence of three major dust episodes on the 24, 26 and 28th of February, as shown in Figure 3. This rural station is located at the top of a hill (elevation 150 m) in the Southern coast of Crete, eastern Mediterranean Sea (35I 20'N, 25I 40'E), and 70 km away from the nearest urban centre Heraklion, Crete.

A series of simulations, in both the forward and backward/receptor mode, using the LPD models HYSPLIT (forward) and FLEXPART (backward) were performed. Meteorological data were retrieved from the ECMWF Mars archive, using custom written routines. Dry deposition was switched off, following Draxler (2002). The results of the forward simulation (HYSPLIT) are compared with PM10 concentration values measured at Finokalia and Aghia Marina (Figure 3) and with satellite Aerosol Index data from the OMI instrument (Figure 4).

Although the emission module of HYSPLIT under-predicted concentrations during the three episodes (24/02, 26/02 and 28/02) in Crete and the prolonged episode in Cyrpus (25/02-01/03), the PM10 figures gave an accurate indication of the timing and the magnitude of the events, even though the dispersion was over a long distance and a considerable time span. Part of the under-prediction is due to pre-existing high background PM10 concentrations not accounted for in the model. The under-prediction is partly balanced by the lack of precipitation in the simulation.

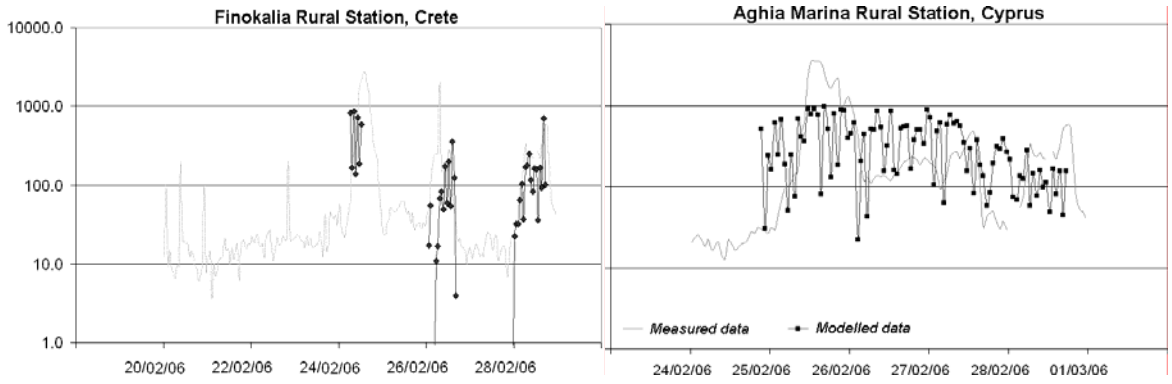

Figure 3: PM10 concentrations (μg/m3), measured at the rural stations of Finokalia, Crete (left) and Aghia Marina Cyprus (right) together with predicted levels (circles)

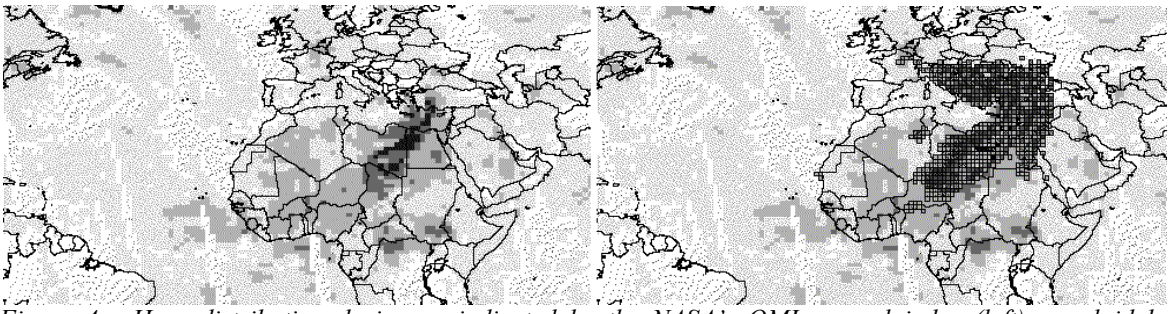

Figure 4: Haze distribution during as indicated by the NASA's OMI aerosol index (left), overlaid by HYSPLIT's predicted dust plume location (right,dark area). The data correspond to the second dust event (26/02/06).

4. CONCLUSIONS

This paper demonstrates the capability of LPD type models in predicting the transport of sand particles from Saharan storms with good accuracy. In particular, the ability to model the entrainment of sand in the atmosphere due to wind shear, coupled with advanced weather forecasting may serve to predict the onset of desert dust storms days before their effects are felt. The combination of forward and reverse (receptor) modes available in both models is useful in confirming the findings, especially where conflicting emission sources exist.

Episodes of windblown dust will make some contribution to the annual average. However even the extreme February 2006 episodes over Crete and Cyprus of several hundred μg/m3 would not be significant as annual averages. An important health impact may therefore by neglected in the implementation of the Directive. Where any assessment thresholds, limit values or exposure reduction target values or concentration cap plus any relevant margin of tolerance is exceeded due to significant transboundary transport of pollutants or their precursors, the draft Directive proposes that the Member States concerned shall cooperate and, where appropriate, draw up joint activities, such as the preparation of joint or co-ordinated plans or programmes in order to remove such exceedences, through the application of appropriate but proportionate measures. There are no appropriate actions in this case which can ameliorate the situation, but simulation studies of transport and atmospheric dispersion of desert dust, as shown in this paper, are necessary to interpret these episodes.

5. REFERENCES

Alpert P., Kishcha P., Shtivelman A., Krichak S. O., Joseph J. H., 2004. Vertical distribution of Saharan dust based on 2.5-year model predictions. Atmospheric Research 70, 109–130.

Astitha M, Katsafados P, Kallos G, Air quality in the Mediterranean urban regions from anthropogenic and natural particulate matter, Proc. HARMO 10, pp213-215, 2005

Draxler, R.R, Gillette, D.A., Kirkpatrick, J.S., Heller, J., 2001, Estimating PM10 Air Concentrations from Dust Storms in Iraq, Kuwait, and Saudi Arabia, Atmospheric Environment, 35: 4315-4330.Gerasopoulos E, et al., ATMOSPHERIC ENVIRONMENT, 40 , 25, 4679-4690 , 08/2006

Karyampudi, V.M., et al., 1999. Validation of the Saharan dust plume conceptual model using lidar, Meteosat, and ECMWF data. Bulletin of the American Meteorological Society 80, 1045–1075.

Maryon Roy, Atmospheric Dispersion Branch, Met Office "NWP Gazette", 3rd Quarter, 1996

Meloni, D., D. Meloni, A. di Sarra, G. Biavati, *et al*., Seasonal behavior of Saharan dust events at the Mediterranean island of Lampedusa in the period 1999–2005. Atmospheric Environment (2007), doi:10.1016/j.atmosenv.2006.12.001

Mihalopoulos N. and Kouvarakis: Personal communication; Finokalia sampling station (ECPL, University of Crete)

NGO, 31 January 2006: Position paper on the proposed directive on ambient air quality and cleaner air for Europe, online PDF file: http://www.acidrain.org/pages/news/NGOs_Ambient_Air_Qual_Directive.pdf

Moulin, C., *et al*., 1998. Satellite climatology of African dust transport in the Mediterranean atmosphere. Journal of Geophysical Research 103, 13137–13144.

Pericleous K. A., Plainiotis S., Fisher B. E. A., 2006. Airborne Transport of Saharan Dust to the Mediterranean and to the Atlantic. Proc. IASTED Conf. Environmental Modelling and Simulation 2006, St Thomas, Nov. 2006

Plainiotis S., Pericleous K. A., Fisher B. E. A., Shier L., 2005. Proc. 16th Int. IASTED Conf. MS-2005, pp.164-169

Plainiotis S., Pericleous K. A., Fisher B. E. A., Shier L., 2005. Proc. HARMO 10, Crete, October, 2005, pp. 398-403

Plainiotis S., Pericleous K. A., Fisher B. E. A., Shier L., 2005. Proc. 5th Int. Conf. on Urban Air Quality, Valencia, Spain

Prospero et al, 2002. Environmental characterization of global sources of atmospheric soil dust identified with the NIMBUS 7 Total Ozone Spectrometer (TOMS) Absorbing Aerosol Product. Reviews of Geophysics 40 (1), 2-1–2-31.

Pulles T *et al*., CEPMEIP Database, http://www.air.sk/tno/cepmeip/, 2003

Rodriguez, S., Querol, X., Alastuey, A., Kallos, G., Kakaliagou, O., 2001. Saharan dust contributions to PM10 and TSP levels in Southern and Eastern Spain. Atmospheric Environment 35, 2433–2447

Ryall, D.B. et al. (2002) The origin of high particulate concentrations over the United Kingdom, March 2000. Atmospher. Env. 36, 1363–1378.

WHO 2004: Health Aspects of Air Pollution. Online PDF file: http://www.euro.who.int/document/E83080.pdf

Proceedings of the 6th International Conference on Urban Air Quality
Limassol, Cyprus, 27-29 March 2007

AIR QUALITY AND POLLUTION DISPERSION MODELING IN SINGAPORE

M. Skote
Institute of High Performance Computing,
1 Science Park Road, #01-01 The Capricorn,
Singapore Science Park II
Singapore 117528
skote@ihpc.a-star.edu.sg +6564191427

ABSTRACT

Recently, a simulation package has been implemented to numerically capture the detailed three dimensional spatial pollutant distributions and time variance over Singapore. The chemistry transport equations are solved with the code CMAQ, developed by US EPA. These simulations require input of weather data, which is produced by the simulation code MM5, and emission data, which is obtained through the program package SMOKE. Comparison of the results from the model with monitoring stations shows that realistic results are obtained. The levels of the concentration, as well as the diurnal variation are captured well by the model.

1. INTRODUCTION

In recent years, the focus on air quality in mega-cities has given great insight into the chemical processes in the lower atmosphere. Also the atmospheric flow is more understood, albeit for the tropical atmosphere some issues remain to be solved; such as the question if the atmospheric flow is dominated by convective clouds or if there is a balance between the diabatic heating and the vertical advection (in the large-scale tropical atmosphere). See Sobel et al. (2001) for a discussion on this topic.
A number of investigators have been using meso-scale numerical models applied to air quality in Asia. A few examples are Siniarovina and Engardt (2005), who applied the Swedish model MATCH to Malaysia, and Joshua Fu et al. (2005) who applied CMAQ to east China. A large number of models are also used by different groups of investigators in Taiwan, Hong Kong, and Japan.
Development of models for the unresolved dynamics of the tropical atmosphere is just in its beginning. The classical scaling laws of the planetary boundary layer may be improved using convective eddy velocity scales following the work by Zilitinkevitch (2006).
The air quality in Singapore is generally good. Almost every year however (usually in October), the island is covered in a haze which originates from forest and peat fires in Indonesia (Sumatra and Borneo). The haze is not considered here since we are mainly interested in the more constant air pollution from local sources.

2. METHODOLOGY

In Singapore, the National Environment Agency (NEA) has generated an efficient air quality monitoring network for real time studies. However, so far the numerical model for prediction/analysis has been limited to a steady state Gaussian model, mainly used for air pollution impact evaluation based on local historic wind and emission data.
In a recently implemented modeling framework, the chemistry transport equations are solved with the code Community Multiscale Air Quality (CMAQ) which was developed by U.S. Environmental Protection Agency (EPA). These simulations require input of weather and emission data. The latter are produced through the program package Sparse Matrix Operator Kernel Emissions (SMOKE). The weather data are created by the simulation code MM5 and then processed by the stand-alone pre-processor program MCIP before being used by CMAQ. See Figure 1 for sketch of the data flow within the modeling framework.
The MM5 package originates from Pennsylvania State University/National Center for Atmospheric Research (NCAR). Predictions are not considered here, but rather the construction of a data set on a fine scale that matches the large scale observational data (taken from the global data base NCEP) and fine scale boundary conditions.
Several steps are required to construct the weather data with the simulation package MM5. The starting point is a simulation with a coarse grid resolution covering a large area (several 1000 km). Then boundary and initial conditions are extracted from this first run to be used for a finer grid simulation covering a smaller geographical region. This nesting procedure is then repeated, and in each step the resolution is increased three times. The same period of time is considered in each step, but the area is reduced in order to zoom in on the area of interest. Five nested simulations were performed using 81, 27, 9, 3, 1 kilometers grid resolution respectively. The first level covers the Southeast Asia region while the fifth and last level with the finest resolution covers Singapore, see Figure 2. Boundary and initial conditions for first and largest grid are taken from a global data base (NCEP).

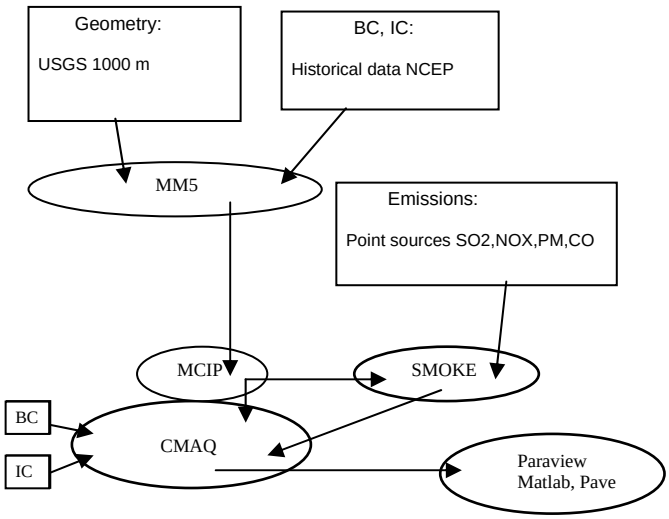

Figure 1: Data flow within the modeling framework. Rectangles represent data and oval the programs.

Examples of the physical processes modeled in MM5 are the cumulus parameterization scheme, for which we use Kain-Fritsch for grid 1-3 and none for grid 4 and 5, where the resolution is high enough to capture the clouds; planetary boundary layer flow, for which we use the Pleim-Chang scheme, together with the land-surface model of Pleim-Xiu.
The emission inventory consists mainly of power plants and oil refineries, and was converted to source terms using SMOKE. Basically, what this program does is to increase the resolution of the emission inventory to match that of the meso-scale method. Here the word "resolution" not only refers to the spatial one, but also to the temporal and speciation resolutions. In Figure 3 we show the SO2 emission sources which are predominantly located in the southwest of Singapore.
When the weather data and the source terms have been created for the time period of interest, the dispersion simulations are performed using CMAQ with a time step of one hour, and with the finest resolution of one kilometer retained.
The simulations were performed on a AMD Opteron Linux cluster and a IBM p575 power5+ super computer. Up to 16 processors were used for the finer grid resolution simulations. Due to excellent speed-up the wall clock time stays within 8 hours for 240 hours real time simulation.
There are four important features that are currently absent in the modeling framework. Firstly, the transboundary transport which sets the boundary conditions on our final domain is neglected. A remedy for this would be to do nesting in CMAQ in the same manner as for MM5, using the emission data base for the whole Southeast Asia region compiled by Streets et al. (2003). Secondly, the traffic and biogenic emission data may have a significantly effect on the distribution and composition of the air pollution. These emissions can be included in the future when a GIS (geographical information system) is integrated with the modeling framework. Thirdly, the land use data used need to be updated. Singapore is increasing its urbanized area, and also the size of the island grows due to land reclamation projects. In Hong Kong, one has observed (Huang et al. 2005) that the increased urbanization the last 15 years has worsen the air quality, not only due to increased emissions, but also due to changed pattern of the sea breeze which causes entrapment of pollutants. The fourth and final feature lacking is the assimilation of observational data into MM5. However, in this project we do not put any effort into predict or capture the weather pattern accurately, but rather try to create a typical weather scenario for the specific season of interest. Also the quality of the air pollution dispersion simulations themselves may be enhanced by assimilation of data from the monitoring stations, see Hogrefe et al. (2006).

2. RESULTS AND DISCUSSION

Singapore lies just north of the Equator and its climate is characterized by uniform temperature and pressure, high humidity and abundant rainfall. The climate can be divided into two main seasons, the Northeast Monsoon (with prevailing winds from the northeast) and the Southwest Monsoon (with winds from southwest) season, separated by two relatively short inter-monsoon periods. We concentrate our simulation work on the south-west monsoon period, since the largest emission sources are located in the southwest of the

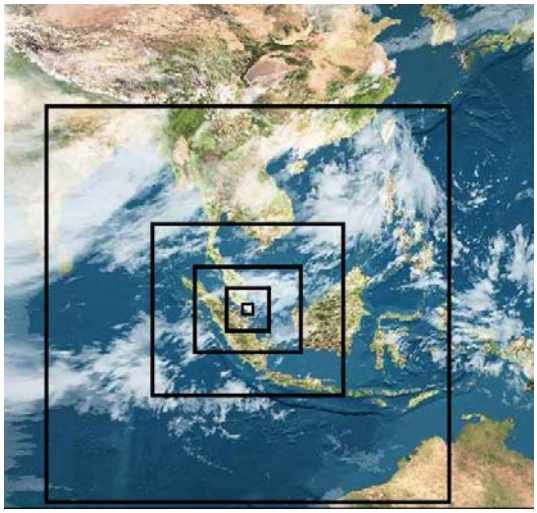

Figure 2: The five nested grids used in the MM5 simulations. The simulations are step by step zoomed in to Singapore Island.

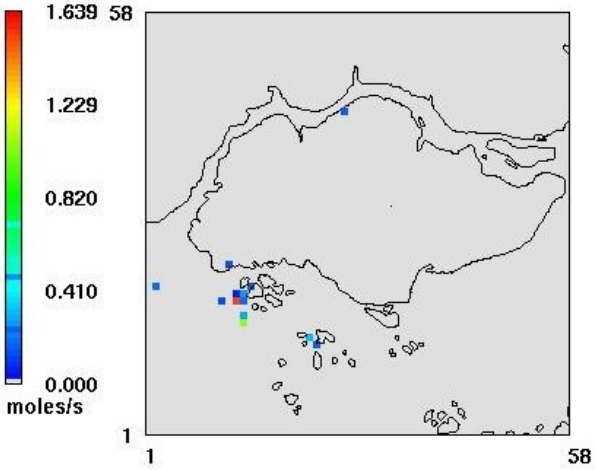

Figure 3: Emissions of SO2 are located mainly in the southeast of the island. Note that the background map is old and is not used in the simulations. The sources that appear to be over water are actually on nowadays reclaimed land.

country. During this period the air pollution emitted by the petrochemical industries is being transported by the winds over the Singapore Island itself. The results shown here are from the month of May 2005.
Example from the CMAQ simulation is shown in Figure 4 where the concentration of SO2 at the first vertical level (36 meter) is shown. Comparison of the simulation results for the concentration of SO2 with monitoring stations shows that realistic results are obtained. See Figure 5 where the variation over time (days in May on the x-axis) at a specific location (in the west of the island) is shown. The sources are stationary, thus the variation is due to advection and chemical transport. Note that the simulation and measured data deviates because the weather data used in the simulations differs from reality. Hence we only compare statistical measures such as levels and frequency of the diurnal cycles (not shown). The levels of the concentration, as well as the diurnal variation are captured well by the model.
These results point towards that the local contribution to the SO2 levels are the most dominant and the transboundary influence is secondary. The level of concentration is not shown in Figure 5 (the y-axis) since the numbers may be sensitive to the National Environment Agency (NEA) in Singapore, for whom we conduct the current investigation. However, the annual and 24-hour daily mean values are far from the current ambient air quality standard set by USEPA. (For SO2 it is 0.03 and 0.14 ppm respectively). In Figure 4, the maximum value is 0.14 ppm, which is also the maximum during the simulation period. But this value is not sustained for more than an hour.
The rest of the emission inventory (NOX, PM and so on) is not of as high quality as for SO2. Hence, the results for species like Ozone are not as reliable. Furthermore, the traffic data is currently absent from the data base, which is a major contributor to the NOX emission. Also, the chemistry mechanisms involved in the formation of Ozone are arguably different in the tropical climate than in the temperate zone, for which the reaction rates in the mechanisms were calibrated.

4. CONCLUSIONS

The package MM5/SMOKE/CMAQ has been implemented and adjusted to the local conditions for the small city-state of Singapore. The most interesting species from the ambient air quality point of view is SO2. The conclusions from simulations suggest that the main contributor to the concentration is the local sources, mainly oil refineries and power plants. Four features that are currently missing in the modeling framework need to be implemented in the near future: (i) Nesting in CMAQ. (ii) Traffic and biogenic emissions. (iii) Updated land use data. (iv) Accurate weather data.

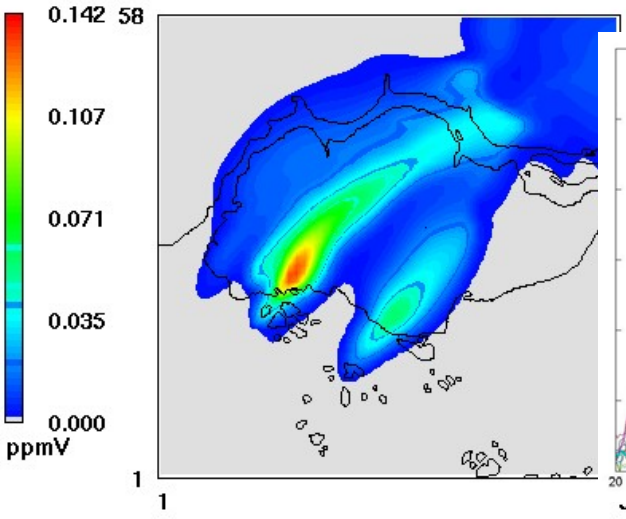

Figure 4: SO2 concentration over Singapore from simulations. A local maximum appears in the western part due to winds at this specific time. The high values persist only for a short moment.

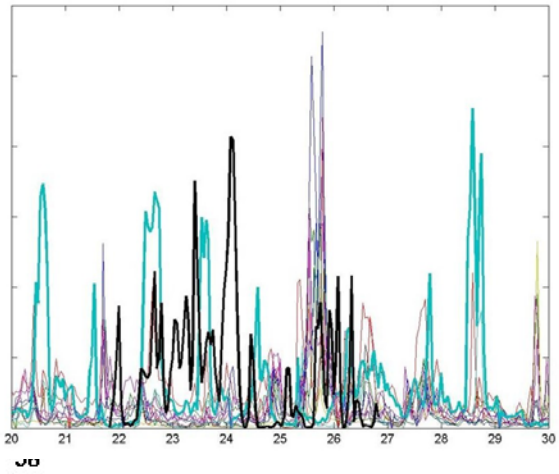

Figure 5: SO2 at a position in the west of the island from simulation (black) and measurements (cyan). The thinner curves are from other positions. Days in May 2005 on the x-axis.

5. ACKNOWLEDGEMENTS

My colleagues Dr Lou Jing, Dr Hua Jin Song and Mr Zhang Baili are recognized for their efforts to initialize and contribute to the project. Mr Lim Cheng Choon at the National Environment Agency in Singapore is greatly acknowledged for providing the emission and monitoring station data.

6. REFERENCES

Fu, J. S., Jang, C., Streets, D., Li, Z., He, K., Wang, L., Zhang, Q. 2005. Regional/Urban Air Quality Regional/Urban Air Quality Modeling in Beijing and Shanghai, Modeling in Beijing and Shanghai, China. 4th Annual CMAS Models-3 User's Conference September 26-28, 2005, Chapel Hill, USA.

Hogrefe, C., Hao, W., Civerolo, K., Ku1, J.-Y. and Sistla, G. 2006. Exploring approaches to integrate observations and cmaq simulations for improved air quality forecasts. 5th Annual CMAS Models-3 User's Conference, October 16 – 18, 2006, Chapel Hill, USA.

Huang, , J.-Y., Fung, J. C.H., Zhang, Y., Lau, A. K.H., Kwok, R., Lo, J. C.F. improvement of air quality modeling in Hong Kong by using MM5 coupled with LSM. 4th Annual CMAS Models-3 User's Conference September 26-28, 2005, Chapel Hill, USA.

Siniarovinaa, U. and Engardt, M. 2005. High-resolution model simulations ofanthropogenic sulphate and sulphur dioxide in Southeast Asia. Atmos Environ. 39, 2021-2034.

Sobel, A. H., Nilsson J. and L. M. Polvani. 2001. The weak temperature gradient approximation and balanced tropical moisture waves. Journal of the Atmospheric Sciences, 58, 3650-3665.

Streets D. G., Bond, T. C., Carmichael, G. R., Fernandes, S. D., Fu, Q. , He, D., Klimont, Z., Nelson, S. M., Tsai, N. Y. , Wand, M. Q. Woo, , J.-H. and Yarber K. F. (2003), An inventory of gaseous and primary aerosol emissions in Asia in the year 2000, J. Geophys. Res., 108(D21), 8809, doi:10.1029/2002JD003093.

Zilitinkevich, S. S., Hunt, J. C. R., Esau, I. N., Grachev, A. A., Lalas, D. P., Akylas, E., Tombrou, A., Fairall, C. W., Fernando,
H. J. S., Baklanov, A. A. and Joffre, S. M. 2006. The influence of large convective eddies on the surface layer turbulence. Quarterly Journal of the Royal Meteorological Society, 132, 1423-1456.

THE DEVELOPMENT AND EVALUATION OF DISPERSION MODELS FOR URBAN AREAS

Wenjun Qian, David Pankratz, Jing Yuan, Tao Zhan, and Akula Venkatram
University of California, Riverside, CA, 92521

ABSTRACT

The paper summarizes results from a five year program to develop dispersion models for releases in urban areas at source-receptor distances ranging from tens of meters to tens of kilometers. Field studies were conducted in several urban locations to collect data required to develop and evaluate these models. In these studies, a tracer, SF_6, was released at several heights within the urban layer and sampled along arcs at distances ranging from a few meters to several kilometers from the release. Concurrent measurements were made to characterize the mean and turbulent structure of the urban boundary layer.

1. INTRODUCTION

The urban boundary layer can be divided into the following regions (Rotach, 1993): 1) the urban canopy, which refers to the layer below the average building height, 2) the roughness sub-layer (RSL), which extends to 2-5 times the average building height, 3) the urban boundary layer, and 4) the inertial layer, which represents transition between the RSL and the urban boundary layer. In modeling dispersion, it is convenient to divide the boundary layer into layers: the RSL, and the rest of the boundary layer (BL). In the RSL, the mean flow and turbulence are modified by the details of the building geometry. The flow above the RSL senses the average roughness of the buildings, and the turbulence is generated by surface heating as well as shear. The field studies, described next, were designed to examine dispersion in each of these layers.

2. DUGWAY AND CE-CERT STUDIES

Two field studies were conducted to understand dispersion within the urban canopy and the RSL. The first was conducted at the Dugway Proving Ground, Utah, from 17 to 26 July 2001. The experiment was designed to simulate a source in an urban area modeled at a scale of roughly 1:10. The model urban canopy was constructed with 55-gallon drums laid out in a 5 by 9 array. Propylene (C_3H_6), the tracer, was released and sampled at 3 receptor arcs both within the barrel array and over flat terrain. Turbulence, velocity, and temperature were measured with sonic anemometers.

The second experiment was conducted at a parking lot of the College of Engineering's Center for Environmental Research and Technology (CE-CERT) at the University of California, Riverside. During the experiment, SF_6 was released at ambient temperature from the top of a trailer situated in a parking lot surrounded by buildings. The height of release was 3.2 m. SF_6 concentrations were measured continuously along two arcs, located to the east and downwind of the emission source at 10 and 20m arcs. In addition, SF_6 concentrations were continuously measured at six locations on all sides of the trailer, each at a distance of 2–5m from the source. Meteorological observations were made at 3 m using a sonic anemometer located on the 20m arc.

Our analysis of the data from Dugway and the CE-CERT experiments indicate that

1. Horizontal and vertical plume spreads observed within the urban canopy and RSL are enhanced over those in flat terrain.
2. The dilution velocities observed with the urban canopy were about twice of those measured in the absence of obstacles, resulting in smaller centerline concentrations in the presence of obstacles.
3. Given appropriate on-site measurements of mean wind and turbulence within the urban canopy, a simple dispersion model, formulated in terms of the probability density function of the wind direction, can explain the maximum ground-level concentrations near the release. The enhanced horizontal plume dispersion associated with the urban canopy is automatically accounted through the use of on-site meteorology.

3. BARRIO LOGAN STUDY

This study was conducted in Barrio Logan, a suburb of San Diego, over a five day period between 21 August, 2001 to 31 August, 2001. A tracer, SF_6, was released from a height of 5 m in the middle of a shipyard over periods lasting from 7 to 10 h each day. The tracer was sampled with bag samplers at ground-level on four arcs at 200, 500, 1000 and 2000 m from the release. The meteorological conditions that governed dispersion were measured using sonic anemometers and a SODAR with a range of 200 m in the vertical. The detailed design and implementation of this field study are described in Venkatram et al (2004).

The ground-level concentrations were governed by the meteorological variables in the urban boundary layer, and are described by

$$C_{max}(x) = \frac{Q}{\pi u_{dil} x^2}, \quad (1)$$

where the dilution velocity, u_{dil}, is given by

$$u_{dil} = \frac{\sigma_w \sigma_v}{U}. \quad (2)$$

The variables in Equation (2) represent averages over a height of 50m.

The analysis of meteorological and dispersion data collected during the Barrio Logan experiment led to the following conclusions:

1. The turbulent intensities varied by less than 20% in the vertical in the BL. This allowed us to describe the turbulent spread of plumes embedded in this layer in terms of an overall turbulent intensity and distance from release.
2. The plume from the near surface source underwent rapid horizontal growth within the urban canopy before dispersing into the urban boundary layer. In our case, the rapid vertical growth was not discernable at the closest receptor at 200 m.

4. WILMINGTON FIELD STUDIES

The first field study was conducted in Wilmington, a suburb of Los Angeles, during 8 days in the period 26 August–10 September 2004. The tracer, SF_6, was released at a height of 3 m from a power plant site on the shoreline, and the concentrations of the tracer were sampled on five arcs at 100, 400, 1000, 3000, and 5000 m from the source during 6 h of the day starting at 7 a.m. The meteorological conditions that governed dispersion were measured using sonic anemometers and sodars. The temperature from near surface to up to about 600 meters was measured there using a remote sensing microwave temperature profiler.

The data analysis indicated that even during summer, the stability of the onshore flow was strong enough to keep the height of the thermal internal boundary layer (TIBL) below 150 m at distances of 5000 m from the shoreline. Yuan et al (2006) showed that Equation (1) provided an adequate explanation of the behavior of the ground-level concentrations until the vertical spread of the plume was limited by the height of the thermal internal boundary layer.

Another field study, which focused on elevated tracer releases, was conducted in Wilmington between June 24th and June 28th 2005. Two types of releases were used: non-buoyant releases 3 m below the top of the 67 m stack, and releases into the buoyant stack gases. Each experiment involved release of the tracer gas, sulfur hexafluoride (SF_6), over periods lasting from 5 to 6 hours during each day of the four day experiment. Integrated box samplers were deployed along three arcs with distances of 1000 m, 3000 m and 5000 m north to the source.

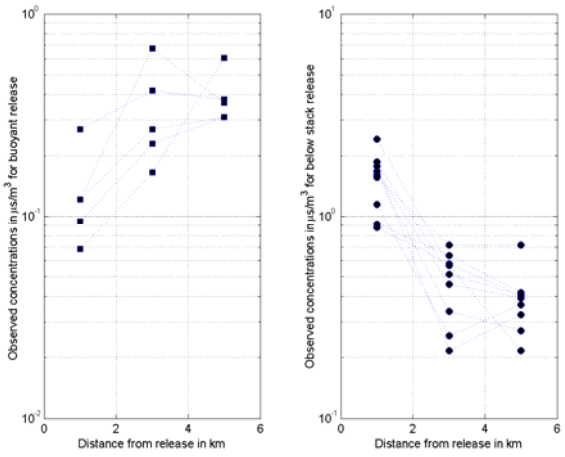

Figure 1: Variation of observed concentrations with distance from release.

Figure 1 compares the concentrations observed during the two sets of experiments, one corresponding to the release 3 m below stack height, and the other corresponding to the release into the exhaust gases. The left panel shows that concentrations resulting from the in-stack buoyant release results in concentrations around 0.1 μs/m^3 at a distance of 1 km, which then increase to about 0.5 μs/m^3 at distances between 3 and 5 km. The concentrations for the below stack top release at 64 m behave similarly to the surface releases conducted in 2004: the concentrations decrease with distance. Most of the observations are above 1 μs/m^3 at 1 km from release, and decrease to about 0.4 μs/m^3 at 5 km.

The gradual entrainment of the elevated plume by the internal boundary layer was modeled using Misra's (1980) model which treats the entrained plume as a series of point sources whose strength depends on the rate of entrainment by the TIBL and the vertical growth of the plume. Assuming that the entrained plume material is instantaneously mixed through the depth of the TIBL, the ground-level concentration is given by the sum of the contributions of all the upwind point sources. The model applies to both buoyant and non-buoyant releases, as long as different buoyant parameters and release heights are used for these releases.

The major conclusions of the Wilmington studies are:

1. Relatively simple dispersion models can be used to estimate ground-level concentrations caused by near surface or elevated sources, such as power plants. The inputs to these models consist of turbulent and mean velocities averaged over the depth of the thermal internal boundary layer that forms when stable air over water flows onto warmer land.
2. The thermal internal boundary layer (TIBL) plays a crucial role in determining concentrations associated with both surface as well as elevated releases on the shoreline. Concentrations caused by elevated sources are sensitive to the growth of the TIBL as a function of distance from the shoreline because ground-level concentrations are determined by the entrainment of the plume by the growing TIBL. The TIBL height limits the vertical extent of the plume for surface releases.

Thus, the problem of estimating concentrations in an urban area reduces to estimating the characteristics of the urban boundary layer using routinely available information, such as that from airports. The next section describes progress in this area.

5. RELATIONSHIPS BETWEEN URBAN AND RURAL MICROMETEOROLOGY

Dispersion of releases in urban areas can be estimated with information on micrometeorological variables in the urban boundary layer. Because this information is not generally available, we developed a method to estimate urban variables from rural measurements. The method is based on a two-dimensional internal boundary layer (Luhar et al, 2006) model that uses Monin-Obukhov surface similarity theory and rural variables as upwind inputs. The model assumes that the urban Obukhov length is the same as that in the rural area under unstable conditions and is infinity (neutral) when rural conditions are stable. The model was evaluated with data from the Basel UrBan Boundary Layer Experiment (BUBBLE), conducted during June and July 2002 around Basel, Switzerland. The internal boundary-layer (IBL) scheme incorporates the effects of the urban roughness length and, to a limited extent, those of thermal properties of the surface and anthropogenic heat flux by assuming a neutral stability in the nighttime. Although this scheme yields results that compare well with observations, it cannot estimate the urban heat flux when rural conditions are stable.

We have also developed a method to compute variables in the TIBL relevant to dispersion. The expression for the convectively generated component of turbulence in the TIBL is

$$\sigma_{wc} = \alpha Q_o^{1/2} \left(\frac{g}{T_o} \right)^{1/3} \left(\frac{2(1+2A)x}{U\gamma} \right)^{1/6}, \qquad (3)$$

The surface heat flux, Q_o, required to compute the TIBL height is estimated through a surface energy balance over land. The surface friction velocity is computed by assuming that we know the mean wind speed well above the urban canopy. In practice, this wind speed can be estimated by extrapolating upwards from routinely available surface information, such as that from an airport, and assuming that the wind speed at the chosen level is the same at the urban location.

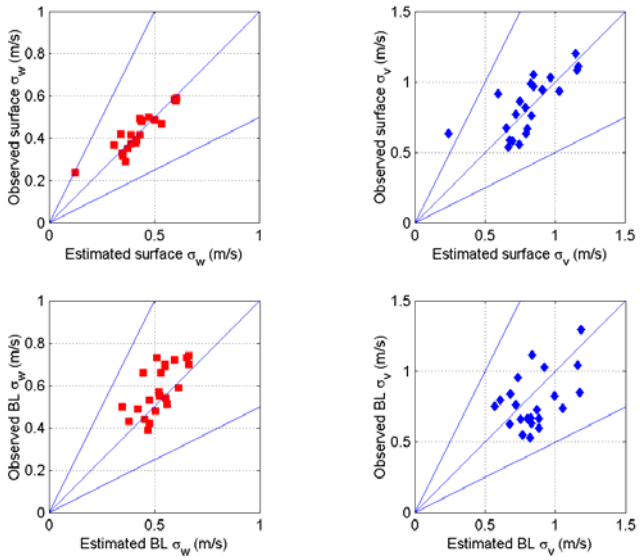

Figure 2: Comparison of estimated surface and 50 m (BL) turbulence levels with observations made at the LADWP site for Wilmington 2004 study.

Figure 2 compares estimated turbulence levels at the surface and at 50 m with observations made with the sonic anemometer and the sodar during the Wilmington 2004 study. The convective component of the turbulent velocity is evaluated at a distance of 100 m from the shoreline, corresponding to the location of the measurements at the release. The estimated values of turbulent velocities are well within a factor of the observations. The comparison between estimated and observed values of σ_v might be fortuitous because observations are likely to be controlled by large scale wind meandering that is not accounted for in the estimates.

6. ACKNOWLEDGEMENTS

The research summarized here was funded by California Air Resources Board (CARB), California Energy Commission (CEC), and the National Science Foundation through Grant ATMOS 0430776.

.

7. REFERENCES

Luhar, A.K., Venkatram, A., Lee, Sang-Mi, 2006: On relationship between urban and rural surface meteorology for diffusion applications. Atmospheric Environment 40, 6541-6553

Misra, P. K., 1980: Dispersion from tall stacks into a shore line. Atmospheric Environment 14, 397-400.

Rotach, M.W., 1993: Turbulence close to a rough urban surface part I: Reynolds stress. Boundary-Layer Meteorology 65, 1-28.

Venkatram, A., Isakov, V., Pankratz, D., Heumann, J., and Yuan, J., 2004: The analysis of data from an urban dispersion experiment. Atmospheric Environment, 38(22), 3647-3659

Yuan, J., Venkatram, A., and Isakov, V., 2006: Dispersion from ground-level sources in a shoreline urban area. Atmospheric Environment, 40(7), 1361-1372

ON THE REPRESENTATION OF THE STABLE BOUNDARY LAYER OVER THE LONDON METROPOLITAN AREA IN MESOSCALE MODELS

C. Chemel*, Y. Yu, E. Somervell, and R. S. Sokhi
Centre for Atmospheric & Instrumentation Research (CAIR), University of Hertfordshire, Hatfield, UK

ABSTRACT

Under stable conditions numerous boundary-layer parameterization schemes can fail to correctly reproduce momentum and heat fluxes over flat and homogeneous terrain. In the case of urban areas, which are intrinsically heterogeneous, the representation of stable boundary-layer (SBL) characteristics in numerical models is even more challenging. The overall objective of this study is to investigate the performance of urban boundary-layer modelling under stable conditions, using a set of models (namely ARPS, MM5 and UM) which contain some similarities but also differences in the way urban areas are treated. Numerical simulations are used to characterize the SBL over the London urban area (UK) for a selected pollution episode in February 2003, which led to high concentrations of pollutants including PM_{10} over Southern England. The results are discussed focusing on identification of most appropriate ways of representing the effects of the urban area on the SBL.

1. INTRODUCTION

The atmospheric boundary layer is usually stably stratified during night over land or sea ice when heat is lost at the surface due to either imbalance in radiation or advection of warm air above a colder surface. Near the surface, turbulence drives the vertical exchanges of momentum, heat, moisture and other atmospheric constituents. Note that in the stable boundary layer (SBL), turbulence is mainly generated by wind shear. Whilst vertical fluxes in the convectively-driven boundary layer are carried by large convective motions spanning most of the mixed layer, vertical motions are strongly inhibited in the SBL, especially in nocturnal conditions. Nonetheless dynamical instabilities can appear and contribute significantly to the mixing of the air mass. In addition, over complex terrain and in urban areas, the boundary layer is characterized by enhanced mixing as well as larger drag effect when compared with homogeneous flat terrain in rural areas. The increase in surface heating in urban areas is an additional source of mixing which can be further promoted by the large surface roughness. Hence, the stability of the boundary layer is somewhat compensated by the urban heat island (UHI) that is likely to form over urban area. Urban areas may be regarded as highly heterogeneous terrain, over which the boundary layer is affected by changes of both surface roughness and heat flux. The typical vertical structure of the boundary layer over urban areas is illustrated in Figure 1.

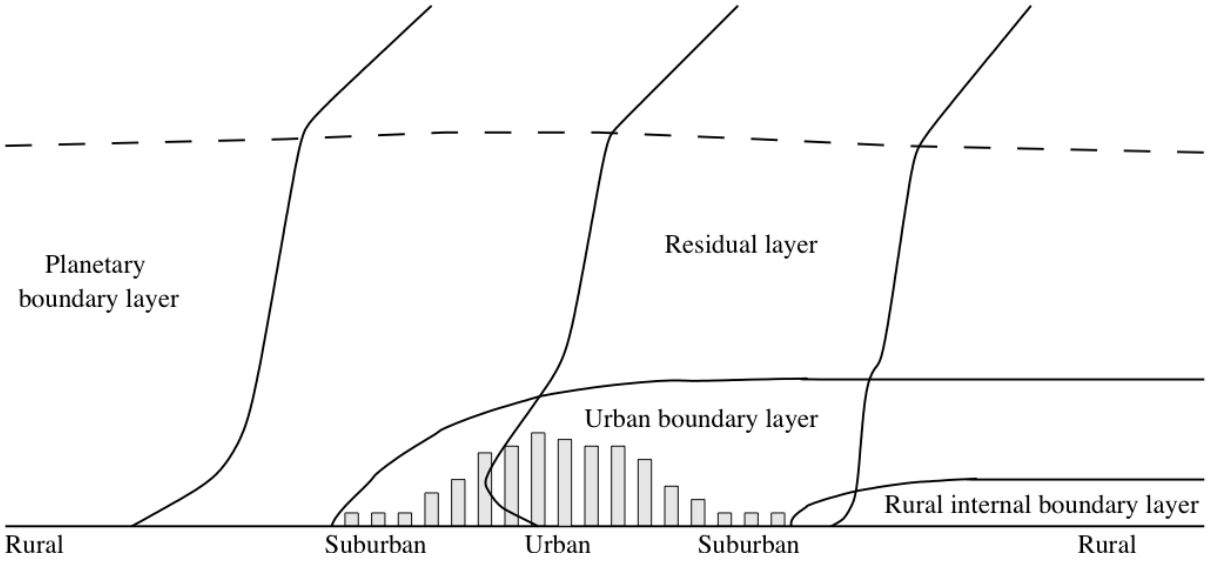

Figure 1. Structure of the urban boundary layer under stable conditions (adapted from COST715, 2005, p. 41)

*Corresponding author address: Dr. Charles Chemel, Centre for Atmospheric and Instrumentation Research, University of Hertfordshire, College Lane Campus, Hatfield, Herts AL10 9AB, United Kingdom (e-mail: c.chemel@herts.ac.uk).

The key issue is the understanding of turbulence and mixing in stable layers and its representation in numerical models, i.e. the parameterization of fluxes. When a fine description is adopted, as in meso-scale or large-eddy simulation models, the urban features modify subgrid-scale quantities, especially fluxes (e.g. Oke, 1988). At larger scales, the cornerstone of the current understanding of turbulence in the SBL is the Monin-Obukhov similarity theory. However this theory, and the parameterizations based on it, is deficient either when turbulence is strongly intermittent, as is the case in the SBL (e.g. Steeneveld et al., 2006), or in the urban roughness sublayer (e.g. Rotach, 1993). Hence, the representation of stable boundary-layer characteristics in numerical models is particularly challenging for urban areas. The main purpose of this study is to investigate the performance of urban boundary-layer modelling over the London urban area during (weak wind) stable conditions for a selected pollution episode in February 2003. Numerical simulations have been conducted with a set of models (namely ARPS, MM5 and UM), which contain similarities but slightly different functionalities such as the degree of complexity of the representation of the urban canopy. The outline of this short paper is as follows. In § 2, the case study is detailed and the modelling tools are described, the emphasis being put on the representation of urban features. In § 3, selected results from one of the models (namely MM5) are used to highlight the balancing effect between the suppression of mixing due to the strong stability of the atmosphere and the enhancing of mixing by the urban area. Conclusions are given in § 4.

2. METHODOLOGY

During the episode (19-23 February 2003), particularly stable and weak wind atmospheric conditions led to high concentrations of smog-forming pollutants and PM_{10} over Southern England, UK (e.g. Kukkonen et al., 2005). Nocturnal temperature profiles show that there was a slight ground-based temperature inversion continuously during this episode. Nonetheless, the temperature only increased from approximately 1 to 4 K within the lowest 200 m of the atmosphere. Hence, it is likely that the UHI reduces the stratification of the lower layers of the atmosphere and mixes surface-based pollutants, which are trapped below the shallow temperature inversion.

As mentioned previously, a set of models, namely ARPS (Xue et al., 2000), MM5 (Grell et al., 1995) and UM (Davies et al., 2005), have been used with several nested grids to reproduce this episode down to a horizontal resolution of 1 km. In § 3, we will present results from the 3-km horizontal resolution domain. Whichever model is used to parameterize the urban surface, its characteristics are usually based on classes of land use. The urban environment represents only one class in most of the parameterization schemes. In our case, the simplest approach to account for the presence of an urban area is to use the same as in rural areas but use larger surface roughness lengths and different soil thermal characteristics for each urban grid cell. This approach is used in our MM5 calculations. As for UM, it treats urban areas through the urban tile for each grid cell that covers an urban area. The urban tile then contributes to the average fluxes in proportion to its percentage in each grid cell. This approach is more realistic than the single urban class assigned to each grid cell in MM5. However, the approach used in either MM5 or UM may be insufficient since it considers sink of momentum at the first grid level only rather than all over the height of the buildings. Indeed, on site observations (e.g. Roth and Oke, 1993) as well as wind tunnel experiments (Kastner-Klein et al., 2001) showed that fluxes are height-dependent in the roughness sublayer. Hence, an add-on urban surface exchange parameterization module (Martilli et al., 2002) has been implemented into the ARPS model to represent urban area using possibly more than one urban class. This module (referred as to BEP) considers roofs, walls and canyon floor as active surfaces and discretizes the buildings within an urban grid. BEP is set up so that the effects of urban surfaces on momentum and heat fluxes are calculated in proportion to the corresponding surface fraction at each level of the urban grid. On top of that, BEP uses fractional volumes, which can actually break up the flow through the grid. Note that for grid cells containing both urban and rural areas, fluxes are calculated separately for the two surface types and are then weighted according to the percentages of each type within each grid cell.

3. RESULTS AND DISCUSSION

For this short paper only results from MM5 are discussed. As urban surfaces (roofs, walls and canyon floor) convert incoming radiation into sensible heat flux and also store it more efficiently than rural area, urban areas are generally warmer than its surroundings. Rural and suburban temperature evolutions reveal larger diurnal amplitude than in urban areas (not shown), where heat accumulated during daytime is released during nighttime. The average urban heat island index was usually found to be in the order of 1 K at night and 3 K during the day. This result is consistent with the range of values obtained in previous studies (e.g. Watkins et al., 2002). This suggests that the urban area is appropriately described in the model. Nonetheless, it was found that the model overestimates nighttime cooling over urban areas. Thus, to evaluate further the ability of the urban parameterization scheme to mimic urban effects, we can quantify its impact on the local friction velocity and

sensible heat flux during both nighttime and daytime.

The friction velocity u_* is increased in urban areas when compared with values over rural areas during both nighttime and daytime (see Figure 2). Consequently, the flow decelerates within the urban canopy, consistently with observations. However, the model is not able to reproduce any velocity gradients at roof level because the first grid level only is modified by urban features. The UM is similar in this respect and is not able to capture this effect either, but the ARPS model using BEP produces more promising results (not shown).

The impact of urban land cover on sensible heat flux H is rather strong. Indeed, H values may be up to twice in urban areas as those over rural areas during daytime (see Figure 3a). As for nighttime conditions, H does not remain significantly larger in urban areas than over rural areas (see Figure 3b). This supports the fact that the model overestimates nighttime cooling over urban areas. Also, the presence of large park areas in the city has the effect of cooling the air temperature within and downwind of the parks. However this modelled effect is too strong when compared to measurements (not shown). It suggests that heat (and momentum fluxes) actually needs to be weighted by the fraction of each landuse type as is the case for UM and ARPS. Note that results from UM as well as ARPS are in better agreement with measurements than MM5 (not shown).

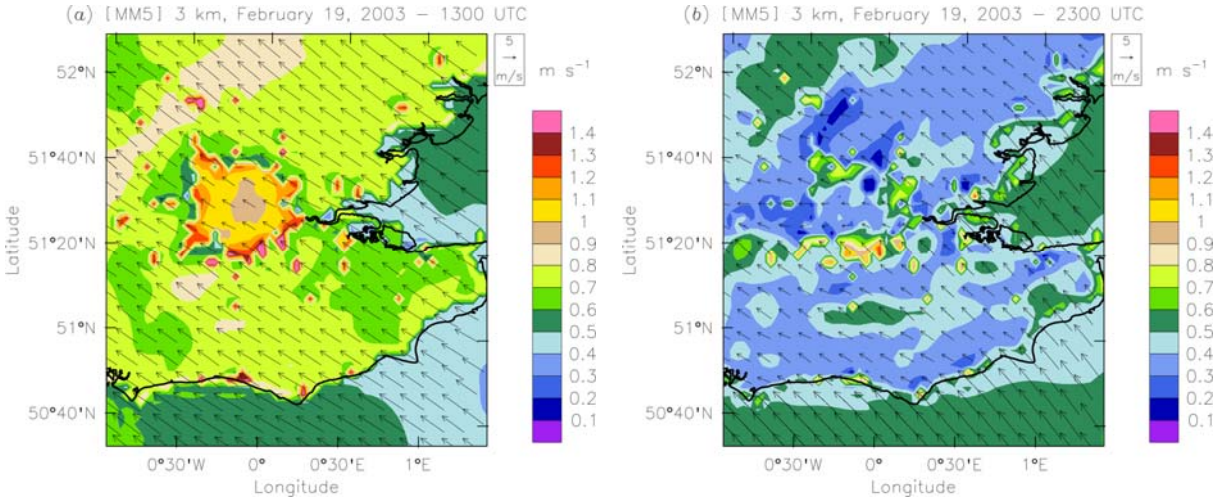

Figure 2. Friction velocity u_* from MM5 calculations on February 19, 2003: (*a*) 1300 UTC and (*b*) 2300 UTC

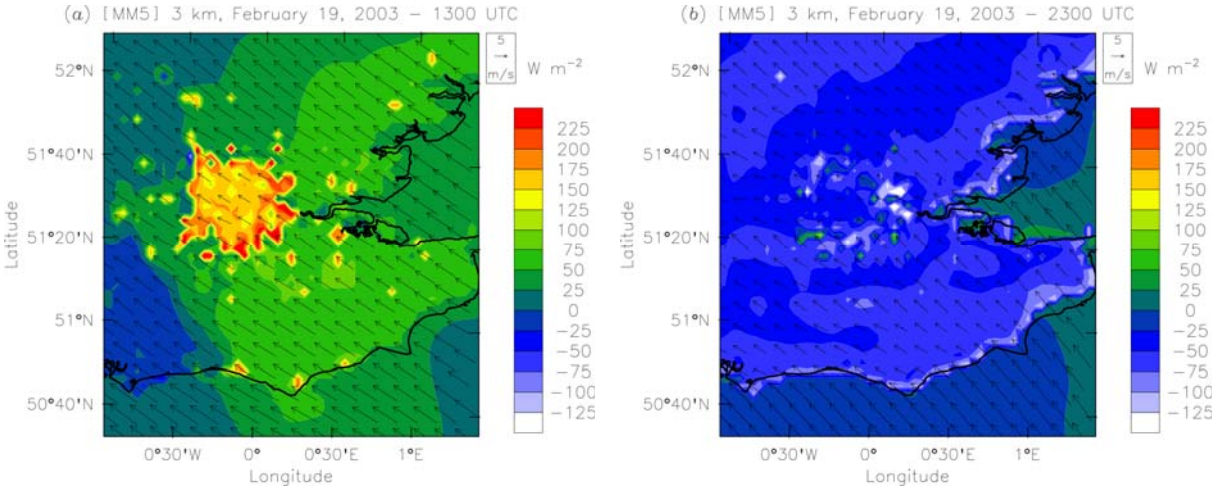

Figure 3. Sensible heat flux H from MM5 calculations on February 19, 2003: (*a*) 1300 UTC and (*b*) 2300 UTC

4. CONCLUSIONS

The selected MM5 results presented in this paper have shown that, for the specific pollution episode of February 2003, the London metropolitan area is on average 1 K warmer than the outskirts during nighttime whilst being 3 K warmer during daytime. The urban heat island index also varies with time of day as well as weather conditions, but is overall quite large during daytime. It should be noted that wind speeds measured in the city were low during that period. That might enable the canyon streets to develop their own microclimate when compared with days with advection and mixing with air masses from adjacent areas. The representation of the urban areas in our calculations is able to capture most of the urban-induced processes such as the UHI. It was found (not shown) that when using either UM or ARPS, both simulated temperature and wind fields are in better agreement with measurements. Nonetheless, the sensible heat flux is still too low at night in UM. The simulated heat flux in ARPS is more realistic possibly due to redistribution of the heat flux throughout the roughness sublayer.

As stated in our initial objective, further research is required on the performance of the numerical weather prediction models to take the step forward by focusing on identification of most appropriate ways of representing the effects of the urban area on the SBL.

5. ACKNOWLEDGEMENTS

This study has been conducted as part of COST Action 728, which aims at enhancing meso-scale meteorological modelling capabilities for air pollution and dispersion applications (see http://www.cost728.org). We thank Alain Clappier for providing us with the BEP module and for helpful discussions on urbanization of meso-scale model.

6. REFERENCES

COST715, 2005. The urban surface energy budget and mixing height in European cities: data, models and challenges for urban meteorology and air quality. Final report of Working Group 2. Demetra Ltd Publishers, Bulgaria, 239 pp.

Davies, T., M. J. P. Cullen, A. J. Malcolm, M. H. Mawson, A. Staniforth, A. A. White, and N. Wood, 2005. A new dynamical core for the Met Office's global and regional modelling of the atmosphere. *Quart. J. Roy. Meteorol. Soc.* **608**, 1759-1782.

Grell, G. A., J. Dudhia, and D. R. Stauffer, 1995. *A description of the Fifth-Generation Penn State/NCAR Meso-scale Model (MM5).* NCAR Technical Note NCAR/TN-398+STR, NCAR, Boulder, CO, USA, 117 pp.

Kastner-Klein, P., E. Fedorovich, and M. W. Rotach, 2001. A wind tunnel study of organized and turbulent air motions in urban street canyons. *J. Wind Eng. Ind. Aerodyn.* **89**, 849-861.

Kukkonen, J., M. Pohjola, R. S. Sokhi, L. Luhana, N. Kitwiroon, L. Fragkou, M. Rantamäki, E. Berge, V. Ødegaard, L. H. Slørdal, B. Denby, and S. Finardi, 2005. Analysis and evaluation of selected local-scale PM10 air pollution episodes in four European cities: Helsinki, London, Milan and Oslo. *Atm. Environ.*, **39**, 2759-2773.

Martilli, A., A. Clappier, and M. W. Rotach, 2002. An urban surface exchange parameterization for mesoscale models. *Boundary-Layer Meteorol.* **104**, 261-304.

Oke, T. R., 1988. The urban energy balance. *Prog. Phys. Geogr.* **12**, 471-508.

Rotach, M. W., 1993. Turbulence close to a rough urban surface. Part II: Variances and gradients. *Boundary-Layer Meteorol.* **66**, 75-92.

Roth, M. and T. R. Oke, 1993. Turbulent transfer relationships over an urban surface. I: Spectral characteristics. *Quart. J. Roy. Meteorol. Soc.* **119**, 1071-1104.

Steeneveld, G. J., B. J. H. van de Wiel, and A. A. M. Holtslag, 2006. Modeling the evolution of the atmospheric boundary layer coupled to the land surface for three contrasting nights in CASES-99. *J. Atmos. Sci.* **63**, 920-935.

Watkins, R., J. Palmer, M. Kolokotroni, P. Littlefair, 2002. The London heat island - results from summertime monitoring. *Build. Serv. Eng. Res. Tech.* **23**, 97-106.

Xue, M., K. K. Droegemeier, and V. Wong, 2000. The Advanced Regional Prediction System (ARPS) – A multi-scale non hydrostatic atmospheric simulation and prediction model. Part I: Model dynamics and verification. *Met. Atm. Phys.* **75**, 161-193.

SWISS-CANADIAN RESEARCH ON AEROSOL MODELLING (SCRAM)

Ş. Andreani-Aksoyoğlu[1], J. Keller[1], M.R. Alfarra[1], A.S.H. Prévôt[1], J.J. Sloan[2], S. Taghavi[2], S. Nikzad[2], Z. He[2]

[1]Laboratory of Atmospheric Chemistry (LAC), Paul Scherrer Institute, Switzerland
[2]Waterloo Centre for Atmospheric Sciences (WCAS), University of Waterloo, Canada

ABSTRACT

The SCRAM Project (Swiss-Canadian Research on Aerosol Modelling) is a collaboration between two research groups to assess the importance of particulate matter in the regional atmospheres in Switzerland and southern Ontario. In this study, two state-of-the-art chemical transport models are applied to simulate meteorology and tropospheric chemistry with a focus on the formation and transport of particulate matter (PM) in Switzerland for a period in winter 2006 and in Southern Ontario in summer 2001. The application of two models with different aerosol modules (CAMx and CMAQ-MADRID) on the same domains will provide unique information about the strengths and/or weaknesses of models. In this paper, the progress of the SCRAM project is reported. The preparation of emission inventory and the modelling of the meteorological parameters for the period between 1 January and 10 February 2006 over the Swiss domains have been completed and simulations with the air quality model CAMx have already started. The results of the first 14 days of the Swiss simulations look promising. The measurements with the aerosol mass spectrometer (AMS) and model predictions show that the particle mass concentrations are dominated by organic and nitrate aerosols at urban and motorway sites. The modelled concentrations of inorganic aerosols agree better with the measurements while organics are underestimated. The CAMx model predicts that the organic aerosols are mostly primary and the secondary organic aerosols (SOA) formed from biogenic emissions dominate the total SOA concentrations at the urban site. The detailed comparison of the model results with measurements will be reported later as soon as the modelling of whole period is completed. The meteorological modelling and preparation of emission inventory have also been completed over the Southern Ontario domains and simulations with CMAQ-MADRID model are in progress.

1. INTRODUCTION

The important role of aerosols in many issues such as climate change, acid rain and human health has been qualitatively known for a long time, but there is still a lack of quantitative knowledge of the important atmospheric processes they affect, such as heterogeneous chemistry and cloud formation. Aerosol effects depend strongly on their chemical compositions and size distributions. This makes prediction of their influences very complicated because of their chemical diversity and their rapid evolution in the atmosphere.

Detailed modelling of atmospheric aerosols has only recently been undertaken in the context of regional chemical transport modelling (CTM) systems (Zhang et al., 2004, Held et al., 2004). Modelling secondary organic aerosol (SOA) formation is among the most demanding aspects associated with atmospheric organic photo-oxidation. Recent experimental evidence for polymerization reactions of organic aerosols indicated the need to readdress the current assumptions in models about the partitioning of oxidation products in the gas and the particle phase (Kalberer et al., 2004). In order to develop appropriate control strategies, the partitioning behaviour of semi-volatile species between the gas and aerosol phases must be well understood.

In the project SCRAM, we are using two state-of-the-art CTMs to simulate the formation and transport of aerosols in Switzerland and in Southern Ontario under different meteorological conditions. At the Laboratory of Atmospheric Chemistry (LAC) in Switzerland, we currently use the photochemical model CAMx Version 4.40 (Comprehensive Air Quality Model with extensions) (Environ, 2006) and the meteorological model MM5 Version 3.7.2 (PSU/NCAR, 2005). The aerosol modelling is done using the ISORROPIA and SOAP modules of CAMx. The CTM used by the Waterloo Centre for Atmospheric Sciences (WCAS) in Canada consists of the Models-3/CMAQ system, driven by MM5 meteorology. Aerosol modelling in the CMAQ system is done using the Model of Aerosol Dynamics, Reaction, Ionization, and Dissolution (MADRID) model (Zhang, et al., 2004). The combination of the models used in this study is capable of addressing all of the state-of-the-art nonlinear chemical interactions encountered in these complex air-particle systems and their results can be used as the basis for alternative control strategies. Application of two different aerosol models to study the formation and transport of aerosols over the complex terrain of Switzerland and in the Great Lakes region in southern Ontario will provide unique information about the strengths and weaknesses of the models.

2. METHODOLOGY

We applied the MM5/CAMx system to the Swiss region of interest using three nested domains with 27 (Europe), 9 (Switzerland and neighbouring countries) and 3 km (Switzerland) resolution. The winter period for the Swiss simulations starts on 1 January and ends on 10 February 2006. The concentrations of aerosols with diameters smaller than 2.5 µm were calculated. Initial and boundary conditions for the Swiss domains were prepared using model data for similar winter periods calculated by the global model MOZART. A standard emission inventory for Switzerland and surrounding countries has been developed including both anthropogenic and biogenic gaseous as well as particle emissions. The methodology of meteorological modelling is described by Keller et al., (2007).

Quantitative measurements of the size-resolved mass distribution of aerosols with diameters smaller than 1 µm were performed by an Aerosol Mass Spectrometer (AMS) at the urban site Zurich and at the motorway site Reiden. There are also hourly average gaseous and PM10 concentrations available from the national air pollution monitoring network stations (NABEL).

The MM5/CMAQ-MADRID system is operated by the WCAS. The Canadian domains have 36, 12 and 4 km resolution, covering Eastern North America, the Great Lakes and Southern Ontario, respectively. Canadian simulations cover July-August 2001. Emissions are prepared using the SMOKE emission model.

3. RESULTS AND DISCUSSION

The AMS measurements performed at urban (Zurich) and motorway (Reiden) sites in northern Switzerland indicated that organics and nitrates are the major components of the aerosol composition in winter (Figure 1). The total concentrations of the aerosol mass reached values of about 70 µg/m^3 on 13 January in Zurich. The particle concentrations decreased later due to precipitation. They started increasing again towards the end of the month. On the other hand, particle concentrations measured at the motorway site Reiden reached 150 µg/m^3 at the beginning of February.

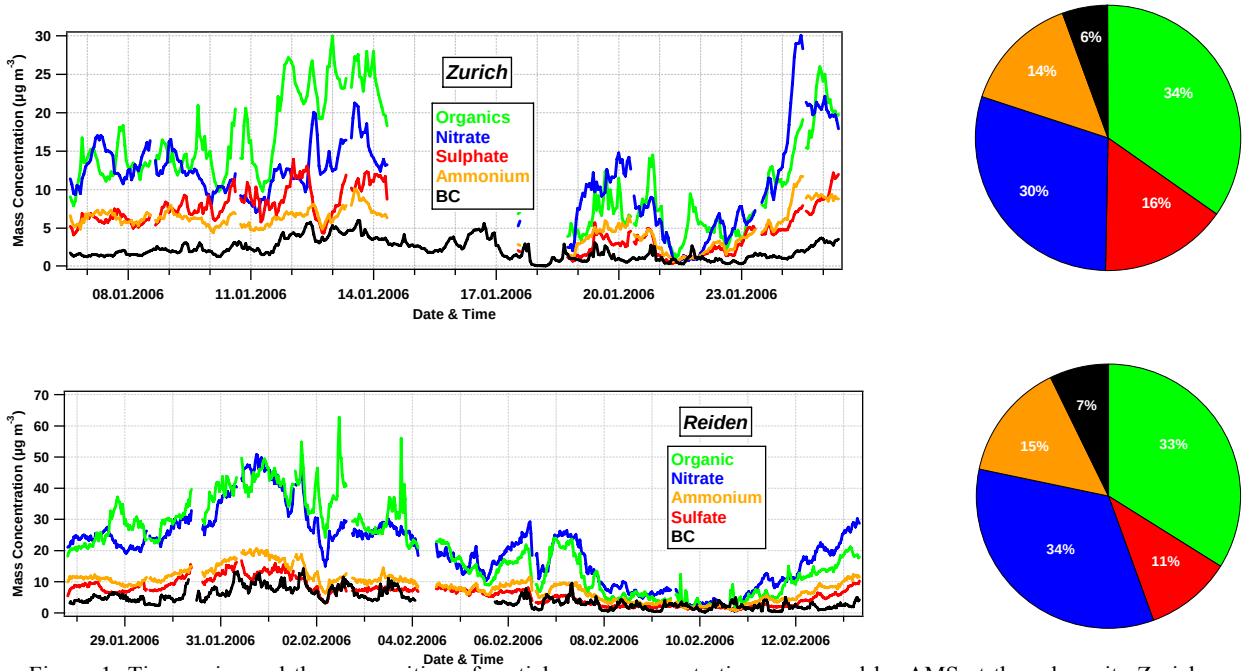

Figure 1: Time series and the composition of particle mass concentrations measured by AMS at the urban site Zurich (above) and motorway site Reiden (below). The pie charts are the averages over the whole period.

At present, the preliminary results of the CAMx model are available for the first 2 weeks of January. The concentrations of gaseous species (CO shown as an example in Figure 2) were reproduced quite well at Zurich during the first week when the wind speed was moderate. The agreement with the measurements becomes worse during the second week when the wind speed was very low and meteorological modelling was difficult.

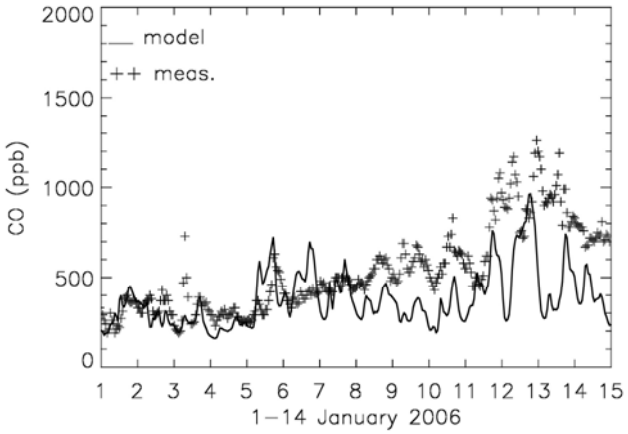

Figure 2: Measured (BAFU/NABEL) and modelled (CAMx) concentrations of CO (ppb) at Zurich.

The daily variations of the modelled aerosol concentrations look similar to those of the measurements (Figure 3). The highest aerosol concentration during the first 2 weeks was on 13 January both by the model and the measurements (see Figures 1 and 3). The aerosol mass concentrations of inorganic aerosols such as particulate nitrate, sulphate and ammonium are in acceptable agreement with the measurements. The contribution of individual particles to the total mass concentration was predicted reasonably well by the model. The model results indicate that the aerosol composition is dominated by organics and nitrate aerosols at the urban site showing a good agreement with the AMS measurements. The primary particle emissions might be overestimated. On the other hand, the modelled concentrations of the total organic aerosols are lower than the measurements, probably due to underestimation of SOA formation. This leads to a general underestimation of the total aerosol concentrations. The predicted organic aerosol concentrations are mainly from the primary sources (POA). On the other hand, the contribution of SOA formed from the biogenic emissions to the total SOA concentrations is much larger (80 %) than that of the anthropogenic sources.

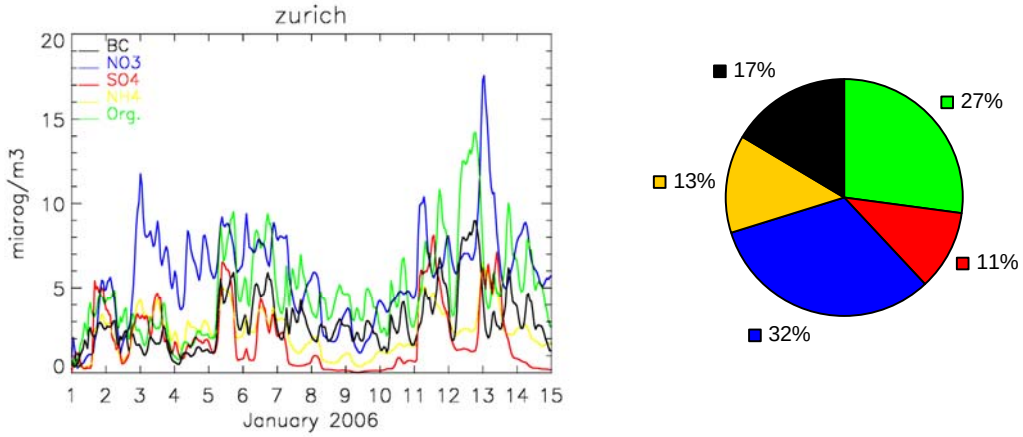

Figure 3: Aerosol concentrations and the composition of particles (d < 2.5 μm) modelled by CAMx in Zurich.

The detailed evaluation of the model results will be carried out when the simulations of the whole period is completed. Improvement of the meteorological model parameterization may help improving the CAMx results. Modelling of the same period with CMAQ-MADRID will provide us with information about the capabilities of the two different aerosol modules.

The meteorological modelling and the preparation of emission inventory have also been completed for the Southern Ontario domains and simulations with CMAQ-MADRID model are in progress (Sloan et al., 2007). Measurements of PM in Southern Ontario and Western Quebec suggest that particulate sulphate is in general the major component of the aerosol composition (Sloan et al., 2007).

4. CONCLUSIONS

The progress in the SCRAM project was reported in this paper. The project covers the modelling of aerosols in winter and summer periods over Switzerland and Southern Ontario, respectively, using two state-of-the-art aerosol models. The meteorological modelling and the preparation of emission inventories for both domains have been completed. Modelling studies with the CAMx model over the Swiss domains have started and preliminary results of the first two weeks were reported here. Simulations for the rest of the period are still ongoing.

The preliminary results of the first 2 weeks look promising in spite of the difficulties in modelling of winter periods. Both measurements and model results indicate that the aerosol concentrations are dominated by organic and nitrate aerosols at urban and motorway sites. Highest particle concentrations during the first two weeks were measured on 13 January. CAMx predicted the daily variations of the aerosol concentrations very well. The predicted composition of particle mass concentrations by CAMx is similar to that from the AMS measurements, although total concentrations are underestimated probably due to the underestimation of SOA levels. Model results suggest that the organic aerosols are dominated by the primary particles. However, the primary particle emissions might be overestimated. On the other hand, biogenic SOA seems to dominate the total SOA concentrations in Zurich. The detailed evaluation of the results will be reported in the future when simulations of the whole period are completed.

5. ACKNOWLEDGEMENTS

This project is financially supported by the Federal Office for the Environment (FOEN) in Switzerland. In addition, the collaboration between PSI and WCAS was supported by the Interdisciplinary Tropospheric Research: from the laboratory to global change (INTROP) grant of the European Science Foundation (ESF). We acknowledge M. Schultz for providing us with MOZART data. PM10 data were taken from the national air pollution monitoring network stations BAFU/NABEL.

6. REFERENCES

Environ. 2006. User's Guide, Comprehensive Air Quality Model with Extensions (CAMx), Version 4.40, Environ International Corporation, California.

Held, T., Ying, Q., Kaduwela, A. and Kleeman, M. 2004. Modelling particulate matter in the San Joaquin Valley with a source-oriented externally mixed three-dimensional photochemical grid model, Atmospheric Environment, 38, 3689-3711.

Kalberer, M., Paulsen, D., Sax, M., Steinbacher, M., Dommen, J., Prévôt, A.S.H., Fisseha, R., Weingartner, E., Frankevic, V., Zenobi, R. and Baltensperger U. 2004. Identification of polymers as major components of atmospheric organic aerosols, Science, 303, 1659-1662.

Keller, J., Andreani-Aksoyoğlu, S., Prévôt, A.S.H, Sloan, J.J., He, Z., Foppa, N. 2007. Meteorological Modelling of winter and summer periods for the Swiss-Canadian Research Project on Aerosol Modelling (SCRAM). 6th International Conference on Urban Air Quality (UAQ 2007), March 27-29, 2007, Limassol (CYP), this conference.

PSU/NCAR. 2005. PSU/NCAR Mesoscale Modelling System. Tutorial Class Notes and User's Guide: MM5 Modelling System Version 3.

Sloan, J.J., Taghavi, S., Nikzad, S., He, Z., Brook, J., Andreani-Aksoyoğlu, S., Keller, J., Alfarra, M.R., Prévôt, A.S.H. 2007. Results of Regional Air Quality Model Simulations for the Swiss-Canadian Research on Aerosol Modelling (SCRAM) Project. 6th International Conference on Urban Air Quality (UAQ 2007), March 27-29, 2007, Limassol (CYP), this conference.

Zhang, Y., Pun, B., Vijayaraghavan, K., Wu, S.-Y., Seigneur, C., S. Pandis, N., Jacobson, M.Z., Nenes, A., Seinfeld, J.H. and Binkowski, F.S. 2004. Development and application of the model of aerosol dynamics, reaction, ionization and dissolution (MADRID), Journal of Geophysical Research, 109, doi:10.1029/2003JD003501.

SIMULATING THE ATMOSPHERIC TRANSPORT AND DEPOSITION OF BENZO(A)PYRENE OVER EUROPE IN 2000 WITH DIFFERENT TIME-VARIANT EMISSION SCENARIOS

Armin Aulinger, Volker Matthias, Markus Quante

GKSS Research Center, Max-Planck-Strasse 1, 21502 Geesthacht, Germany, armin.aulinger@gkss.de

1. Abstract

The effect of temporal variation of polycyclic aromatic hydrocarbon (PAH) emission data on transport and deposition patterns were simulated with the Community Multiscale Air Quality modelling system (CMAQ) for Europe, 54 km grid, for the year 2000. The carcinogenic benzo(a)pyrene (B(a)P) was used as a representative for the group of PAHs. The official emission data are only provided as one-year bulk emissions without information on temporal variability. However, the major emission sources of B(a)P vary within seasonal, diurnal and weekly cycles, respectively. An approach for implementing temporal variation on emission data is presented and compared to models that use constant or simply seasonally varying emissions.

2. Introduction

Polycyclic aromatic hydrocarbons (PAHs) are semivolatile, lipophilic persistent organic pollutants (POPs), which originate primarily from incomplete combustion of organic material. Surveys have revealed that a variety of PAHs possess a high carcinogenic potential to animals and humans (ATSDR, 1995) and are bio-accumulated in the food chain. They can be transported over long distances in the atmosphere resulting in a widespread distribution across the earth, including regions where they have never been used. Due to their toxic and ecotoxic characteristics they pose a threat to humans and the environment, and therefore the international community has called for actions to reduce and eliminate the release of POPs, such as the Protocol to the UN-ECE Convention on Long-range Transboundary Air Pollution (CLRTAP) on POPs.

To study the atmospheric transport and deposition of PAHs over Europe our research group used the Community Multiscale Air Quality (CMAQ) Modeling System developed under the leadership of the US Environmental Protection Agency (Byun and Ching, 1999; Byun and Schere, 2006) as basic model and extended it to treat semivolatile POPs, in particular PAHs. Benzo(a)pyrene (B(a)P) is one of the best investigated PAHs both because of its severe toxicity and its relatively good availability to measurements. In our modeling study it was for this reason used as a marker for carcinogenic PAHs. The release of PAHs into the environment is highly dependent on human activities whereas their distribution over e.g. Europe is driven by their physical-chemical characteristics and meteorological conditions. Emission data for B(a)P is sparse connected with large uncertainties (Breijvik at al. 2006). Emissions are reported on an annual basis by the European countries. These data completed with expert estimates where official data is missing is usually used to create model ready emission data. Denier van der Gon et al. (2005) published a technical report on emissions of B(a)P and other POPs for Europe that contain yearly bulk emissions projected on a 50 x 50 km² grid in polar stereographic projection for 2000. Unfortunately, neither the official nor expert estimate emission data give any information on the temporal assignment of the data even though it is known that B(a)P emissions are strongly dependent on air temperature because its main sources are connected with domestic heat production. Due to this lack of knowledge many models use constant emissions or a simplified scheme that differentiates emission strength only by different factors for each season. In this work a new approach for creating time-variant emissions from yearly bulk emissions is presented and results from the chemical transport model gained from these emissions are compared with the results produced when invariant or only seasonally variant emissions were applied.

3. Model Description

CMAQ is a 3D Eulerian regional model which is in our case configured for the European continent. The entire model domain covers Europe from the Mediterranean Sea to the North Polar Sea and from Iceland to Western Russia with a grid cell size of 54x54 km². The CMAQ system consists of three primary components which are devoted to meteorology, emissions, and chemical transport, respectively. The chemistry transport module is mainly designed for classical air pollutants like SO_2, NO_x, O_3, and particulate matter (PM).

At GKSS the CMAQ systems was extended to cope with the transport of B(a)P in the gas phase and adsorbed to particles (Aulinger et al., 2006). Thereby, special emphasis was laid on considering the mass transfer of B(a)P between the gaseous and the particulate phase. The partition of the compound between the gas and the particle phase as well as its distribution between the Aitken, accumulation and the coarse particle mode is dependent on temperature and particle surface, mass of organic aerosols and aerosol water content in each mode. The physical-chemical properties of B(a)P which determine the partition are hence its liquid vapor pressure, octanol-air partitioning coefficient and Henry's Law constant. Owed to the fact that B(a)P occurs at temperatures prevailing in middle Europe mainly bound to aerosols, the degradation of particle bound PAHs is orders of magnitude slower than those of gaseous PAHs (Esteve et al. 2005) and knowledge about heterogenous reactions of B(a)P is scarce it is treated inert as a first approach.

4. Emissions

The first step to create emissions ready for the CMAQ model was to interpolate the data provided by Denier van der Gon et al. to the 54x54 km² CMAQ grid with the inverse distance weighting method considering conservation of mass (Figure 1, left). Next, the bulk emissions for 2000 that were provided in tons were recalculated to g/s and a matrix of 81x90 data points was formed for each model time step of one hour. In the constant-emissions data matrix each time step contained the same value. To achieve seasonal variability the emission values for winter and autumn were multiplied by 1.2 and for spring and summer by 0.8 according to a scheme proposed by Baart et al. (1995).

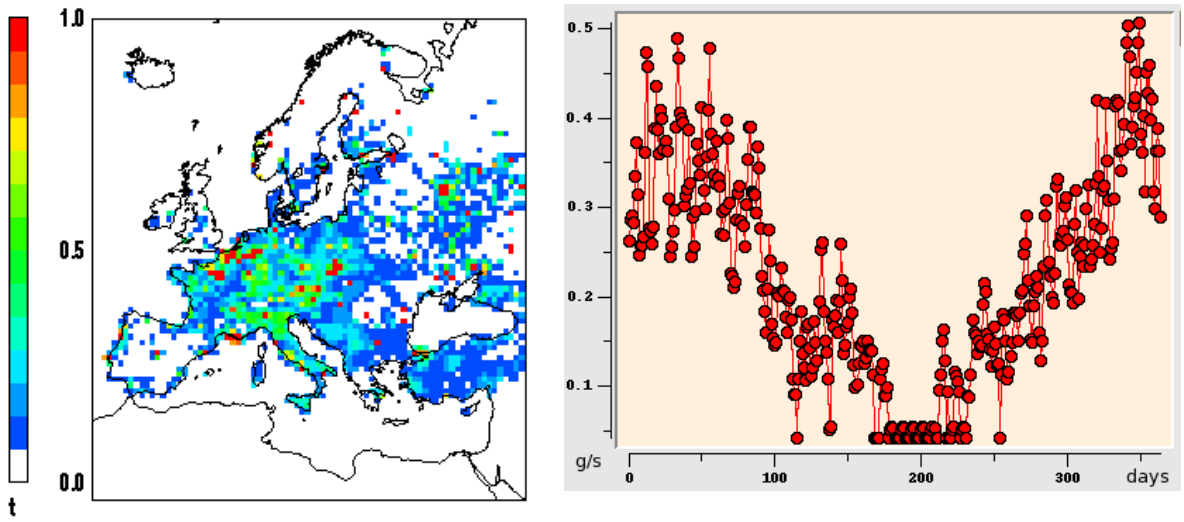

Figure 1: B(a)P emissions in 2000 over Europe (left) and a profile of temperature dependent emission over 365 days (right).

The emissions within the report of Denier van der Gon et al. are attributed to different emission sectors. Because more than 80 % of the B(a)P emissions emanate from the sector “residential combustion”, a strong dependence of the emissions on temperature is expected. To consider the temperature dependence of B(a)P emissions, therefore, emissions from sector “residential combustion” were linearly correlated to the ambient air temperature whereas the yearly total emissions in each grid cell were kept constant. This resulted in winter emissions to be about a factor of 2.5 higher than the annual average while emissions in summer were only about one tenth of the annual average (Figure 1, right). Concerning weekly and diurnal cycles that were additionally superimposed on the temperature dependent variations, emissions from residential combustion follow the same temporal evolution as the CO emissions in the same grid cell while emissions from traffic follow that of NO. Industrial emissions, as the second important sector follow only weekly but no diurnal cycles.

5. Model Results

To evaluate the model performance monthly mean ground level B(a)P concentrations measured in 2000 at six measurement stations belonging to the Environmental Monitoring and Evaluation Program (EMEP) were compared to modeling results. At most of the sites a good correlation between measured and simulated concentrations of the year 2000 could be observed, where the highest correlation occurred at sites in the vicinity of source regions. The correlation coefficient at Kosetice, Czech Republic was 0.84 with constant emissions (case A), 0.83 with seasonally varying emissions (case B) and 0.97 with temperature dependent emissions (case C) and at Preila, Lithuania 0.64 (case A), 0.65 and 0.80 B(a)P as a mostly particle bound substance is primarily deposited near its sources. The good correlation even when using constant emissions indicates that the concentrations near the ground are also highly dependent on the meteorological conditions, above all the boundary layer thickness and precipitation rates. However, the correlations increase significantly for case C showing that the time variation of the emissions applied is sound. Also, at sites further away from the main sources, some correlation between measured and simulated concentrations could be established. As an example, the correlation at Roervik, Sweden was 0.48 (case A), 0.64 (case B) and 0.69 (case C) which confirms the atmospheric transport processes used by the model. Further, it seems to be important for the long range transport of substances whether certain weather condition that promote vertical transport meet with emission peaks. Looking at monthly mean concentrations it made a significant difference if constant or time-variant emissions were used. At Kosetice, for example, the mean concentration in January simulated with constant emissions was 1.1 ng/m^3, while with case C emissions it was 1.8 ng/m^3. In July, the mean concentration was 0.54 ng/m^3 (Case A) and 0.35 ng/m^3 (Case C). The differences at Roervik were 0.39

ng/m^3 (Case A) against 0.55 (Case C) in January and 0.38 ng/m^3 (Case A) against 0.23 ng/m^3 (Case C) in July.

The yearly mean concentrations differed for the study year 2000 at the EMEP sites about ten percent while on the other hand, the absolute deviations between measured and simulated means were relatively high. The measured concentrations were on average five times overestimated by the model. The highest discrepancy could be observed at Pallas, Finland where the measured mean concentration in 2000 was 0.006 ng/m^3 whereas the simulated mean concentration was 0.079 ng/m^3. As it is unlikely that this deviation is only caused by omitting the degradation reactions in our model at its current state it seems to be also necessary to revisit the total emissions.

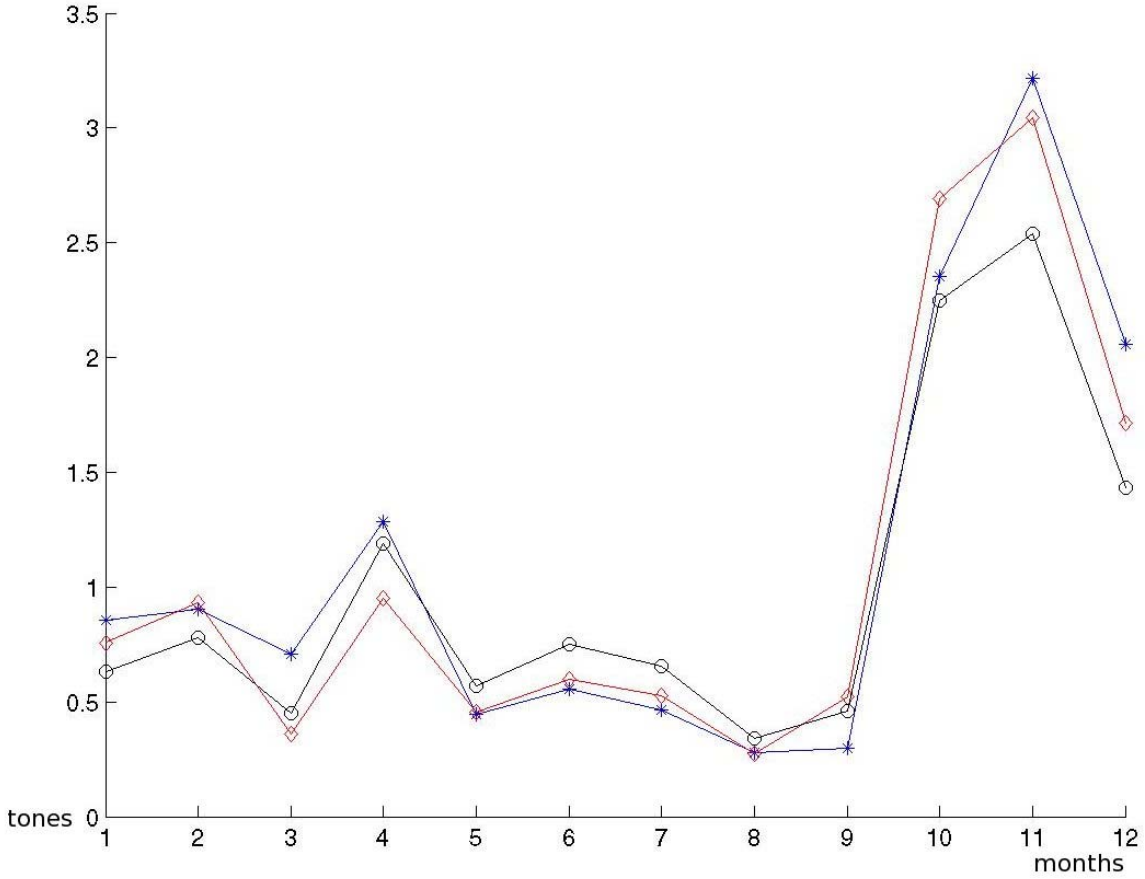

Figure 2: Accumulated monthly deposition of B(a)P into the Baltic Sea

Wet deposition is the dominant sink for atmospheric B(a)P and other PAHs. Over the Baltic Sea without any emissions – ship emissions are not considered so far – the average deposition rate for 2000 was 0.32 g/ha when using temperature dependent emissions which sums up to 13.4 tones direct atmospheric input of B(a)P into the Baltic Sea. The reason for this relatively high rate is that B(a)P is transported mainly from middle and eastern European regions in northern direction towards the Baltic Sea where it is scavenged by rain water. The dominating influence of rain events on the deposition pattern can be seen from the fact that the highest deposition fluxes occurred in October and November, the months with the highest precipitation rates, and not in December and January, when emissions were at its maximum. With case A the total deposition was 12.0 tones and with case B 12.8 tones. Concerning monthly differences between results produced with constant or variable emissions the pattern was similar as for the concentrations (Figure 2).

6. Conclusion

The new approach for deriving time variant B(a)P emissions produced results that were in better correlation with measurements when comparing the monthly variations. The annual concentration and deposition values varied between the three emission cases within about ten percent. Significantly more pronounced were the results for single months.

References

Agency for Toxic Substances and Disease Registry (ATSDR), Toxicological Profile for Polycyclic Aromatic Hydrocarbons (PAHs). Public Health Service, US Department of Health and Human Services, Atlanta, GA, USA, 1995

Aulinger, A., V. Matthias, M. Quante, Introducing a partitioning mechanism for PAHs into the Community Multiscale Air Quality modelling system and its application to simulating the transport of benzo(a)pyrene over Europe, J. Appl. Meteorol., accepted 2007

Baart, A.C., J.J.M. Berdowski, J.A. Van Jaarsveld, Calculation of atmospheric deposition of contaminants on the North Sea -TNO-report. TNO-MEP-R 95/138. Schoemakerstraat 97, P.O. Box 6011, 2600 JA Delft, The Netherlands, 1995

Breivik, K., V. Vestreng, O. Rozovskaya, J.M. Pacyna, Atmospheric emissions of some POPs in Europe: a discussion of existing inventories and data needs, Env. Sci. Pol. **9**, 663-674, 2006

Byun, D., J.K.S. Ching, Science Algorithms of the EPA Models-3 Community Multiscale Air Quality Modelling System. --EPA report, EPA/600/R-99/030, Office of Research and Development, Washington DC 20406, 1999

Byun, D., K.L. Schere, Review of the Governing Equations, Computational Algorithms, and Other Components of the Models-3 Community Multiscale Air Quality (CMAQ) Modeling System. -Appl. Mech. Rev. **59**, 51-77, 2006

Denier van der Gon, H.A.C., M. van het Bolscher, A.J.H. Visschedijk, P.Y.J. Zandveld, Study of the effectiveness of UNECE Persistent Organic Pollutants Protocol and cost of possible additional measures. Phase I: Estimation of emission reduction resulting from the implementation of the POP Protocol. -TNO-report. B&O-A R 2005/194. Laan van Westenenk 501, P.O. Box 342, 7300 AH Appeldoorn, The Netherlands, 2005

Esteve, W., H. Budzinski, and E. Villenave, Relative rate constants for the heterogeneous reactions of NO2 and OH radicals with polycyclic aromatic hydrocarbons adsorbed on carbonaceous particles. Part 2: PAHs adsorbed on diesel particulate exhaust SRM 1650a. *Atmos. Environ.*, **40**, 201–211, 2005

THE IMPACT OF BIOGENIC VOC EMISSIONS ON PHOTOCHEMICAL OZONE FORMATION DURING A HIGH OZONE POLLUTION EPISODE IN THE IBERIAN PENINSULA IN THE 2003 SUMMER SEASON.

Nuria Castell[1], Rosa Salvador[1], Enrique Mantilla[1], Ariel Stein[2] and Millán Millán[1].
[1] Centro de Estudios Ambientales del Mediterráneo, Valencia, Spain. (nuria@ceam.es).
[2] Earth Resources and Technology on assignment to NOAA/Air Resources Laboratory.

ABSTRACT
During the 10 - 15 August 2003 ozone pollution event, anticyclonic conditions were accompanied by long residence times of polluted air masses in the atmospheric boundary layer, inhibiting the renovation of air masses. These atmospheric conditions, together with a cloudless sky and elevated temperatures, favored photochemical ozone formation. During meteorological conditions with a weak pressure gradient the complex topography of the Iberian Peninsula favors the development of mesoscale flows such as mountain winds, topographic injection, and land/sea breeze. These mesoscale structures affect ozone distribution over the Iberian Peninsula (Millán, et al., 1997).

The aim of this paper is to understand and quantify computationally the influence of biogenic volatile organic compound (BVOC) emissions in the formation of tropospheric ozone during this high ozone episode. Being able to differentiate how much ozone comes from biogenic emissions alone and how much comes from the interaction between anthropogenic and biogenic emissions would be helpful to develop a feasible and effective ozone control strategy.

1. INTRODUCTION

In this paper, we investigate the influence of biogenic volatile organic compound (BVOC) emissions in relation to anthropogenic emissions in the Iberian Peninsula. The points of interest in this region are: (i) it is characterised by the presence of a large variety of biogenic compound emitters that are quite different from the usual vegetation in northern latitudes or in the US; (ii) the cities and the industries are not as large as the ones in northern Europe or the US; (iii) an anticyclonic pressure system generally leads to high photochemical activity and to the formation of mesoscale re-circulation systems such as the sea breeze and mountain slope winds; (iv) ozone exceedances occur all summer in the Iberian Peninsula.

Previewed air quality modelling researches range from an urban airshed (several hundred to several thousand km^2) to a regional airshed (million km^2) to a continental airshed (Europe). They concluded that: (1) biogenic emissions generally enhance ozone formation in most areas, and the magnitude of their impact varies from location to location; (2) a large biogenic impact normally occurs during high-temperature periods because biogenic sources tend to emit more VOCs at high temperatures; and (3) naturally emitted VOCs, especially isoprene, play a significant role in ground-level ozone due to their relatively high reactivity (Tao et al., 2003).

In this paper, we consider the impact of biogenic emissions on surface ozone concentrations in the Iberian Peninsula. Although high-resolution photochemical models are more computationally suitable to investigate small domains, a large-domain study with lower resolution could still provide a good representation of regional phenomena. Understanding these regional simulations may be crucial to solve local ozone problems.

This study reports the “total impact” on ozone formation due to biogenic sources, i.e. the sum of ozone contributions from biogenic emissions alone (the pure impact) and those from the interactions between anthropogenic and biogenic emissions (the synergistic impact), and the isolated contribution of each of these factors (pure and synergistic) to ozone concentrations. Thunis and Cuvelier (2000) addressed these issues by applying a factor separation approach to ozone modeling in the Burriana area (east coast of Spain) for a two-day ozone episode. We apply this approach to the Iberian Peninsula over a six-day episode to determine the total, pure and synergistic impacts of biogenic and anthropogenic sources to ground-level ozone concentrations.

The impact on ozone formation is also studied in the context of various anthropogenic emissions reduction strategies, i.e., when anthropogenic VOC emissions and/or NOx emissions are reduced.

2. METHODOLOGY

Numerical simulations have been carried out using, , independently, the MM5 meteorological model and the CAMx photochemical model, version 4.31. The anthropogenic emissions (traffic and industry) in the Iberian Peninsula have been estimated from the EMEP/CORINAIR emissions inventory. The BVOCs emission model for vegetation (isoprene, monoterpenes and other VOCs) uses the algorithm from Guenther et al.

(1993), suited and adapted for the particular emitter behavior of some Mediterranean species.

In order to quantify the amount of ozone originating from pure biogenic emissions as well as that from the synergistic effect between anthropogenic and biogenic emissions, the factor analysis technique proposed by Stein and Alpert (1993) was employed.

We consider factors A (Anthropogenic emissions) and B (Biogenic emissions), and denote S_{AB}, S_A, S_B, and S_O simulation results to include both factors A and B, factor A alone, factor B alone, and neither of the two factors, respectively. Then the pure impacts (denoted by a prime) of factor A and B are given respectively by: $S'_A = S_A - S_O$ and $S'_B = S_B - S_O$.

Since the run including both factors is expressed as $S_{AB} = S_O + S'_A + S'_B + S'_{AB}$, the effect of the mutual interaction between the two processes is given by: $S'_{AB} = S_{AB} - S'_A - S'_B - S_O = S_{AB} - S_A - S_B + S_O$.

On the other hand, the total impact of factor B is defined by $S_{AB} - S_A$ (equivalent to $S'_B + S'_{AB}$), so that the interaction can also be written as the difference between the total and the pure impacts, i.e., $S'_{AB} = (S_{AB} - S_A) - (S_B - S_O)$.

This implies that the evaluation of the contribution from the two factors, and from their possible interaction, requires four simulations, namely S_{AB}, S_A, S_B and S_O.

3. RESULTS AND DISCUSSION

3.1. Impact of BVOC emissions on ozone levels

In this section, the BVOC impact is characterized by simulations with and without BVOC emissions. The total impact of biogenic emissions is studied by differentiating two simulations: with (S_{AB}) and without (S_A) biogenic emissions; however, both simulations include anthropogenic emissions.

Figure 1b shows for each grid point in the computational domain, the maximum biogenic impact (in ppb), i.e., $S_{AB} - S_A$ on ozone levels during the episode. The map is therefore not a snapshot at a specific time, since the maximum impact occurs at different times for different locations.

From Figure 1a we deduce that the greatest impact of biogenic emissions is produced in areas where there is a pre-existing high photochemical production, close to zones where there are high emissions of ozone precursors. Thus, the total impact of the biogenic emission (the pure one in addition to the one that includes the biogenic/anthropogenic interaction) on the area of Madrid, Barcelona or Valencia can surpass 90 ppb in the hourly maximums, and 60ppb in the 8-hour maximums. It should be noticed that this impact does not necessarily occur on the ozone peak. However, both the information and the human health protection thresholds could be surpassed by considering only the contribution from the anthropogenic emissions.

In the western part of the Iberian peninsula there is a vast area where the total impact from biogenic emissions is smaller. This is a zone with fewer anthropogenic emissions. Thus, the most important impact of biogenic emissions seems to take place in areas where large sources of NOx exist.

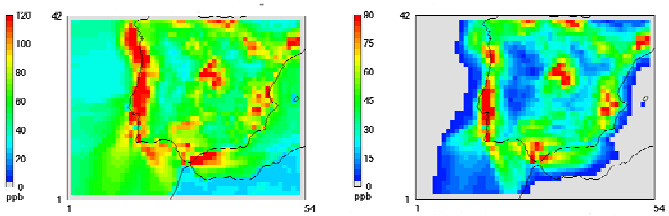

Figure 1: (a) Hourly maximum of ozone for every grid during the episode. (b) Maximum hourly impact of biogenic emissions, $S_{AB} - S_A$ (ppb) for the 10-15 August 2003 episode. Note that the difference does not necessarily occur on the ozone peak.

3.2. Separation between biogenic and anthropogenic impacts

Results of the factor analysis of the two types of emissions are shown in Figure 2. It depicts the maximum hourly contribution to the ozone concentration (not necessarily over the ozone maximum), from pure anthropogenic emission (S'_A); from pure biogenic emission (S'_B); and from the interaction between biogenic and anthropogenic emissions (S'_{AB}), during the 10-15 August 2003 episode. The total contribution of the biogenic emissions ($S'_B + S'_{AB} = S_{AB} - S_A$) is represented in figure 1b.

It can be observed that the biogenic emission contribution is due mainly to its interaction with the anthropogenic emissions. In fact, the pure BVOC contribution does not reach 1ppb of maximum in any area of the Iberian Peninsula. This means that in a photochemical simulation that considers only BVOC emissions, the ozone concentration will be kept around the typical values of "clean air".

On the other hand, the contribution from pure anthropogenic emissions assumes impacts higher than 60ppb across a large area of the peninsula. It is presumed that adding these impacts to the background concentrations could result in exceedances of the legal thresholds defined in the European Directive. The contribution due to the interaction between biogenic and anthropogenic emissions assumes threshold values of 90ppb and 120 ppb in different areas of the Peninsula.

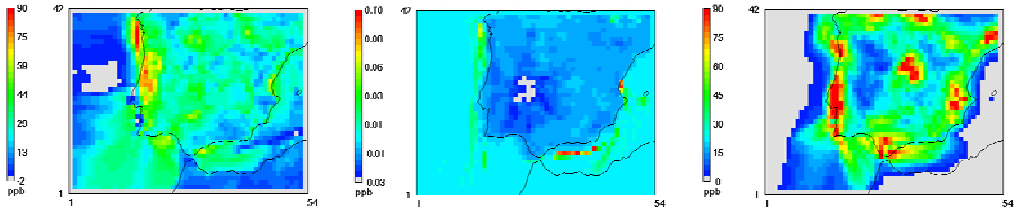

Figure 2: Factor separation analysis. Hourly maximum impact. S'a, pure contribution of anthropogenic emissions to ozone formation; S'b, pure biogenic contribution; S'ab, mutual interaction between anthropogenic and biogenic emissions.

3.3. Sensitivity to NOx/AVOC emission reductions

In this section the BVOC impact on ozone production is analyzed when the anthropogenic emissions are reduced (50% NOx and/or AVOC). This is interesting because of the hypothesis that a reduction in the AVOCs will cause the competition between BVOCs and AVOCs for the OH radical to be less intense, and result in a larger BVOC impact on photochemical ozone formation.

It is observed that the BVOC impact has a clear dependence on NOx and AVOCs availability. In all the reduction scenarios, as well as in the actual scenario, the largest impacts are located around the zones with the greatest precursor emissions, or downwind from them, moving inland along the natural channels. Nevertheless, if we compare the BVOC impact in these scenarios with the impact in the actual scenario, both show zones in which the biogenic impact has increased and decreased. The biogenic emissions impact thus depends on the reduction scenario, i.e., whether it is an NOx or an AVOC reduction scenario. We have found zones where reducing the NOx decreases the BVOC impact, as well as zones where decreasing the AVOCs increases the BVOC contribution to ozone formation.

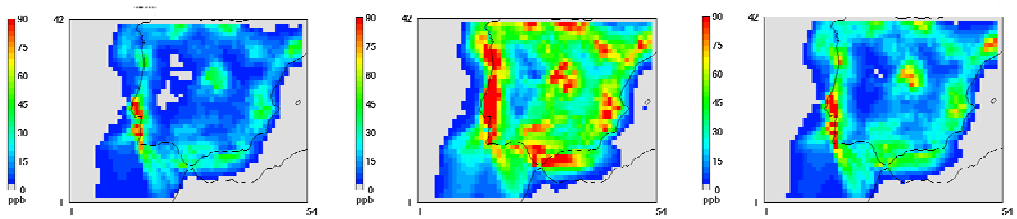

Figure 3: Maximum hourly impact of biogenic emissions, $S_{AB} - S_A$ (ppb) for the different control scenarios: 50% NOx; 50% AVOC; and 50% NOx and AVOC, respectively.

The result of applying factorial analysis to the anthropogenic reduction emission scenarios shows that the largest mutual impact is produced in the AVOC reduction scenario. The explanation for this is that when AVOCs are reduced, the BVOC, which has a high reactive power, plays a more active role in the OH chemistry. In coastal zones, big cities and industrial areas, the synergistic impact could be greater than 90 ppb. The second scenario where the synergy between anthropogenic and biogenic emissions is greater is the one in which both VOCs and NOx have been reduced by 50%. In this scenario, the areas with large anthropogenic emissions have an impact up to 90ppb. This means that the contribution from the interaction between anthropogenic and biogenic emissions is high enough to surpass the information threshold.

4. CONCLUSIONS

Including biogenic emissions in the photochemical simulation of the episode promotes ozone production substantially, yielding higher maximum values and also a greater number of exceedances of the thresholds

established in the Directive.

The factor analysis technique has been used to separate the purely biogenic emission contribution from the synergistic anthropogenic and biogenic emission contribution. It is observed that for the whole of the Iberian Peninsula, the purely biogenic VOC emission contribution is very small. In fact, in a simulation that included only BVOCs, the ozone levels stayed at nearly "clean air" conditions. The largest contribution of biogenic emissions comes from its non-linear interaction with anthropogenic emissions. At some points in the Peninsula, this mutual contribution between both types of emissions surpasses 90 ppb in the hourly values, and 60 ppb in the 8-hour ones. This would assume exceedances of the legal threshold values established in the European Directive.

Another large contributor to ozone concentrations is the purely anthropogenic one; its concentration can also exceed the legal thresholds mentioned above.

The impact of biogenic emissions on ozone formation has also been studied in combination with some anthropogenic emissions reduction strategies, i.e., when anthropogenic VOC emissions and/or NOx emissions are reduced by 50%. The greatest impact is found for the scenario in which the NOx emissions are not changed, but the anthropogenic VOCs are reduced. This may be due to a lower anthropogenic competition in the ozone production reactions involving the OH radical.

Finally, this preliminary study on biogenic and anthropogenic VOC emissions in photochemical ozone formation over the Iberian Peninsula is limited over urban zones, and can introduce mistakes due to the fact that all the emissions are mixed in a cell of 24x24 km (normally, anthropogenic sources are concentrated in smaller areas). Nevertheless, this type of mesh permits a first analysis of ozone formation behavior at regional scale, which is necessary to understand the ozone behavior at scales with a larger spatial resolution, but a small domain.

5. ACKNOWLEDGEMENTS

The Fundación CEAM is financed by the Generalitat Valenciana and BANCAIXA. Thanks also to CESCA for its computer support.

This work is a contribution to COST 728.

6. REFERENCES

Fiala, J., Cernikovsky, L., de Leeuw, F., and Kurfuerst, P., 2003. Air pollution by ozone in Europe in summer 2003. Overview of exceedances of EC ozone threshold values during the summer season April-August 2003 and comparisons with previous years. Copenhagen, European Environment Agency (EEA Topic Report 3/2003).

Guenter, A.B., Zimmerman P.R. and Harley, P.C. 1993. Isoprene and monoterpenes Emission Rate Variability: Model Evaluations and Sensitivity analysis. Journal of Geophysical Research, 98(D7), 12609-12617.

Millán M.M., Salvador, R., and Mantilla, E., 1997. Photooxidant dynamics in the Mediterranean Basin in summer: results from European Research Projects. Journal of Geophysical Research. 102 (D7), 8811-8823.

Solberg, S., Coddeville, P., Forster, C., Hov, O., Orsolini, Y., and Uhse K., 2005. European surface ozone in the extreme summer 2003. Atmos. Chem. Phys. Discuss. 5, 9003-9038.

Stein, D. and Alpert, P., 1993. Factor separation in numerical simulations. Journal of Atmospheric Sciences, 50, 2107-2115.

Tao, Z., Larson, M.S., Wuebbles, D., Williams, a. and Caughey, M., 2003. A summer simulation of biogenic contributions to ground-level ozone over the continental United States. Journal of Geophysical Research, 108, D14, 4404.

Thunis, P., and Cuvelier, C., 2000. Impact of biogenic emissions on ozone formation in the Mediterranean area. A BEMA modeling study. Atmos. Enrironment, 39, 317-334.

STUDY OF PHOTOCHEMICAL SMOG INCIDENCE IN THE INFLUENCE AREA OF "LA PLANA DE CASTELLON"

Juana M Delgado-Saborit[1, 2], Maria A. Querol-Balaguer[2] & Vicente J Esteve-Cano[2]*

(1) University of Birmingham, Division of Environmental Health & Risk Management, Birmingham (UK)

(2) Universtat Jaume I, Dept. Quimica Inorganica y Organica, Castellon, (Spain)

ABSTRACT

The aim of the present work is to study the incidence of photochemical smog episodes in the area of influence of "La Plana de Castellon". Passive sampling methodology has been employed to assess surface ozone levels in the area of study instead of conventional continuous monitoring in order to cover a wide area of study with a low cost as well as to avoid the use of electric power on the selected sites. Measurements were made during the higher photochemical activity period during the years 2001, 2002 and 2003 for four consecutive months, from June to September. Measurement campaigns were divided in sampling periods of one week. Data were collected from twenty different sampling points covering an area of 8000 km2. Samples were taken in peripheral points around the main city as well as the main precursor pollutants sources. Ozone maps have been created with data provided by passive samplers. Areas with high concentration of ozone have been identified in inland rural areas whereas low concentration levels are recorded by the coast where the main city and industrial areas are located. Surface ozone concentrations close to direct precursor's sources were generally lower than elsewhere, mainly as a result of the scavenging of ozone by nitric oxide. On the contrary, ozone levels were always higher in inland rural sites as a consequence of the transport of polluted air masses downwind of urban/industrial centres and the development of the photochemical generation system.

1. INTRODUCTION

Ozone is a tropospheric air pollutant formed in the atmosphere under conditions of bright sunlight and warm temperature as a result of photochemical reactions involving nitrogen oxides, carbon monoxide and volatile organic compounds as primary pollutant precursors (EPA 1996; Skelly et al. 2001). Sources of these primary pollutants come mainly from motor-vehicle emissions, stationary combustion sources, and industrial and domestic use of solvents and coatings (Denison et al. 2000). Among all of them, urban traffic becomes the principal source of ozone precursors (Bernard et al. 1999).

The area of study, know as "La Plana de Castellón", has some features that make it of some interest to measure surface ozone levels. Meteorologically, it is described by high levels of sunlight and very stable weather in summer. In addition, all the primary pollutants of surface ozone are emitted in the area by traffic and industries (Delgado-Saborit et al. 2006).

Passive sampling methodology has been employed to assess the ozone levels in the area of study instead of conventional continuous monitoring in order to cover a wider area with low cost as well as to avoid the necessity of using electric power at the sampling sites. The passive sampling technique is regarded as a viable option to measure ambient ozone concentrations for the purposes of ecological assessment. Passive samplers are inexpensive and easy to deploy in the field; they require no power supply or supporting equipment and offer flexibility of placement. These features make them attractive for monitoring in complicated environments, such as forest (Cox et al. 1999; Krupa et al. 2000).

The aim of the present work is to study the incidence of photochemical smog episodes in the area of influence of "La Plana de Castellon".

2. METHODOLOGY

2.1. Area of Study

The area of study, located in "La Plana de Castellón" and its surroundings (Figure 1), is in the East coast of Spain. The area is a semicircular plain terrain enclosed on the east by the Mediterranean Sea and surrounded by mountains of 700 m in height.

Meteorologically, the area has a Mediterranean climate with hot summers and mild winters. It has an average amount of sunlight of about 900 W/m^2 and has more than 2800 hours of sunlight, which represents around 70% of the theoretical sunlight period. Rainfall is irregular and heavy, mostly in the fall season and in spring. The relative humidity is around 65% to 70% all the year. Winds are very low. Less than 3% of winds are above 50 km/h and more than 90% are lower than 20km/h. The prevailing winds are maritime winds from NE and SE in summer and winds from the West in winter (Delgado-Saborit et al. 2006). Nevertheless, breezes are the most important mechanism and impose a synoptic circulation which affects the ozone formation mechanism (Sanz et al. 1998).

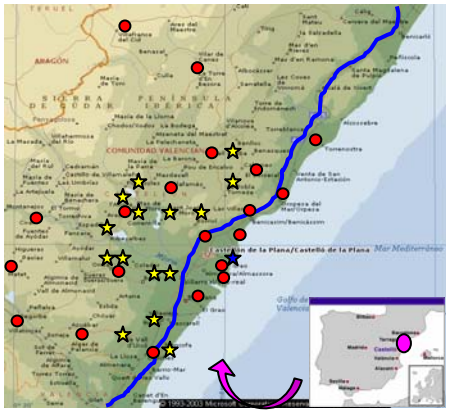

Fig. 1: Area of Study where light stars are tile and glaze factories, dark star is an Oil Refinery and a Power Plant, dark line is a main road and highway and spots shows sampling sites.

As regards of sources of ozone precursors, the area is of special interest due to the fact that there is an industrial area called "El Serrallo" which has an oil-fired power plant, an oil refinery and a chemical factory that works with by-products from the oil refinery (Figure 1, dark star). In addition, there are more than three hundred tile factories and glaze factories (Figure 1, light stars). The area is also crossed by one of the main Spanish and European highways, the A7-E15 and the Spanish trunk road, the N-340 (Figure 1, dark line).

Therefore, the area of study has some important sources of ozone precursors as well as weather conditions favorable to the formation of ozone at ground level.

2.2. Passive Samplers

Measurements were made with Radiello passive sampler which is based on the principle that ozone is adsorbed onto a microporous polyethylene cartridge filled with 4,4-dipyridelethylene coated silica gel. This principle of measuring ozone was firstly used by Hangartner, Kirchner and Striedner and validated in ambient air by different groups (Hangartner et al. 1996; Bernard et al. 1999). During the exposure period one mol of 4,4-dipyridelethylene is oxidized with one mol of ozone to form two moles of 4-pyridinecarboxaldehyde. During the analysis, in the laboratory, the 4-pyridinecarboxaldehyde is reacted with 3-methyl-2-benzothiazolinonehydrazone hydrochloride to form a yellow colored hydrazide, which is measured in an espectrofotometer. The hydrazide concentration is proportional to the amount of ozone reacted over the sampling period.

For analysis, the silica spheres inside the sampling cartridge were poured into an 11-ml polyethylene tube and 5 ml of the MBTH solution was added. The solution was stirred well for 1 hour to allow the reaction of the MBTH with the 4-pyridinecarboxaldehyde (formed with the ozone) to give a yellow colored hydrazide. After stirring, the solution was filtered with a pre-filter (Whatman 45 μm) and a syringe. The yellow hidrazide sample extracts were analyzed immediately colorimetrically by means of a Hewlett Packard 8453 spectrophotometer at 430 nm. The analytical software employed was UV-VIS ChemStation. If the extracts were not going to be analyzed immediately, they were stored in a refrigerator at 4^{o}C for no longer than 48 hours to avoid the breakdown of the hidrazide.

2.3. Measuring Campaign

2.3.1. Periods and frequency. Measurement campaigns were made during the higher photochemical activity period in summer 2001, from 11th July to 10th September, summer 2002, from 2nd July to 23rd September and

summer 2003, from 9th of June to 6th October. Measuring campaigns were divided into sampling periods of one week.

2.3.2. Sampling sites. Twenty samples were collected each sampling period to cover an interest area of 8000 km^2. Samples were located around the sampling area of interest, in radial peripheral points around Castellón city and the main precursor pollutants sites. Figure 1 shows the distribution of the sampling sites in the area of interest.

Samples were located away from sources of nitrogen oxides, far from walls, in a distance of 20 cm or more from vertical surfaces and 1.5-2 m above the ground. As passive samplers were at first thought to assess indoor quality air, in assessing the quality of air outdoors is advisable to protect them with a rain/wind shelter. Even in the absence of rain, the shelter is required to minimize dust contamination and the effects of advection on the passive sampler (Roadman et al. 2003). In this study shelters supplied by the manufacturer were employed. The shelter was fixed by means of a flange to a post, wall or streetlight.

2.3.2. Sampling protocol. Special care was taken when handling passive samplers. Except during sampling, all samplers were kept in airtight bags. Samplers prepared in the lab were transported to and from the field in airtight containers placed in cold boxes. After exposure and once back in the lab, the sampler's cartridges were transferred to plastic tubes and kept at 4^{o}C until preparation for analysis.

3. RESULTS AND DISCUSSION

The average surface ozone levels for each sampling campaign were plotted as concentration isopleths on regional maps with Surfer 7.0, Golden Software Golden, INC (Surfer) using the interpolation model (Kriging) to understand spatial variability. Figure 3 represent average ozone levels measured by means of Radiello passive samplers in each sampling campaign.

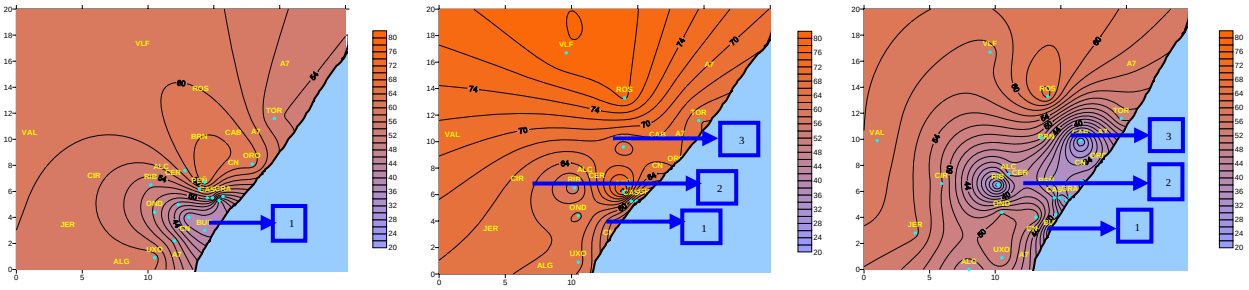

(a) 2001 (b) 2002 (c) 2003

Fig. 3: Campaign averaged ozone levels measured by means of Radiello passive samplers

Figure 3 shows that there are three different areas where in all measuring campaigns the lowest values of ozone were registered. The first area, coded as 1 in Figure 3, corresponded with "El Serrallo" area (where the power plant, the oil refinery and the petrochemical factory are located) jointly with Castellón city and its downwind surroundings. This area is clearly identified in the three studied years. The other two areas, coded as 2 and 3 in figure 3, matched with the distribution of the ceramic and glaze factories. In contrast with area coded as 1, areas 2 and 3 are not clearly identified in all years.

Concentrations close to direct precursors focus are generally lower than elsewhere, mainly as a result of the scavenging of ozone by nitric oxide (WHO 2000). In this way the decrease in ozone levels is produced due to the vicinity to NO emissions (Winner et al. 1989; Monn 2001), in this case, the vicinity of the petrochemical area, Castellon city area and the ceramic area.

In the rest of the areas, ozone levels were always higher. These results are consistent with literature where rural sites tend to have higher long-term ozone exposures as polluted air masses are transported downwind of urban/industrial centers and the photochemical generation system continues to develop with little scavenging of ozone precursors (Skelly et al. 2001).

The average of weekly ozone levels for each campaign were in the range of 40-44 µg/m^3 in 2001, 54-74 µg/m^3 in summer 2002 and in the range 34-44 µg/m^3 in summer 2003. Those values are in consonance with European background levels of ozone which are in the range 40–70 µg/m^3 (WHO 1995).

4. CONCLUSION

Passive samplers have been successfully employed to determine ozone levels in a Mediterranean area. Areas with high concentration of ozone have been identified in inland rural areas whereas low concentration levels are recorded by the coast where the main city and industrial areas are located. Surface ozone concentrations close to direct precursor's sources were generally lower than elsewhere, mainly as a result of the scavenging of ozone by nitric oxide. On the contrary, ozone levels were always higher in inland rural sites as a consequence of the transport of polluted air masses downwind of urban/industrial centres and the development of the photochemical generation system.

5. ACKNOWLEDGMENT

Authors are grateful to Mr. Carlos Felis and to Conselleria de Medi Ambient of Generalitat Valenciana for facilitating the necessary data from their Regional Monitoring Ambient Network. Authors recognize to Ms. Carmen Clemente her technical support in this study. Dr. Delgado-Saborit and Ms. Querol-Balaguer are grateful to Generalitat Valenciana for the FPI grant. Ms. Querol-Balaguer is grateful to Generalitat Valenciana for the financial support from GV00-2-137 project and the FPI00-02-328 grant.

6. REFERENCES

Bernard, N. L., M. J. Gerber, C. M. Astre and M. J. Saintot (1999). "Ozone measurement with passive samplers: Validation and use for ozone pollution assessment in Montpellier, France." Environmental Science & Technology **33**(2): 217-222.

Cox, R. M. and J. W. Malcolm (1999). "Passive ozone monitoring for forest health assessment." Water Air and Soil Pollution **116**(1-2): 339-344.

Delgado-Saborit, J., M. Querol-Balaguer and V. Esteve-Cano (2006). Use of passive samplers as a tool for health risks assessment due to tropospheric ozone. 6th International symposium on Advanced Environmental Monitoring, Heidelberg, Germany.

Denison, L., K. Rolfe and B. Graham (2000). Review of the Ambient Air Quality Guidelines. Health Effects of Five Common Air Contaminants and Recommended Protective Ranges. Wellington, New Zealand, Ministry for the Environment.

EPA (1996). Air quality criteria for ozone and related photochemical oxidants., U.S. Environmental Protection Agency. Research Triangle Park, NC, National Center for Environmental Assessment, RTP Office,.

Hangartner, M., M. Kirchner and H. Werner (1996). "Evaluation of passive methods for measuring ozone in the European Alps." Analyst **121**(9): 1269-1272.

Krupa, S. V. and A. H. Legge (2000). "Passive sampling of ambient, gaseous air pollutants: an assessment from an ecological perspective." Environmental Pollution **107**(1): 31-45.

Monn, C. (2001). "Exposure assessment of air pollutants: a review on spatial heterogeneity and indoor/outdoor/personal exposure to suspended particulate matter, nitrogen dioxide and ozone." Atmospheric Environment **35**(1): 1-32.

Roadman, M. J., J. R. Scudlark, J. J. Meisinger and W. J. Ullman (2003). "Validation of Ogawa passive samplers for the determination of gaseous ammonia concentrations in agricultural settings." Atmospheric Environment **37**(17): 2317-2325.

Sanz, M. J. and M. M. Millan (1998). "The dynamics of aged airmasses and ozone in the Western Mediterranean : Relevance to forest ecosystems." Chemosphere **36**(4-5 (7 ref)): 1089-1094.

Skelly, J. M., J. A. Ferdinand, J. E. Savage and J. D. Mulik (2001). "A 13-week comparison of passive and continuous ozone monitors at forested sites in north-central Pennsylvania." Journal of the Air & Waste Management Association **51**(9): 1280-1287.

Surfer Golden Software, INC., Golden, Colorado, USA.

WHO (1995). Update and revision of the air quality guidelines for Europe, WHO Regional Office for Europe.

WHO (2000). Chapter 7.2. Ozone and other photochemical oxidants. Air Quality Guidelines - Second Edition. Copenhaguen, Denmark, WHO Regional Office for Europe.

Winner, W. E., A. S. Lefohn, I. S. Cotter, C. S. Greitner, J. Nellessen, L. R. McEvoy, Jr., R. L. Olson, C. J. Atkinson and L. D. Moore (1989). "Plant Responses to Elevational Gradients of O3 Exposures in Virginia." Proc. Natl. Acad. Sci.. **86**: 8828-8832.

PHOTOCHEMICAL MODELING AND OZONE IMPACT OF NEW INDUSTRIAL FACILITIES IN THE SOUTHWESTERN IBERIAN PENINSULA

Enrique Mantilla[1], Nuria Castell[1], Rosa Salvador[1], Ariel Stein[2], and Millán Millán[1]

[1] Centro de Estudios Ambientales del Mediterráneo (CEAM), Valencia, Spain (enrique@ceam.es).
[2] Earth Resources and Technology on assignment to NOAA/Air Resources Laboratory.

ABSTRACT

This paper presents an objective estimation of the impact of a new thermal power plant in the area of Huelva, in the South-West of the Iberian Peninsula. Simulations were carried out with a photochemical transport model (CAMx). The lack of information on some of the critical input data required by the photochemical model, particularly emissions, confers a high degree of uncertainty on the simulated results. To handle this uncertainty, a methodology based on a matrix of potential emission scenarios is defined. This methodology will serve to analyze the expected ozone impact from a new power plant in the area under the different emission scenarios. This kind of study could be used as an effective tool to support environmental managing policies in the context of the current European Union Directive 2002/3/EC on tropospheric ozone.

1. INTRODUCTION

In the troposphere, ozone is formed as a result of complex photochemical reactions, involving nitrogen oxides (NOx) and volatile organic compounds (VOC) precursors. The chemical production of O_3 in the atmosphere is highly non-linear, making it difficult to estimate the behavior (both qualitatively and quantitatively) of ozone levels in response to changes in emissions. Under certain conditions, O_3 concentrations increase with increasing NOx and remain quite insensitive to changes in VOCs, while for other scenarios, the rate of O_3 formation will rise mainly with increasing VOCs (Atkinson, 2000; Sillman, 2002).

The use of numerical models for air quality studies has to include all the significant factors taking part in the complex and non-linear atmospheric dynamics. In this respect, a very important aspect to be considered is the effect of uncertainties in the input information on the model outputs. When studying the photochemical impact due to new emissions, it has to be taken into account that the emissions inventory could have errors as large as 300% (Castell et al., 2006; Simpson, 1995).

As a result, suitable solutions must be proposed for the following aspects:

- *temporal response*; frequently a climatic answer is required (especially when the impact of a new industrial activity is evaluated), but modeling long time periods with a high-resolution model has an elevated computational cost. Thus, choosing a representative case requires a meteorological study of the area.
- *interaction between different scales*; many of the processes that determine the pollutant dynamics occur at different scales. The tools must include interaction at different scales, both for the meteorology and for the emissions.
- *realistic description of the physical-chemical mechanisms*; this requires the use of complex tools that include the main mechanisms involved. Its description must be sufficiently realistic.
- *uncertainty in the information*; the input information is usually scarce and incomplete. It does not satisfy the spatial and temporal resolution needs of the models, which forces a preprocessing of the initial data.
- *management of the uncertainty*; the models must be used with a strategy that permits adapting their results to the initially established needs, in order to delimit the range of uncertainty.
- *management of the information*; the numerical models provide a copious amount of information; this makes it necessary to adapt the generated information to a useful answer (in this case, to the impact of a new industry on the ozone levels).

2. METHODOLOGY

The methodology established in this study to estimate the impact of a new thermal power plant in the area of Huelva is as follows:

─Analysis of two simulations: with and without the new industry. This will help to minimize the uncertainty associated with the initial conditions.

─ Identification of significant episodes from the meteorological and pollution point-of-view. They must be representative of and favorable to ozone production. The results are conservative in relation to the general behavior of the system ("worst-case scenario").

─ Application of state-of-the-art simulation technologies to represent the atmospheric processes involved in the ozone formation and dispersion.

─ Use the best information available to diminish the uncertainties associated with the input information.

─ Run a series of simulations (with different input emissions) that allow the evaluation of the uncertainty in the results. For this, a matrix of probabilities obtained from a collection of nine emission scenarios is used (see figure 1).

─ Transformation of an important volume of the information generated by the model to a dataset with a reasonable amount of data.

─ Management of the information taking into account the European Directives. Two types of results are presented:

  ─ Statistics relative to the increase in the ozone concentrations.

  ─ Spatial distributions of pollutants to show the impact zones.

The non-hydrostatic MM5 v3.5 model has been used to simulate the meteorological pattern. Four nested grids (one-way) have been used with a 2, 6, 24, and 72 km horizontal resolution and a variable vertical resolution up to 15 km. For the photochemical simulation the CAMx v.4.3 air quality model operating with the CBIV chemical mechanism has been used.

Both the biogenic and the anthropogenic emissions have been computed for the three domains used in the photochemical model.

The figure 1 shows the matrix of emission scenarios used in this study. The base case (B) corresponds to the scenario of emissions, using the best available information. Other emission scenarios have been computed using a factor of 3 from the base case to estimate the anthropogenic and biogenic emissions. Each of the scenarios have been used to model with and without the new thermal power plant.

The potential emissions and the characteristics of the new thermal power plant are shown in table 1.

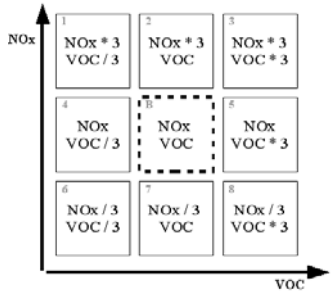

Figure 1: Emission scenario matrix used in this study.

Table 1: Characteristics of the new power plant.

Height	65 m
Diameter	6.5 m
Temperature	348 K
Flow rate	2238194 Nm3/h
Emission: NOx	60 mg/Nm3
Emission: SO_2	23.4 mg/Nm3

3. RESULTS AND DISCUSSION

The topography of the Huelva river basin has a notable influence in the atmospheric dispersion of pollutants. Huelva is located between two rivers, the Tinto and the Odiel. The Aracena mountain range, with a maximum altitude of 1035m, is located around 40km from Huelva. Figure 2 shows the main topographical characteristics of the finer grid of 2km. The points with meteorological measurements and the position of the new power plant (in the Nuevo Puerto industrial area) are also represented in Figure 2.

Two dispersion scenarios were selected: 10-15 August 2003 and 14-19 June 2004. Both scenarios frequently occur in the Iberian Peninsula in summer. The meteorological conditions corresponding to these episodes feature a weak pressure gradient along with a relative low-pressure development in the southern part of the peninsula (Iberian Thermal Low). Under these atmospheric conditions, with a cloudless sky and elevated temperatures, photochemical ozone formation is favored (Salvador et al., 2006).

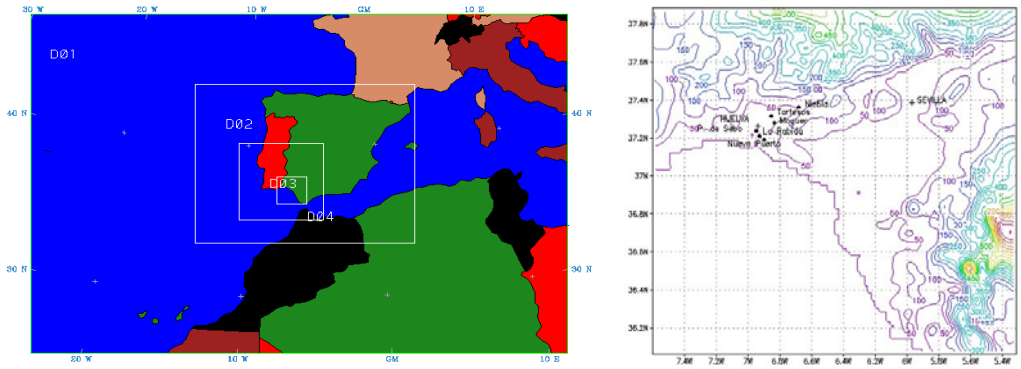

Figure 2: (left) MM5 grid configuration. (right) main topographical characteristics of the Huelva river basin corresponding to Domain 4 (2 km).

Figure 3 shows the spatial distribution of the expected increase in hourly maximum ozone for the matrix of nine emission scenarios. The impacts distribution shows intense spatial variations, strongly dependent on the meteorological conditions considered.

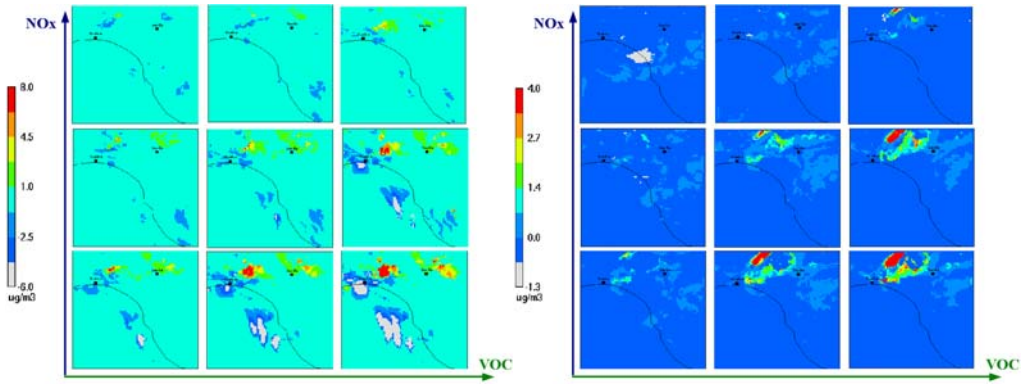

Figure 3: Spatial distribution of the expected increase in the hourly ozone maximum for the nine emission scenarios shown in figure 1: (left) 10-15 August 2003, (right) 14-19 June 2004.

Figure 4 shows the distribution of the increase in the ozone daily hourly maximum as a function of distance to the power plant for the nine emission scenarios shown in figure 1. For the August meteorological episode, two regions clearly show impact areas: the first one located approximately between 15 and 40 km, and the second one, further away, between 75 and 125 km. They correspond to the regions located around the cities of Huelva and Seville, respectively.

For the second meteorological episode (June 2004) the largest impacts are located approximately between 30 and 60 km from the point source. For this meteorological episode, the impact downwind of the city of Seville is smaller than in the August one.

Increases in maximum ozone concentrations are obtained over 95% of the population considered, with the hourly averages varying between 3 and 5 ug/m3. Therefore, the maximum increase in the ozone peak can reach 15 ug/m3 for the hourly averages.

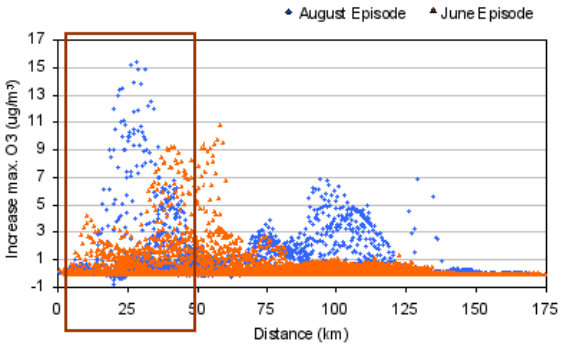

Figure 4: Distribution of the expected increases in maximum ozone levels as a function of distance to the new industry. The rectangle marks the location of the current air quality monitoring network.

4. CONCLUSIONS

The distribution of impacts shows intense spatial variations and marked temporal evolution, strongly dependent on the meteorological conditions considered. The variability between different meteorological episodes is very relevant.

The spatial influence of the new emissions seems to spread to a certain degree over the entire domain studied (172x172 km). The maximum impacts are distributed in a strip between 20 and 70 km, although one can observe a clear variation in the distance/maximum-ozone-increase rate as a function of the meteorological episode.

The potential impact has variable consequences that could be summarized within an interval ranging from 3 to 5 ug/m3 of ozone increase in the daily maximum hourly average.

This uncertainty should be reduced by improvements in the emission inventories (both natural and anthropogenic).

5. ACKNOWLEDGEMENTS

The project has been supported by the Andalucia Goverment and was developped under the technical coordination of the CSIC. The Fundación CEAM is financed by the Generalitat Valenciana and BANCAIXA. Thanks also to CESCA for its computer support.

This work is a contribution to ACCENT.

6. REFERENCES

Atkinson, R. 2000. Atmospheric chemistry of VOCs and NOx. Atmospheric Environment, 34. 2063-2101.

Sillman, S., HE, D., 2002, Some theoretical results concerning O3-NOx-VOC chemistry and NOx-VOC indicators. *Journal of Geophysical Research*, 107 (D22), pp. 4659.

Castell, N., Mantilla, E., Salvador, R., Stein, A., Hernández, L., Millán, M. 2006. Emission Inventory for a Photochemical Modelling Exercise over the South-west of Spain. *6th Annual Meeting of the EMS / 6th ECAC.* 4-8 September 2006. Ljubljana (Slovenia)

Salvador, R., Mantilla, E., Castell, N., Stein, A., Hernández, L., Millán, M. 2006. Analysis of Meteorological Conditions during Photochemical Episodes over South-West of the Iberian Peninsula. *6th Annual Meeting of the EMS / 6th ECAC.* 4-8 September 2006. Ljubljana (Slovenia).

Simpson, D., Guenther A., Hewitt, C.N. and Steinbrecher R. 1995. Biogenic emissions in Europe. Estimates and uncertainties. *Journal of Geophysical Research*, 100 (D11), 22 875- 22 890.